Characterization and elucidating the functional role of uroplakins in the male reproductive tract

Thesis submitted to the University of Hyderabad for the award of Doctor of Philosophy in the Department of Animal Biology

By

Suresh Babu Munipalli

(Reg. No. 14LAPH10)



Department of Animal Biology
School of Life Sciences
University of Hyderabad
Hyderabad - 500 046
Telangana, India

JULY-2022



University of Hyderabad

School of Life Sciences Department of Animal Biology

DECLARATION

I, Suresh Babu Munipalli, hereby declare that this thesis entitled "Characterization and elucidating the functional role of uroplakins in the male reproductive tract" submitted by me under the guidance and supervision of Prof. Suresh Yenugu is an original and independent research work. I also declare that it has not been submitted previously in part or in full to this University or any other University or Institution for the award of any degree or diploma.

Prof. Suresh Yenugu

(Supervisor)

Dr. SURESH YENUGU
Professor
Department of Animal Biology
School of Life Sciences
University of Hyderabad
Hyderabad-500046. (TS), INDIA

M. Swith Below.

Suresh Babu Munipalli

(Reg.No.14LAPH10)



University of Hyderabad

School of Life Sciences

Department of Animal Biology

CERTIFICATE

This is to certify that this thesis entitled "Characterization and elucidating the functional role of uroplakins in the male reproductive tract" is a record of bonafide work done by Mr. Suresh Babu Munipalli, a research scholar for Ph.D. programme in the Department of Animal Biology, University of Hyderabad under my guidance and supervision for a full period prescribed under Ph.D. ordinances of this University. The thesis has not been submitted previously in part or full to this or any other University or Institution for the award of any degree or diploma. We recommend his thesis entitled for submission for the degree of Doctor of Philosophy of the University.

Prof. Suresh Yenugu

Supervisor

Dr. SURESH YENUGU
Professor
Department of Animal Biology
School of Life Sciences
University of Hyderabad
Hyderabad-500046. (TS), INDIA

Department of Animal Biology

अध्यक्ष / HEAD जंतु जैविकी विभाग

Department of Animal Biology

Dean

School of Life Sciences

DEAN

School of Life Sciences University of Hyderabad Hyderabad-500 046.



University of Hyderabad

School of Life Sciences Department of Animal Biology

CERTIFICATE

This is to certify that this thesis entitled "Characterization and elucidating the functional role of uroplakins in the male reproductive tract" is a record of bonafide work done by Mr. Suresh Babu Munipalli, a research scholar for Ph.D. programme in the Department of Animal Biology, School of Life Sciences, University of Hyderabad under my guidance and supervision. This thesis is free from plagiarism and has not been submitted in part or in full to this or any other University or institution for the award of any degree or diploma. Parts of the thesis have been:

A. Published in the following journal:

- Babu Munipalli, S. and S. Yenugu, Uroplakin expression in the male reproductive tract of rat.
 General and Comparative Endocrinology, 2019. 281: p. 153-163.
 (https://pubmed.ncbi.nlm.nih.gov/31181195/).
- B. Presented in the following conferences:
 - 1. **Suresh Babu Munipalli**, & Suresh Yenugu. Characterization of Uroplakin expression in the male reproductive tract. Poster presentation in "International Symposium on Comparative Endocrinology and Integrative Physiology (CEIP 2015)", Thiruvananthapuram, Kerala.
 - Suresh Babu Munipalli, & Suresh Yenugu. Characterization of Uroplakin expression in the male reproductive tract. Poster presentation in "International Symposium on Integrative Physiology and Comparative Endocrinology (ISIPCE-2016)", Banaras Hindu University, Varanasi.

Further, the student has passed the following courses towards the fulfillment of the coursework requirement for Ph.D.

Course Code	Name	Credits	Pass/Fail
AS 801	Analytical Techniques	4	Pass
AS 802	Research Ethics, Data Analysis and Biostatistics	3	Pass
AS 803	Lab Work and Seminar	5	Pass

Prof. Suresh Yenugu

Supervisor

Dr. SURESH YENUGU
Professor
Department of Animal Biology
School of Life Sciences
University of Hyderabad
Hyderabad-500046. (TS), INDIA

Head No. 1.22

Department of Animal Biology

अध्यक्ष / HEAD जंतु जैविकी विभाग Department of Animal Biology

Dean

School of Life Sciences

School of Life Sciences University of Hyderabad Hyderabad-500 046.

Acknowledgements

I express my sincere gratitude to my teacher and research supervisor, **Prof. Suresh Yenugu** for his overall guidance and suggestions throughout the period of my work. As a supervisor, he has given full freedom to execute the experiments with critical suggestions. I express my deepest gratitude for his magnanimous and kind heartedness. In addition to research, I am very grateful to him for his kind help even in many situations of my personal life across this period.

I would like to thank my doctoral committee members Prof. Aparna Dutta Gupta, Prof. B. Senthilkumaran and Prof. Naresh Babu V Sepuri, for their insightful comments and suggestions for this study.

I sincerely acknowledge the Head of Department- Current and previous heads for providing equipment in good condition and facilities to carry out this work. I sincerely acknowledge the dean of the school of Lifesciences - Current and previous deans for allowing me to use school facilities to carry out this work.

I thank animal house In-charge Prof. K, Arun Kumar, for allowing me to use animal facilities to carry out this work.

I thank all the animal house staff for their kind help throughout this period.

I thank FACS In-charge/s Dr. Radheshyam Mourya, and Dr. Roy Karnati for allowing me to use FACS facilities.

I express my sincere thanks to all my teachers at PG level, at UG level, Inter, high school and primary school.

I thank RGNF (JRF and SRF) for providing financial assistance to carry out this work. Financial support from VoH, CSIR, ICMR, IOE, DBT and DST to the laboratory is highly acknowledged.

I am grateful to my laboratory colleagues Aisha Jamil, Mounika Marri and Priyanka Patra for their help cooperation, and support in all respects during my work. I would like to thank my laboratory seniors Dr. Bernali Biswas, Dr. Madhu Babu Golla, Dr. Rajesh Anjireddy, Dr. G. Narmadha and P. Lavanya, Dr. Anandha Rao, Dr. Sangeeta for their help and efforts to establish the lab. I thank laboratory helper Narasihanna for his timely help.

I think to late Prof. Aparna Dutta Gupta, and Prof. B. Senthilkumaran for my expertise in Wax sectioning and H and D staining.

I thank Prof. Arun Kumar for allowing me to use the animal house facility and for helping me whenever I need.

I thank the NIAB Animal house facility for maintaining Knockout mice and taught me animal handling and mating study.

I thank Dr. Aurélie Jory for generated Upk1a heterozygous mice and special thanks to National Center for Biological Sciences (NCBS).

I thank Dr. Nirmalya Ganguli for teaching me about testicular microinjection.

I Thank Dr. Radheshyam Maurya and Mr. Prince Sebastian for FACS assistance and analysis.

I thank Dr. Prasad Tammineni, Deepti madam, and Nalini madam for the high-resolution imaging.

I thank Dr. J. Madhupraksh for teaching me protein modelling.

I thank Dr. Sireesh Kumar for the infection model generation.

I thank Mr. Mahesh and Mr. Sridhar for the Histopathology study.

I special thanks to the Novel gene Technology team Bipin Sir, Abhishek sir, Naveen, and Aman, for the transcriptome studies.

I am incredibly thankful to Dr. Gurranna and Dr. Jyothi Chaitanya Pagadala for their continuous support.

I am highly thankful to all my friends at the University of Hyderabad.

I am highly thankful to all juniors in the life science for their help.

I am so fortunate to having a lovable and fabulous sister Sujatha, and my brother Ravi Kumar for their constant encouragement, support, and cooperation across this journey and I would have not reached to this level without them.

Thanks to the almighty for everything!

FINALLY, I THANK MY EVER-LOVING PARENTS, BULLEIAH AND NIRMALA

Suresh Babu Munipalli....

Contents

P	age No
Abbreviations	_
Title page	
Introduction	
References	
References	12
Chanter 1	
Chapter 1	17
In silico and in vivo Characterization of Rat Uroplakins	
1.1 Introduction	
1.2 Materials and methods	
1.2.1. <i>In silico</i> analyses	
1.2.2. Molecular modelling	
1.2.3. Animals and tissue collection	
1.2.4. Polymerase chain reaction (PCR)	22
1.2.5. Immunoblotting	
1.2.6. Immunofluorescence	23
1.2.7. Treatment with LPS in vitro and in vivo	.24
1.2.8. Statistical analyses	25
1.3. Results	25
1.3.1. In silico analyses	25
1.3.2. Uroplakin expression in the rat	
1.3.3. Modulation of <i>Upk</i> gene expression by LPS	
1.4. Discussion	
1.5. References	
1.3. References	32
Chapter 2.	
Functional characterization of Uroplakin1a (<i>Upk1a</i>) using knock-out model	58
2.1. Introduction	59
	60
1	60
2.2.2. RT-PCR	62
2.2.3. Assessment of fecundity	63
2.2.4. Assessment of capacitation and acrosome reaction	63
2.2.5. Histological evaluation	64
2.2.6. UPEC infection and assessment	
2.2.7. Gene chip hybridization, data collection and enrichment	64
2.2.8. Statistical analyses	65
2.2.9. Ethics approval statement	65
2.3. Results	66
2.3.1. Genotypic characterization of knockout mice	66
2.3.2. Body and organ	
2.3.3. Fecundity, sperm count and sperm.	68

2.3.4. Histopathology	70
2.3.5. UPEC infection and bacterial clearance	. 74
2.3.6. Transcriptome analyses	. 76
2.4. Discussion	
2.5. References	
Chapter 3	
Evaluating the functional role of Uroplakin1a at the molecular level	
using Yeast Two Hybrid Screening	. 89
3.1. Introduction	
3.2. Materials and methods	92
3.2.1. Yeast two hybrid screening	92
3.2.2. Performing control experiments for validation	93
3.2.3. Cloning and testing the bait for auto-activation and toxicity.	. 97
3.2.4. Identification of UPK1A / UPK2 interacting partners in	00
the testis cDNA library	
3.3. Results	
3.3.1. Identifying the interaction partners of UPK1A and UPK2	101
3.3.2. Confirmation of the interaction of UPK1A with RGN and PSMB1	106
3.4. Discussion.	
3.5. References.	
<u></u>	110
SUMMARY	117

Abbreviations

UPKs : Uroplakins

PGC: Primordial germ cells

SSCs : spermatogonial stem cells

PTM : Peritubular myoid

LH : luteinizing hormone

FSH : Follicle-Stimulating Hormone

TP1 : Transition protein 1

SPAG11A : Sperm-associated antigen 11A

AUM : Asymmetric unit membranes

VUR : Vesicoureteral reflux

ER : Endoplasmic reticulum

UPEC : Uropathogenic *Escherichia coli*,

PBS : Phosphate buffered saline

SOPMA : Self-Optimized Prediction Method with Alignment

HEK293 : Human embryonic kidney 293 cells

LC540 : Rat Leydig cell line - 540

RCE : Rat caput epididymal cell line

PATE : Prostate and Testis expressed

LYZL : Lysozyme like

PFA : Paraformaldehyde

CDK7 : Cyclin-dependent kinase 7

PPIs : Protein-protein interactions

HE4 : Epididymis protein 4

CFTR : Cystic fibrosis transmembrane conductance regulator

FGF : fibroblast growth factor

Y2H : Yeast two hybrid screening

DNA-BD : DNA-binding domain

DNA-AD : DNA – Activation domain

RGN: Regucalcin

PSMB1 : Proteasome subunit beta 1

TEX44 : Testis expressed 44

SNRPN : Small nuclear ribonucleoprotein polypeptide N

RFP : Red fluorescent protein

GFP : Green fluorescent protein

Title

Characterization and elucidating the functional role of uroplakins in the male reproductive tract

	•			•								•																•						•				•		•	
V.			■ V4					 	▲ ₹⊿		7	N	■ T.	• •	V.	▲ 7.4	 -	V.			-	N.	- ₹ 7.		V.	■ V4			■ V4				▲ T.	 Y 👝 .	~~	_ ~ Y	 7	- T		1	_
\sim	_	_	_	_	_	$\overline{}$	_	 ~	$\overline{}$	_	_	$\overline{}$	_		 ~	_	 -	_	_	_		_	_	 	_	_	 _	~	_	_	_	_	_	 ~	$\overline{}$	_	 _	$\overline{}$	_		_
•	•	•	- 4 -	•																																					

Introduction

Male reproductive system

The male reproductive system combines testes, epididymides, vas deferens, and ejaculatory duct and also includes accessory sex glands (prostate, bulbourethral and seminal vesicles). A pictorial representation of a typical organization of the male reproductive organization is presented in Figure 1.

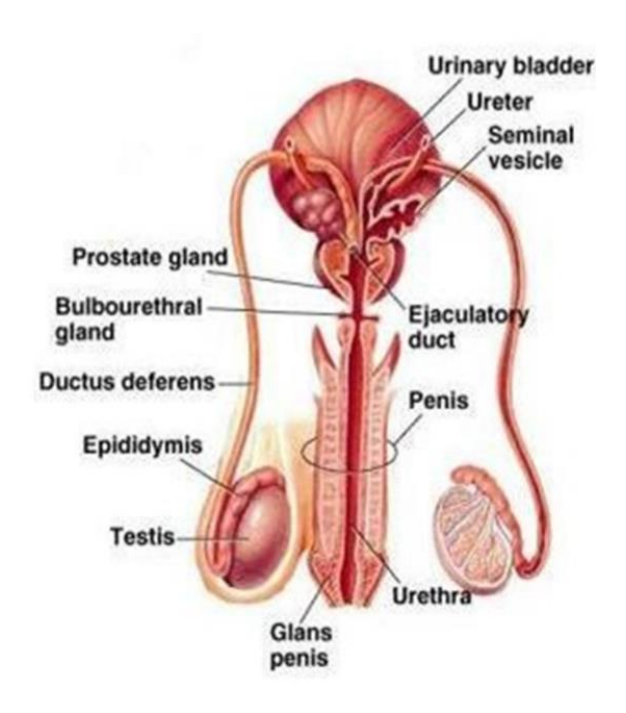


Figure 1. Male reproductive system

Testes

Oval-shaped structures in the scrotal sac (a bag-like structure) just behind the penis. Tunica albuginea (a fibrous capsule) sheaths both the testes. The testis is partitioned into 200–400 wedge-shaped lobes by the fibrous tissue of the tunica albuginea. Three to ten coiled tubules, or seminiferous tubules, are present within each lobe. Testis acts as both exocrine and endocrine glands. Leydig cells of the testis produce testosterone, a factor crucial for spermatogenesis and other physiological functions (bone mass, fat distribution, sex drive muscle size, strength, etc.) The exocrine function of the testis is to produce spermatozoa in the seminiferous tubules.

Epididymis

A highly intricate tubular organ, called the epididymis, is trisected into three portions i.e caput, corpus, and cauda. The sperm passes from the testes to the vas deferens through the epididymis. The immotile testicular sperm attain motility and fertilizing ability when they cross the epididymal regions. The broad portion of the epididymis is represented by the caput, which is located over the testes posteriorly and nourishes the sperm till they start to undergo maturation. Sperm start to become more motile in the corpus epididymis. After development, sperm are stored in the cauda until ejaculation.

Vas deferens

A long muscular tube beginning from the epididymis that extends across the pelvic cavity and ends right outside the bladder. For ejaculation, the vas deferens facilitates the movement of mature sperm to the urethra.

Ejaculatory duct

The ejaculatory duct transports sperm into the urethra with the prostate's essential secretions and supplements for sperm activity.

Seminal vesicles

The two seminal vesicles produce the fluidic compositions of the semen. An estimated 50 to 80 percent of semen's volume is made up of the liquid produced by the seminal vesicles. Seminal fluid contains ingredients intended to keep sperm viable after entering the vagina. Energy-producing fructose aid in sperm motility and prostaglandins prevent an immune response by the tissues of the female genital tract. The seminal fluid alkalinity aids in neutralizing the acidic environment in the female genital tract. Various clotting factors aid in the longevity of sperm.

Prostate gland

The prostate gland is positioned immediately beneath the bladder. The principal purpose of the prostate is to furnish the fluid for sperm transport and nourishment. Enzymes, zinc, and citric acid found in prostatic fluid make semen a perfect environment for sperm cells to live.

Bulbourethral gland:

The bulbourethral glands are a pair of pea-shaped exocrine glands, also known like Cowper's gland, are located posterolateral to the membranous urethra. By secreting lubricating mucus, they add to the final amount of semen.

Spermatogenesis

The primary function of the male reproductive system is the production of sperm (spermatogenesis) in the seminiferous tubules of the testis. This process starts with differentiating primordial germ cells (PGC) into spermatids through mitotic and meiotic divisions. For instance, in humans, the primordial germ cell is the main undifferentiated stem cell that distinguishes connecting gametes, spermatozoa, or oocytes. (Nikolic, Volarevic, Armstrong, Lako, & Stojkovic, 2016).

The multiplication and development of spermatogonial stem cells (SSCs), which come from PGCs in the early embryo, maintain the production of mammalian sperm (Ohta, Wakayama, & Nishimune, 2004). Spermatogonial stem cells (SSCs), which can self-renew and produce daughter cells to bear terminally differentiated cells, or spermatozoa, are necessary for the lifelong maintenance of spermatogenesis (Figure 2). Spermatogenesis occurs in the seminiferous tubules and constitues three main cell types: germ cells, Sertoli cells, and peritubular myoid (PTM) cells. The crucial primary role played by these cells is to provide niche for SSCs (Richardson, Kleinman, & Dym, 1995). Leydig cells in the interstitial space of the testis secrete testosterone in response to stimulation by luteinizing hormone (LH). In spermatogenesis (a process tightly controlled by testosterone), diploid spermatogonia undergo mitosis until they start to transform into gametes. These gametes eventually become primary spermatocytes, which divide once during the initial meiotic phase to produce two haploid secondary spermatocytes. After a second meiotic division, the secondary spermatocytes both resulted in two spermatids, which will eventually mature into sperm. The immature sperm will enter the epididymal caput, and maturation is facilitated by the epididymal secreations. The matured sperm is stored in epididymal cauda.

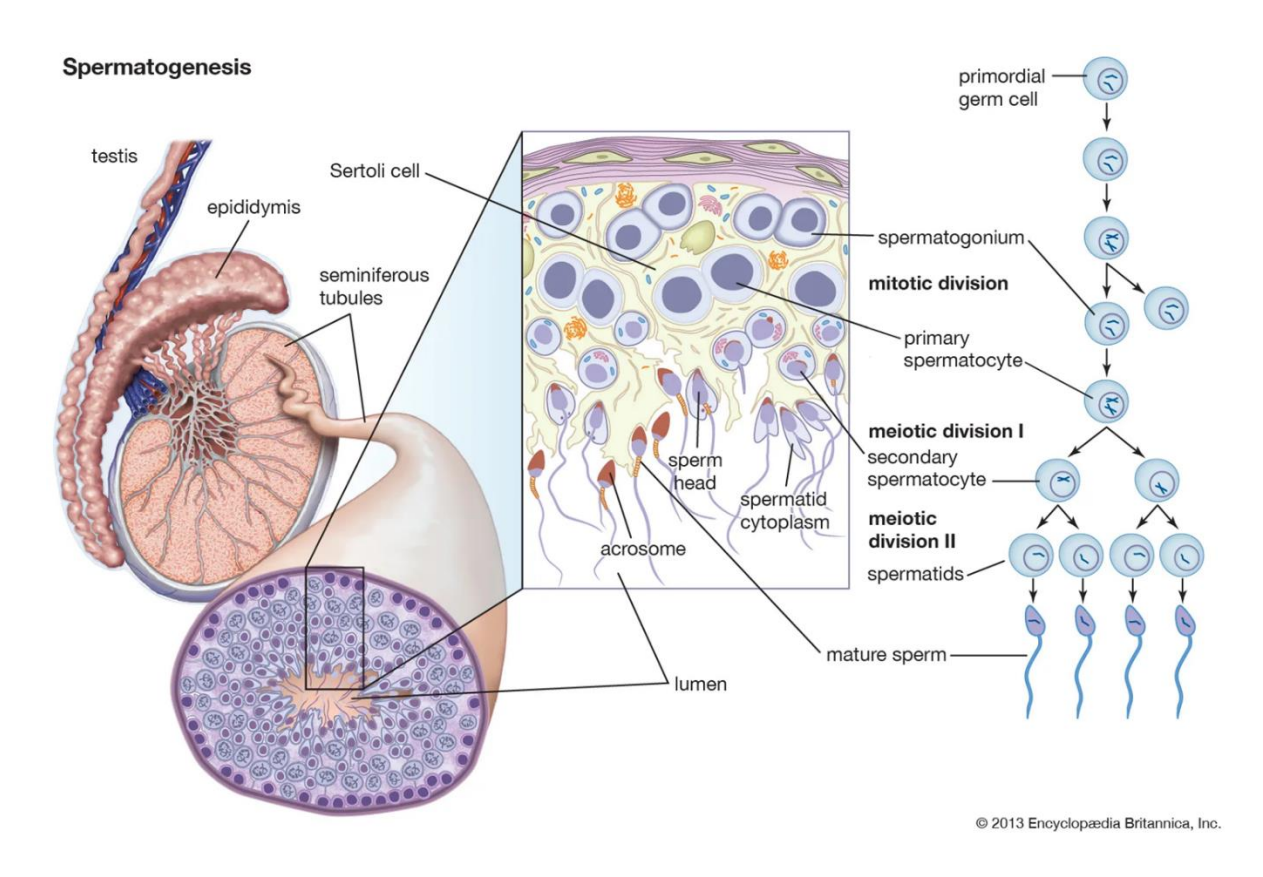


Figure 2. Representation of the Spermatogenesis

Factors involved in spermatogenesis and maturation

Spermatogenesis initially starts from neonatal development through testis and epididymis. In this sequential development process, several factors help form sperm and its maturation. In the period of neonatal development, the progenitor cells convert into gonocytes in the presence of SCF/cKit, which is crucial for maintaining primordial germ cells. Sertoli cells also express SCF when stimulated by Follicle-Stimulating Hormone (FSH). (Rossi, Sette, Dolci, & Geremia, 2000). The pluripotent nature of the PGC is supported by the expression of the Stella and Oct4 and alternative pluripotent genes in germ cells; and repression of *Hoxb1*, *Hoxa1*, *Evx1*, and *Lim1*, homeobox genes that negatively regulate somatic cell differentiation (Saitou *et al.*, 2003; Yeom *et al.*, 1996). The PGCs multiply and move through the mesentery and endoderm of the hindgut before migrating bilaterally to the genital ridges. Meiosis begins in females or mitotic arrest in the case of males and initiates differentiation into each oocyte or spermatozoa. (Molyneaux, Stallock, Schaible, & Wylie, 2001). Postmigration, PGCs are

distinguished by the expression of various RNA binding proteins, namely, *MVH*, *DAZL*, and *NANOS3*. In the female XX embryo, the PGCs constantly proliferate and consequently enter prophase I of meiosis. XY PGCs undergo mitotic arrest and entry into the genital ridges, where they persist in the quiescent G 0/G 1 cell cycle phase during the embryonic period. (McLaren, 2001). PGCs, which move from the embryonic ectoderm postnatally, give rise to SSCs. The transcription factor-encoding genes *Bcl6b*, *Etv5*, and *Lhx1*, as well as the site factor of glial cell line-derived neurotrophic factor (GDNF), significantly impact the self-renewal of rodent SSCs. (Oatley & Brinster, 2008).

During sperm production in the testis, i.e., spermatogonial stage to spermatids, factors that define chromatin modeling, transcription, and RNA binding are involved. Numerous transcription elements involved in spermatogenesis, including heat shock factor 2 (HSF2) and OVOL are implicated in germ cells. Sertoli cells express WT1, RHOX5, SOX8, and FOXI1, contributing to sperm maturation in the epididymis (Bettegowda & Wilkinson, 2010). At the chromatin level, two of the four canonical core histones, H2A, H2B, H3, and H4 (that make up nucleosomes in male germ cells) form octamers to regulate gene expression and fold the DNA (Talbert & Henikoff, 2010). Non-histone proteins like transition protein 1 (TP1) and transition protein 2 (TP2) that are arginine and lysine-rich with an excellent affinity for DNA play a crucial role in the control of chromatin structure of spermatids. The protein BRDT, found in the testis, is implicated by pachytene spermatocytes. Shortened BRDT lacking bromodomain exhibits problems in postmeiotic male germ cells (Shang, Nickerson, Wen, Wang, & Wolgemuth, 2007).

One of the families of RNA-binding proteins (RBPs) found in germ cells is the Y-box protein family, which includes the variants MSY1, MSY2, and MSY4. The role of MSY2 transcription factor promotes the transcription of testis-specific genes. Also, it functions as a structural constituent of messenger ribonucleoproteins (mRNPs) in the cytoplasm of maturing germ cells (Gu et al., 1998). Human testis expresses YBX2, also referred to as "Contrin," the homologue of MSY2. Alterations in the YBX2 gene result in altered protamine expression, which in turn causes aberrant spermatogenesis and infertility in humans.(Hammoud, Emery, Dunn, Weiss, & Carrell, 2009; Yang, Morales, Medvedev, Schultz, & Hecht, 2007)

The three parts that made up the epididymis were the proximal caput, the extended corpus, and the expanded distal cauda. The immature sperm that the testis produces will go into the

epididymis, where maturation will occur. The epididymal caput produces intraluminal components that are necessary for sperm motility and fertilization. (Sullivan & Mieusset, 2016). The expression of the sperm-associated antigen 11A (SPAG11A), which is androgen-dependent and plays a function in sperm maturation, is restricted to the caput epididymis's main cells in mice. (Pujianto, Loanda, Sari, Midoen, & Soeharso, 2013).

Transmembrane proteins in male reproduction

Transmembrane proteins are the cell surface receptors involved in the signal transduction process crucial for gametogenesis and fertilization. The ion channel receptors, namely, calcium channels regulate calcium levels for sperm function and fertilization (Darszon, Nishigaki, Beltran, & Trevino, 2011). The male germ cells express ryanodine receptors (RyRs); and the mobilization of calcium through RyR channels regulates the maturation of male germ cells (Chiarella, Puglisi, Sorrentino, Boitani, & Stefanini, 2004). Similarly, enzyme-linked receptors, such as c-Kit, have a pivotal role in the differentiation of gonocytes and testis maturation (Prabhu *et al.*, 2006). When spermatogonia mature into spermatozoa, differential gene expression and cell-to-cell communication are moderated by the endocrine stimuli resulting from FSH/LH and testosterone. The FSHR, a transmembrane G-protein receptor on Sertoli cells, drives spermatogenesis (Oduwole, Peltoketo, & Huhtaniemi, 2018).

Tetraspanins (also known as tetraspan or TM4SF) are a broad family of integral membrane proteins, and 33 groups make up this superfamily in humans. The homologs of human tetraspanins, which are found in all eukaryotic species, are broadly distributed in cells and tissues. They are involved in various processes, including differentiation, adhesion, motility, cell activation, and proliferation (Maecker, Todd, & Levy, 1997). Tetraspanin family members include membrane protein CD9. Despite CD9's wide tissue distribution, animals lacking CD9 mainly exhibited female infertility caused by a problem with the sperm-egg fusion process(Kaji, Oda, Miyazaki, & Kudo, 2002). The tetraspanin family proteins CD9, CD63, CD81, and CD151 are crucial for immunity, cell-to-cell communication, and fertilization (Desalle, Chicote, Sun, & Garcia-Espana, 2014). The Uroplakin1a (UPK1a) and Uroplakin1b (UPK1b) also belong to 20th and 21st tetraspanin families, present on mammalian bladder epithelium (urothelium)(Jenkins & Woolf, 2007).

Uroplakins (UPKs)

Uroplakins (UPKs) are integral membrane proteins that fall under one of two families: The four-transmembrane domain tetraspanin (TSPAN or TM4SF) family, which includes UPK1a (UPIa) and UPK1b (UPIb) (Yu, Lin, Wu, & Sun, 1994); and the single-spanning transmembrane uroplakins, which include UPK2a, UPK2b, UPK3a (UPIIIa, UPK3A), UPK3b (UPIIIb, UPK3B), UPK3c and UPK3d. UPK2b is predominant in non-mammalian vertebrates, UPK3c exists in mammals, reptiles and birds, while UPK3d is dominat in bony fish (Garcia-Espana et al., 2006; Lin, Wu, Kreibich, & Sun, 1994; Wu et al., 1994). The UPKs are primarily involved in forming urothelial plaques by forming unique structures called asymmetric unit membranes (AUM). UPK1a and UPK1b (both 27 kDa), UPK2 (15 kDa), and UPK3 (47 kDa) are some of the critical integral membrane proteins found in the apical surface of mammalian urinary bladder epithelium (Ryan et al., 1993). In forming urothelial plaques, UPK1a mainly interacts with UPK2, while UPK1b specifically interacts with UPK3a to produce the heterotetramer (Figure 3). Ninety percent of the urothelial apical surface is made up of hexagonally packed, two-dimensional crystals made of urothelial plaque. (Matuszewski et al., 2016). (Figure 3). Excess uroplakins are drawn into the cell once the bladder is emptied, which reduces the amount of uroplakin-covered surface. In reaction to the increasing capacity of the bladder filling the bladder with urine, uroplakins return to the urothelial surface(Lewis, 2000).

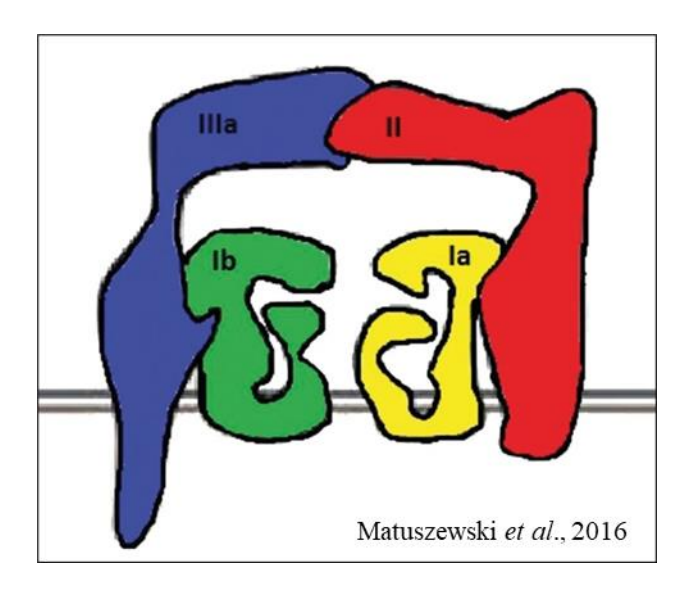


Figure 3: Schematic representation of uroplakin heterotetramer that contributes to the formation of urothelial plaques.

Urothelial plaques maintain a persistent permeability barrier to preserve the blood from toxic elements of the urinary tract (Negrete, Lavelle, Berg, Lewis, & Zeidel, 1996). In *Upk2* or *Upk3a* null-mutant mice, the heterodimeric partner of the specific protein expressed by each mutant gene is disrupted, which causes abnormal plaque formation (Hu *et al.*, 2000; Lewis, 2000). Symptoms include severe vesicoureteral reflux (VUR), reduced renal function, and hydronephrosis in mice lacking UPK2, UPK3a, or both(Hu *et al.*, 2000; Kong *et al.*, 2004). The initial and most crucial step in the infection of the urinary tract and bladder by uropathogenic *E coli* (UPEC) bacteria. The bacteria adhere to the urothelial surface through particular connections between the UPEC FimH and the mannosylated glycoprotein on the urothelial surface (Ofek, Hasty, Abraham, & Sharon, 2000). The primary mannosylated glycoprotein (UP1a/1b) on the urothelial surface can interact with type 1-fimbriated *E. coli* (Wu, Sun, & Medina, 1996). The UPK1a acts as a receptor for the type-1 fimbriated *E. coli*, which causes urinary tract infection (Zhou *et al.*, 2001).

Recent investigations have also reported the role of uroplakins in reproductive physiology. The distribution of uroplakins was consistent in the *Xenopus laevis* bladder, fat cells, oocytes, zebrafish pronephric tubules, and various mammalian nonurothelial organs and malignancies (Garcia-Espana *et al.*, 2006; Mitra *et al.*, 2012).In *Xenopus laevis*, Upk3a and Upk1b function as receptors when sperm and eggs are in contact (Mahbub Hasan *et al.*, 2014). Upk3b is expressed in the epididymis and the ovarian follicle in a time-dependent manner (Kuriyama, Tamiya, & Tanaka, 2017). Double-knockout *Upk2/3a* mice had a reduced litter size. The Uroplakins are also found in subcellular localization in the oocyte of multivesicular bodies such as the endoplasmic reticulum (ER), Golgi bodies, and late endosomes (Liao *et al.*, 2018).

References:

 Bettegowda, A., & Wilkinson, M. F. (2010). Transcription and post-transcriptional regulation of spermatogenesis. *Philos Trans R Soc Lond B Biol Sci*, 365(1546), 1637-1651. doi: 10.1098/rstb.2009.0196

- 2. Chiarella, P., Puglisi, R., Sorrentino, V., Boitani, C., & Stefanini, M. (2004). Ryanodine receptors are expressed and functionally active in mouse spermatogenic cells and their inhibition interferes with spermatogonial differentiation. *J Cell Sci*, 117(Pt 18), 4127-4134. doi: 10.1242/jcs.01283
- 3. Darszon, A., Nishigaki, T., Beltran, C., & Trevino, C. L. (2011). Calcium channels in the development, maturation, and function of spermatozoa. *Physiol Rev*, 91(4), 1305-1355. doi: 10.1152/physrev.00028.2010
- 4. Desalle, R., Chicote, J. U., Sun, T. T., & Garcia-Espana, A. (2014). Generation of divergent uroplakin tetraspanins and their partners during vertebrate evolution: identification of novel uroplakins. *BMC Evol Biol*, *14*, 13. doi: 10.1186/1471-2148-14-13
- Garcia-Espana, A., Chung, P. J., Zhao, X., Lee, A., Pellicer, A., Yu, J., ... Desalle, R. (2006).
 Origin of the tetraspanin uroplakins and their co-evolution with associated proteins: implications for uroplakin structure and function. *Mol Phylogenet Evol*, 41(2), 355-367. doi: 10.1016/j.ympev.2006.04.023
- Gu, W., Tekur, S., Reinbold, R., Eppig, J. J., Choi, Y. C., Zheng, J. Z., . . . Hecht, N. B. (1998).
 Mammalian male and female germ cells express a germ cell-specific Y-Box protein, MSY2. *Biol Reprod*, 59(5), 1266-1274. doi: 10.1095/biolreprod59.5.1266
- Hammoud, S., Emery, B. R., Dunn, D., Weiss, R. B., & Carrell, D. T. (2009). Sequence alterations in the YBX2 gene are associated with male factor infertility. *Fertil Steril*, 91(4), 1090-1095. doi: 10.1016/j.fertnstert.2008.01.009
- 8. Hu, P., Deng, F. M., Liang, F. X., Hu, C. M., Auerbach, A. B., Shapiro, E., . . . Sun, T. T. (2000). Ablation of uroplakin III gene results in small urothelial plaques, urothelial leakage, and vesicoureteral reflux. *J Cell Biol*, *151*(5), 961-972. doi: 10.1083/jcb.151.5.961
- 9. Jenkins, D., & Woolf, A. S. (2007). Uroplakins: new molecular players in the biology of urinary tract malformations. *Kidney Int, 71*(3), 195-200. doi: 10.1038/sj.ki.5002053
- 10. Kaji, K., Oda, S., Miyazaki, S., & Kudo, A. (2002). Infertility of CD9-deficient mouse eggs is reversed by mouse CD9, human CD9, or mouse CD81; polyadenylated mRNA injection developed for molecular analysis of sperm-egg fusion. *Dev Biol, 247*(2), 327-334. doi: 10.1006/dbio.2002.0694
- 11. Kong, X. T., Deng, F. M., Hu, P., Liang, F. X., Zhou, G., Auerbach, A. B., . . . Sun, T. T. (2004). Roles of uroplakins in plaque formation, umbrella cell enlargement, and urinary tract diseases. *J Cell Biol*, 167(6), 1195-1204. doi: 10.1083/jcb.200406025
- 12. Kuriyama, S., Tamiya, Y., & Tanaka, M. (2017). Spatiotemporal expression of UPK3B and its promoter activity during embryogenesis and spermatogenesis. *Histochem Cell Biol, 147*(1), 17-26. doi: 10.1007/s00418-016-1486-8

- 13. Lewis, S. A. (2000). Everything you wanted to know about the bladder epithelium but were afraid to ask. *Am J Physiol Renal Physiol*, 278(6), F867-874. doi: 10.1152/ajprenal.2000.278.6.F867
- 14. Liao, Y., Chang, H. C., Liang, F. X., Chung, P. J., Wei, Y., Nguyen, T. P., . . . Sun, T. T. (2018). Uroplakins play conserved roles in egg fertilization and acquired additional urothelial functions during mammalian divergence. *Mol Biol Cell*, 29(26), 3128-3143. doi: 10.1091/mbc.E18-08-0496
- 15. Lin, J. H., Wu, X. R., Kreibich, G., & Sun, T. T. (1994). Precursor sequence, processing, and urothelium-specific expression of a major 15-kDa protein subunit of asymmetric unit membrane. *J Biol Chem*, 269(3), 1775-1784.
- 16. Maecker, H. T., Todd, S. C., & Levy, S. (1997). The tetraspanin superfamily: molecular facilitators. *FASEB J*, 11(6), 428-442.
- 17. Mahbub Hasan, A. K., Hashimoto, A., Maekawa, Y., Matsumoto, T., Kushima, S., Ijiri, T. W., . . . Sato, K. (2014). The egg membrane microdomain-associated uroplakin III-Src system becomes functional during oocyte maturation and is required for bidirectional gamete signaling at fertilization in Xenopus laevis. *Development*, 141(8), 1705-1714. doi: 10.1242/dev.105510
- 18. Matuszewski, M. A., Tupikowski, K., Dolowy, L., Szymanska, B., Dembowski, J., & Zdrojowy, R. (2016). Uroplakins and their potential applications in urology. *Cent European J Urol, 69*(3), 252-257. doi: 10.5173/ceju.2016.638
- 19. McLaren, A. (2001). Mammalian germ cells: birth, sex, and immortality. *Cell Struct Funct*, 26(3), 119-122. doi: 10.1247/csf.26.119
- 20. Mitra, S., Lukianov, S., Ruiz, W. G., Cianciolo Cosentino, C., Sanker, S., Traub, L. M., . . . Apodaca, G. (2012). Requirement for a uroplakin 3a-like protein in the development of zebrafish pronephric tubule epithelial cell function, morphogenesis, and polarity. *PLoS One*, 7(7), e41816. doi: 10.1371/journal.pone.0041816
- 21. Molyneaux, K. A., Stallock, J., Schaible, K., & Wylie, C. (2001). Time-lapse analysis of living mouse germ cell migration. *Dev Biol*, 240(2), 488-498. doi: 10.1006/dbio.2001.0436
- 22. Negrete, H. O., Lavelle, J. P., Berg, J., Lewis, S. A., & Zeidel, M. L. (1996). Permeability properties of the intact mammalian bladder epithelium. *Am J Physiol*, *271*(4 Pt 2), F886-894. doi: 10.1152/ajprenal.1996.271.4.F886
- Nikolic, A., Volarevic, V., Armstrong, L., Lako, M., & Stojkovic, M. (2016). Primordial Germ Cells: Current Knowledge and Perspectives. *Stem Cells Int*, 2016, 1741072. doi: 10.1155/2016/1741072
- 24. Oatley, J. M., & Brinster, R. L. (2008). Regulation of spermatogonial stem cell self-renewal in mammals. *Annu Rev Cell Dev Biol*, 24, 263-286. doi: 10.1146/annurev.cellbio.24.110707.175355

- 25. Oduwole, O. O., Peltoketo, H., & Huhtaniemi, I. T. (2018). Role of Follicle-Stimulating Hormone in Spermatogenesis. *Front Endocrinol (Lausanne)*, *9*, 763. doi: 10.3389/fendo.2018.00763
- Ofek, I., Hasty, D. L., Abraham, S. N., & Sharon, N. (2000). Role of bacterial lectins in urinary tract infections. Molecular mechanisms for diversification of bacterial surface lectins. *Adv Exp Med Biol*, 485, 183-192. doi: 10.1007/0-306-46840-9
- 27. Ohta, H., Wakayama, T., & Nishimune, Y. (2004). Commitment of fetal male germ cells to spermatogonial stem cells during mouse embryonic development. *Biol Reprod*, 70(5), 1286-1291. doi: 10.1095/biolreprod.103.024612
- 28. Prabhu, S. M., Meistrich, M. L., McLaughlin, E. A., Roman, S. D., Warne, S., Mendis, S., . . . Loveland, K. L. (2006). Expression of c-Kit receptor mRNA and protein in the developing, adult and irradiated rodent testis. *Reproduction*, *131*(3), 489-499. doi: 10.1530/rep.1.00968
- 29. Pujianto, D. A., Loanda, E., Sari, P., Midoen, Y. H., & Soeharso, P. (2013). Sperm-associated antigen 11A is expressed exclusively in the principal cells of the mouse caput epididymis in an androgen-dependent manner. *Reprod Biol Endocrinol*, 11, 59. doi: 10.1186/1477-7827-11-59
- 30. Richardson, L. L., Kleinman, H. K., & Dym, M. (1995). Basement membrane gene expression by Sertoli and peritubular myoid cells in vitro in the rat. *Biol Reprod*, *52*(2), 320-330. doi: 10.1095/biolreprod52.2.320
- 31. Rossi, P., Sette, C., Dolci, S., & Geremia, R. (2000). Role of c-kit in mammalian spermatogenesis. *J Endocrinol Invest*, *23*(9), 609-615. doi: 10.1007/BF03343784
- 32. Ryan, A. M., Womack, J. E., Yu, J., Lin, J. H., Wu, X. R., Sun, T. T., ... D'Eustachio, P. (1993). Chromosomal localization of uroplakin genes of cattle and mice. *Mamm Genome*, 4(11), 656-661. doi: 10.1007/BF00360903
- 33. Saitou, M., Payer, B., Lange, U. C., Erhardt, S., Barton, S. C., & Surani, M. A. (2003). Specification of germ cell fate in mice. *Philos Trans R Soc Lond B Biol Sci*, 358(1436), 1363-1370. doi: 10.1098/rstb.2003.1324
- 34. Shang, E., Nickerson, H. D., Wen, D., Wang, X., & Wolgemuth, D. J. (2007). The first bromodomain of Brdt, a testis-specific member of the BET sub-family of double-bromodomaincontaining proteins, is essential for male germ cell differentiation. *Development*, 134(19), 3507-3515. doi: 10.1242/dev.004481
- 35. Sullivan, R., & Mieusset, R. (2016). The human epididymis: its function in sperm maturation. *Hum Reprod Update*, 22(5), 574-587. doi: 10.1093/humupd/dmw015
- 36. Talbert, P. B., & Henikoff, S. (2010). Histone variants--ancient wrap artists of the epigenome. *Nat Rev Mol Cell Biol*, 11(4), 264-275. doi: 10.1038/nrm2861

- 37. Wu, X. R., Lin, J. H., Walz, T., Haner, M., Yu, J., Aebi, U., & Sun, T. T. (1994). Mammalian uroplakins. A group of highly conserved urothelial differentiation-related membrane proteins. *J Biol Chem*, 269(18), 13716-13724.
- 38. Wu, X. R., Sun, T. T., & Medina, J. J. (1996). In vitro binding of type 1-fimbriated Escherichia coli to uroplakins Ia and Ib: relation to urinary tract infections. *Proc Natl Acad Sci U S A*, *93*(18), 9630-9635. doi: 10.1073/pnas.93.18.9630
- 39. Yang, J., Morales, C. R., Medvedev, S., Schultz, R. M., & Hecht, N. B. (2007). In the absence of the mouse DNA/RNA-binding protein MSY2, messenger RNA instability leads to spermatogenic arrest. *Biol Reprod*, 76(1), 48-54. doi: 10.1095/biolreprod.106.055095
- 40. Yeom, Y. I., Fuhrmann, G., Ovitt, C. E., Brehm, A., Ohbo, K., Gross, M., . . . Scholer, H. R. (1996). Germline regulatory element of Oct-4 specific for the totipotent cycle of embryonal cells. *Development*, 122(3), 881-894. doi: 10.1242/dev.122.3.881
- 41. Yu, J., Lin, J. H., Wu, X. R., & Sun, T. T. (1994). Uroplakins Ia and Ib, two major differentiation products of bladder epithelium, belong to a family of four transmembrane domain (4TM) proteins. *J Cell Biol*, 125(1), 171-182. doi: 10.1083/jcb.125.1.171
- 42. Zhou, G., Mo, W. J., Sebbel, P., Min, G., Neubert, T. A., Glockshuber, R., . . . Kong, X. P. (2001). Uroplakin Ia is the urothelial receptor for uropathogenic Escherichia coli: evidence from in vitro FimH binding. *J Cell Sci*, 114(Pt 22), 4095-4103. doi: 10.1242/jcs.114.22.4095

******************	*
Chapter - 1	
In silico and in vivo Characterization of Rat Uroplakins	
	2

1.1 Introduction

Uroplakins (UPKs) are a group of proteins that form the major constituents of urothelial plaques. In the mammals, five UPKs, namely, UPK1a, UPK1b, UPK2, UPK3a and UPK3b (a minor isoform of UPK3a) are characterized. Besides these, UPK2b and UPK3c and UPK3d were identified in other species (Desalle et al., 2014, Garcia-Espanaet al., 2006, Wu et al., 1994). Mammalian UPKs are divided into two groups. UPK1a and UPK1b belong to the tetraspanin family, whereas UPK2 and UPK3 are grouped under the monospanin family (Yu et al., 1994, Lin et al., 1994, Wu and Sun 1993). The former family of proteins span the plasma membrane four times whereas the later span the plasma membrane only once. The plaques formed by UPKs generates an asymmetric unit membrane (AUM), which in turn functions to provide permeability barrier and structural stability to the urothelium. The formation of plaques involves specific interaction between the UPKs. UPK1a interacts with UPK2 whereas UPK1b interacts with UPK3a (Wu et al., 1994, Hu et al., 2005, Tu et al., 2006, Tu et al., 2002).

The functional significance of UPKs vary across the species. In mammals, though their major function is important for development, differentiation and homeostasis of the urothelium arpenteret al., 2016), in the Xenopus oocytes UPK3a and UPK1b form a complex to mediate sperm-egg interaction and fertilization (Sakakibaraet al., 2005, Hasan et al., 2011, Mahbub Hasan et al., 2005). In the zebrafish, UPK3a related protein contributes to epithelial cell polarization and morphogenesis of pronephric tubules (Mahbub Hasan et al., 2005). A recent study indicates that the UPK2/3 proteins are related to phosphotyrosine phosphatases and thus may have a role in cellular signalling (Chicote et al., 2017). UPK knock out mice display renal failure and high rates of mortality (Kong et al., 2004, Hu et al., 2000). Mutations in the UPK genes resulted in renal hypo dysplasia, adysplasia and renal failure in humans (Jenkins et al., 2005, Schonfelderet al., 2006). Further, UPKs serve as anchors for Uropathogenic E. coli (UPEC) during infections (Wu et al., 2009). They allow binding of the type-1 fimbriae expressing UPEC strains and facilitate their binding to the urothelial surface and triggering a cascade of events that favor bacterial infection and migration not only in the bladder, but also in the upper urinary tract organs such as urethra and renal pelvic urothelia (Wu et al., 1996, Mulvey et al., 1998, Martinez et al., 2000). Altered levels of UPKs in urothelial carcinomas are considered as useful markers for the diagnosis,

detection and prediction of urothelial carcinomas (Wu et al., 2009, Huang et al., 2007, Zupancicet al., 2011).

Because of the tetraspanin nature of UPKs, they are predicted to play a key role in a variety of functions such as cell migration, immune signaling, membrane architecture and infection (Hemler 2003, Levy and Shoham 2005). The presence of UPKs in respiratory, ocular and other epithelial cell types indicate a wider role for these proteins beyond the urothelial functions (Adachi et al., 2000, Olsburghet al., 2003). The spatiotemporal expression of UPK3b in the epididymal and testicular sperm and ovarian follicles implicates them in gametogenesis and the development of gamete delivery organs (Kuriyamaet al., 2017). Recently it was demonstrated that mouse UPKs are expressed in nonurothelial lineages (Liao et al., 2018). All the known uroplakins were found to be expressed on the oocytes and associated with multivesicular bodies. Further, they were localized on the hook of the sperm. In vitro assays demonstrated reduced fertilization rates in mice eggs under conditions of knock down or antibody protection. Further, UPII/IIIa double knock out mice had smaller litter size suggesting are important in reproduction (Liao et al., 2018). Though UPKs have been well characterized in the urinary tract, their role in other organ systems are not well studied. The organs of male reproductive system has many anatomical similarities with the urinary system and both these are subjected to infections by UPEC, the bacterial species that expresses the type 1 fimbriae. In light of these similarities and the scarce of studies on the role of UPKs in other organ systems, the aim of this study was to analyze the expression pattern of UPk gene and their protein products in the male reproductive system of rat and to study their possible functional role during endotoxin challenge was analyzed. We observed that UPKs are abundantly expressed in the male reproductive tract of rat and their expression altered during endotoxin challenge both in vitro and in vivo.

1.2. Materials and methods

1.2.1. In silico analyses

The rat genome available at UCSC Genome Browser rat assembly RGSC6/rn6 was used to download all the known *Upk* gene sequences. Various properties of the genes and their proteins were predicted using *in silico* tools (Table 1). Based on the genome assemblies deposited in Ensembl, gene neighborhood analyses was carried out. Self-Optimized Prediction Method with

Alignment (SOPMA) was used to predict the percentage of all the secondary structures (α-helix, β- turn, extended strand and random coil) (Geourjon and Deléage 1995,Frishman and Argos 1995).

Table 1. Computational tools used for the in silico analyses.

Analysis	Tool used	Website
Sequence retrieval	UCSC Genome	https://genome.ucsc.edu/
	Browser assembly	
Similarity search	NCBI BLAST	http://blast.ncbi.nlm.nih.gov/Blast.cgi
Multiple sequence	T-COFFEE	http://tcoffee.crg.cat/
alignment		
Pairwise alignment	CLUSTALW	http://www.genome.jp/tools/clustalw/
General properties	EXPASY server	http://expasy.org/proteomics
Post translational	Sequence	http://www.bioinformatics.org/sms2/
modifications	manipulation suite	
Genomic	Ensembl	http://asia.ensembl.org/index.html
neighbourhood		
Secondary structure	SOPMA	https://npsa-
prediction		prabi.ibcp.fr/NPSA/npsa_sopma.html
Molecular modelling	GPCR-I-TASSER	https://zhanglab.ccmb.med.umich.edu/GPCR-
		I-TASSER/
Structure validation	PROCHECK	https://www.ebi.ac.uk/thornton-
		rv/software/PROCHECK/

1.2.2. Molecular modelling

Amino acid sequences of UPK1A, UPK1B, UPK2, UPK3A and UPK3B were obtained from NCBI database and submitted to the GPCR-ITASSER server (https://zhanglab.ccmb.med.umich.edu/GPCR-ITASSER/) in the FASTA format. The server usually employs a hybrid approach that integrates experimental mutagenesis data with ab initio transmembrane helix assembly simulations to construct the final 3Dmodel of target proteins (Zhang *et al.*, 2015). Models with high confidence score (C-score) were selected, which is typically

in the range of (-5 to 2), where a C-score of a higher value signifies a model with a higher confidence and vice-versa. Further, the structural validation was performed using PROCHECK (Laskowski *et al.*, 1993) and Ramachandran plot analysis (Ramachandran *et al.*, 1963). Models with 90% and above residues in the most favored or allowed or additionally allowed regions were considered for further analysis. PyMOL was used for visualization of the selected models, structural comparison and picture representation.

1.2.3. Animals and tissue collection

Wistar rats were purchased from National Center for Laboratory Animals, National Institute of Nutrition, Hyderabad, India. The rats were housed at animal facility maintained at ambient temperature (25 °C) with free access to food and water and were daily monitored for their well-being. For collection of tissues, the animals were terminated in a carbondioxide containing jar. All procedures involving animals were conducted using the guidelines for the care and use of laboratory animals to minimize suffering and this study was specifically approved by the Institutional Animal Ethics Committee of University of Hyderabad (IAEC/UH/151/2017/01/SY/P7).

To determine the overall tissue distribution patter of *Upks*, brain, heart, lungs, liver, kidney, spleen, ovary, uterus, cervix, bladder, caput (without the initial segment and corpus), cauda, testis, seminal vesicles and prostate were collected from adult Wistar rats (aged 90 days; n=5 each of male and female). Epididymides and testes obtained from 1- to 60-day old Wistar rats (n=5 for each age group) were used to study the developmental regulation. The tissues were placed in PBS, removed any excess fat and snap frozen in liquid nitrogen and stored at -80 °C until use. For collection of spermatozoa, cauda epididymides from adult Wistar rats were placed in PBS and squeezed gently with forceps. The spermatozoa were resuspended in PBS for further processing.

1.2.4. Polymerase chain reaction (PCR)

Total RNA isolated from different tissues using commercially available kits (Qiagen) was subjected to DNAse digestion to remove any contaminated DNA. 2 μg of total RNA was reverse transcribed and the expression of *Upks* in these tissues was carried out using exon spanning gene specific primers (Table 2) in a thermal cycler (cycling conditions: 94 °C for 1 min followed by 30 cycles at 94 °C for 30 sec, 58 °C for 30 sec and 72 °C for 30 sec, and with a final round of extension at 72 °C for 10 min). No reverse transcriptase and no template controls were included to confirm that the amplification is specific. The PCR amplicons were electrophoresed on 2% agarose gels and the images captured using a gel documentation system. The identity of the PCR amplicons was confirmed by sequencing though a commercial source (Bioserve Technologies Hyderabad, India). For quantification of gene expression, real time PCR was carried out using SYBR master mix kit (Applied Biosystems, Warrington, UK) in a thermal cycler (Applied Biosystems) using standard conditions.

Table 2. Gene specific primers used in this study.

Gene	Primer	Primer sequence (5'>3')	Length	GC	Tm	Amplicon
name	direction		(bp)	(%)	(°C)	size (bp)
Upk1a	Forward	CTCCTGCATCACATCCTACACC	22	55	56.7	187
	Reverse	GTAATTCACCCAGTCCATGG	20	50	51.8	
Upk1b	Forward	GCAGATGCTGATGAGGTATC	20	50	51.8	184
	Reverse	GTAGTCAGCATCGCTATTC	19	47	48.8	
Upk2	Forward	GAGCCAATGACAGCAAAGTG	20	50	59.4	153
	Reverse	ATTTGGTTCCTGGTGTGAGG	20	50	59.8	
Upk3a	Forward	GAAGCCTCTGTGCATGTTCG	20	55	53.8	203
	Reverse	CACAAGGGTCAGGTCAAAGG	21	57	56.3	
Upk3b	Forward	CTGAGTCTAGACCTGATTCCCTAC	24	50	57.4	198
	Reverse	CTTAGCAGCGGTCTGTGGGTTCTG	24	58	60.8	
Gapdh	Forward	CCAATGTATCCGTTGTGGATCT	22	45	60.1	157
	Reverse	GAGTTGCTGTTGAAGTCACAG	21	48	59.5	

1.2.5. Immunoblotting

Urinary bladder, caput, cauda, testes seminal vesicle and prostate tissues of 90day old Wistar rats were homogenated in RIPA buffer (25mM Tris-HCL, pH 7.6; 150mM NaCl; 1% each of NP-40, sodium deoxycholate and sodium dodecyl sulfate) and centrifuged at 12,857g for 10 min. The protein in the supernatant was quantified by Lowry's method. Total protein (100 µg) was electrophoresed on 15% SDS PAGE and transferred to nitrocellulose membrane (Hybond ECLTM; GE Healthcare, Little Chalfront UK) in a transfer buffer (25mM Tris; 192mM Glycine, 20% methanol (v/v); pH 8.3) with a constant voltage of 25 V for 16 h. 5% skim milk was used to block the membrane for 2 h at room temperature followed by probing (for 1 h) with primary antibody against the respective UPK protein. (UPK1A (Cat # ab183503) or UPK1B (Cat# ab185970) raised in rabbit (Abcam Biotechnology, Cambridge, UK) or UPK2 (Cat# sc-15178) raised in goat (Santa Cruz Biotechnology, Dallas, USA) or UPK3B (Cat# sc-165867) raised in goat (Santa Cruz). The blots were then washed thrice with TBS (Tris-buffered saline) and TBS-T (Tris-buffered saline, 0.1% Tween-20) followed by incubation with anti-rabbit secondary antibody (Cat# 65120) raised in goat or anti-goat secondary antibody (Cat# 611620) raised in rabbit (Invitrogen, Carlsbard, USA). After the incubation the membranes were washed thrice with TBS and TBS-T each for 10 min. At the end of washing, the membrane was developed using enhanced chemiluminescence kit (GE Healthcare, Buckinghamshire, UK).

1.2.6. Immunofluorescence

Epididymides (caput, cauda) and testes obtained from adult Wistar rats were fixed in Bouin's solution and 4% paraformaldehyde solution respectively and embedded in paraffin. Five micron sections (obtained by serial sectioning) placed on a glass slide were kept on a platform preheated to 60 °C for 5 min followed by washings with xylene, gradient alcohol (70–100%) and PBS for 10 min each. Slides were placed in a container filled with 10mM citrate buffer, pH 6.5 maintained at 60C for 12 min (for antigen retrieval) and subjected to permeabilization with PBS containing 1% triton X-100 (PBST) for 15 min. 10% goat serum was then added and incubated for 45 min to allow blocking. Sections were incubated for one hour with the respective primary antibody as indicated in the immunoblotting section above. The primary antibody was washed off thoroughly and the sections incubated with anti-rabbit (Cat# 656111; Invitrogen) or anti-goat (Cat# sc-2777; Santa Cruz) -FITC-labelled secondary antibody. Nucleus was stained with 4', 6-

diamidino-2-phenylindole (DAPI; Sigma Aldrich, St. Louis, USA) followed by addition of mounting medium and covered with cover slip. Multiple images (around 10) for each sample were recorded by taken in a trinocular fluorescence microscope with excitation and emission at 495 nm and 519 nm respectively. In the case of spermatozoa, smears on glass slides were prepared, air dried and fixed with 4% paraformaldehyde. They were then permeabilized with PBST, blocked with 10% goat serum and processed in a similar way as that of tissue sections.

To determine the specificity of antibodies, appropriate controls were included. Since UPKs are difficult to express using recombinant technology, pcDNA vector that encodes either one of the UPK proteins was transfected into HEK cells and incubated with primary and FITC labelled secondary antibody (positive control). Untransfected HEK cells incubated with primary and FITC-labelled secondary antibody served as negative control. Further, another negative control to test the nonspecific binding of secondary antibody was also included by incubating the tissue sections with only FITC-labelled antibody.

1.2.7. Treatment with LPS in vitro and in vivo

Rat testicular carcinoma cells (LC540) were obtained from National Centre for Cell Science, Pune, India and were maintained in EMEM medium (Sigma Aldrich, St. Louis, USA) containing 5% FCS at 37 °C. The rat caput immortalized cell lines (RCE) were a kind gift from Dr. Daniel Cyr, University of Quebec, Canada. They were maintained in DMEM medium containing 5% FBS at 32 °C. 1×10⁶ cells were plated in each well of a 24 well plate (Sigma Aldrich, St. Louis, USA) and allowed to adhere. Following replacement of culture medium, they were treated with 100 ng/ml E. coli lipopolysaccharide (LPS; Sigma Aldrich, St. Louis, USA) and incubated up to 24 h. The treatment dose and time points were chosen basing on our previous studies (Biswas and Yenugu 2013). Cells were collected at different time points (0, 3, 6 12 and 24 h after treatment) for RNA isolation. Since LPS was dissolved in phosphate buffered saline (PBS), pH 7.4, control cells were treated with PBS. The experiments were conducted three times in triplicates. To determine the effect of LPS on *Upk*gene expression, adult male Wistar rats (n=5 for each group) were treated intra peritoneally with 1 mg/kg body weight of E. coli LPS and sacrificed at different time points (0, 6, 12 and 24 h after LPS injection). The dosage of LPS was based on our previous studies (Biswas and Yenugu 2011). Control animals (n=5) received PBS equivalent to the volume that was used for LPS treatment. Caput, cauda, testis, seminal vesicle and prostate

were collected at each of these time points. They were then snap frozen in liquid nitrogen and stored at -80 °C until further use.

1.2.8. Statistical analyses

Statistical analyses were performed using one-way ANOVA (multiple comparison; Holm-Sidak test) and Student's t-test available in Sigma Plot software 12.5, Build 12.5.0.38 (SPSS Inc., Chicago, IL, USA). Values shown are Mean \pm S.D. *p < 0.05 denotes statistical significance.

1.3. Results

1.3.1. In silico analyses

To gain insight into the role of UPKs in the male reproductive system, we initiated in silico studies to gather first-hand information on the characteristic features of their genes and proteins. A thorough search in the rat genome indicated that the gene sequence of *Upk1a*, *Upk1b*, *Upk2* and Upk3a (NM 001108911.1, NM 001024253.1, NM 001109523.1 and NM 001130507.1 respectively) are already available in the GenBank. Besides these, alternate transcripts for *Upk1a* (XM 017589474.1; XM 008759176.2; XM 017589475.1) and *Upk1b* (XM 006248367.2; XM 006248368.3) were found to be predicted. Besides the reported Upk gene sequences, identification and characterization of the alternate transcripts is an important aspect in studying the functional characterization. Hence, using cDNA from rat urinary bladder, the amplicons corresponding to Upkla alternate transcript 2 (XM 008759176.2), Upklb alternate transcript 1 (XM 006248367.2) were amplified and sequenced. Rat *Upk3b* is not yet reported. Two alternate transcripts (XM 341056.8 and XM 006249208.3) are predicted. To characterize rat Upk3b further, we amplified XM 341056.8. The sequence obtained was submitted to GenBank and were assigned the accession numbers KU310911 (Upkla alternate transcript 2), KU310910 (Upklb alternate transcript 1) and KU310912.1 (*Upk3b* alternate transcript 1). For practical purposes, in this manuscript, we labelled the *Upk1a* alternate transcript 2, *Upk1b* alternate transcript 1 and *Upk3b* alternate transcript 1 as *Upk1a*, *Upk1b* and *Upk3b* respectively. We observed that *Upk3b* gene was located at chromosome 12q.12 (Figure. 1), whereas Upk1a, Upk1b, Upk2 and Upk3a genes were localized to the chromosomal positions 1q21, 11q21, 8q22 and 7q34 respectively (as per the information available at NCBI). The coding region of the mRNA and the corresponding amino acid sequence of *Upk1a*, *Upk1b* and *Upk3b* characterized in this study are shown in Figures.

2 and 3. The general characteristic features of all the rat *Upk* genes and their protein products were compiled based on the information available in the rat genome at NCBI and are given in Table 3.

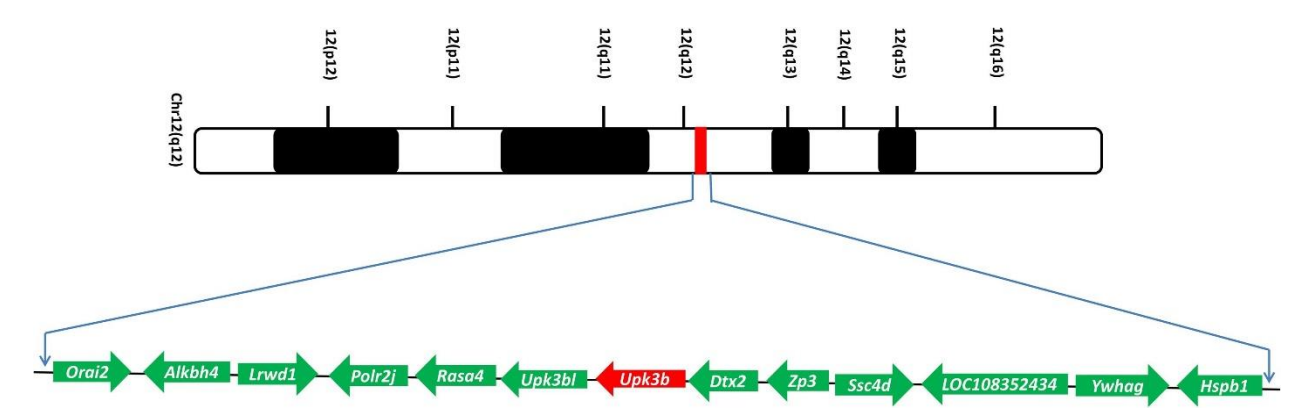


Figure 1. Genomic localization of rat Upk3b gene. Arrows indicate direction of transcription. Positions were taken from UCSC Genome Browser rat assembly RGSC6/rn6. Distance between genes is not to scale. Rat Upk3b sequences was submitted to GenBank and assigned the accession number KU310912.1. Upk3b gene is indicated in red color for better representation.

Upkla (alternate transcript 2)

atggcttctacagcgacagagggagagagagggtctcctgtggftgtggggctgctggtc EGEKGSPVVVGL gtgggcaacatcattattctgctgtcaggcctggccctgtttgcggagacagtgtgggtg SGLAL GNIIIL ${\tt acggctgaccagtaccgtgtgtacccactgatgggcgtctcaggcaaggacgacgtcttc}$ gccggtgcctggatcgccatcttctgcggcttctccttcttcgtggtggccagctttggt AGAWIAIFC G F SFF ASCI TSY gtgtccaacccatccctgataaccaagcaaatgttgaccttctacagtgcggacaccgac KOML cagggccaagagctaacccgcctctgggaccggatcatgattgagcaagagtgctgcggc I M RLWDR acatctggccccatggactgggtgaattacacatcagccttcagggcagccaccccggaa TSGPMDWVNYTSAF gaagatggctgccgagtaggccacatggactacctgtttaccaagggttgcttcgaacac RVGHMDYL atcagccatgccattgacagctacacgtggggcatatcgtggtttggctttgcaatcttg ISHAIDSYTWGISWF atgtggactctccctgtgatgatgatagccatgtatttctacaccattctctga VMMIAM

Upk1b (alternate transcript 1)

 $\verb|atgctgtggagtgagtctgtgcagcatcaggaagaagacggcagaagaagaccaggcagcca|\\$ SVQHQEETAEE KMAKDDST $at \verb|cttcttgtatctgaccaacacagcctttatccacttcttgaagccaccaacaacgat|$ VSDQHSLYPL gttctagccatagtaggaattatgaagtccaacaggaaaatcctcttggcgtacttcatc V L A T V G T M K S N R K T L L atgatgtttatagtgtatggttttgaagtggcgtcttgcatcacagcagccacacaacga gactttttcacgaccaacctcttcctgaagcagatgctgatgaggtatcaaaacaacagc TNLFLKQMLMRYQNNS cccccaaccaatgacgacaaatggaagaacagctatgtcaccaagacctgggataggctc P P T N D D K W K N S Y V T K T W D R L $\verb|atgctgcaggaccactgctgtggggtaaacggtccgtcagactggcagaaatacacctct|$ M L O D H C C G V N G P S D W O K Y gccttccgagtggagaatagcgatgctgactacccctggcctcggcagtgctgtgtcatg NSDADYPWPR LOEP LNLDACKLGV cacagtcagggctgttatgagctaatctctggaccaatggatcggcacgcctggggagtt LISGPMDR $\verb|gcctggtttggatttgctattctctgctggaccttctgggttctcctgggcaccatgttc|\\$ AWFGFAILCWTFWVLLGTM tactggagcagaattgagtactaa

Figure 2. Rat Upk1a and Upk1b mRNA coding region and the predicted protein sequence. Amino acids are indicated in single letters. The rat Upk1a and Upk1b cDNA sequence was submitted to Genbank and was assigned the accession number KU310911 and KU310910 respectively.

Upk3b (alternate transcript 1)

atggagttcacccggatgcggcctcacccttggcccctgcttctcccggtacttatgtggM E F T R M R P H P W P L L L P V L M W $\verb|cttccccaaagcctgagtctagacctgattccctacacgccgcagataactgccagggac||$ LPQSLSLDLIPYTPQITARD $\verb|ctgggagggaaggtcacagccactacgttctctctggagcagcctcggtgcgtctttgat|$ LGGKVTATTFSLEQPRCVFD D F Q N P Q T A A K I P T F P Q L L T D ggccactatatgacattacccctgtccctggatcagctgccatgtgaggacctgaccggt G H Y M T L P L S L D Q L P C E D L T G ggcagtggaggtgttcaggtgcttcgggtgggcaatgacttcggctgttaccagcgaccc G S G G V Q V L R V G N D F G C Y Q R P tattg caac gctccctccccag ccag ggcccttac ag tg tg aa gttcctt gt aa tg gattact gas to be a simple of the control of the controY C N A P L P S Q G P Y S V K F L V M D $\verb|gctggtggcccacccaaggctgaaacgaagtggtctaatcccattttctccaccaaggg|$ AGGPPKAETKWSNPIFLHQG a aga acccca acgccatt gacacat ggcct ggtcggcggagcggctgt at gatcgtcat acgccat acgccatKNPNAIDTWPGRRSGCMIVI acttctatccttccggtcctggccggcctcttgctcctggctttcctggcagcctccactT S I L P V L A G L L L A F L A A S T acgcgtttctccagcctgtggtggcctgaggaagcccctgagcagctgcggattggctccTRFSSLWWPEEAPEQLRIGS $\verb|ttcatgggaaaacgttacatgactcaccatatccccccagcgaggctgccacactgccg|$ F M G K R Y M T H H I P P S E A A T L P $\verb|gtgggctgcgagcctggacccccttcccagtctcagcccatag|$ V G C E P G L D P L P S L S P

Figure 3. Rat Upk3b mRNA coding region and the predicted protein sequence. Amino acids are indicated in single letters. The rat Upk3b cDNA sequence was submitted to Genbank and was assigned the accession number KU310912.1.

Table 3. General predicted and deduced features of rat uroplakin genes and their encoded proteins

Attribute		Upk1a	Upk1b	Upk2	Upk3a	Upk3b
Chromosome		1q21	11q21	8q22	7q34	12q12
Gene accession number		NC_005100.4	NC_005110.4	NC_005107.4	NC_005106.4	NC_005111.4
Gene length (bp)		282763074	90463843	133307652	145729302	52716770
Total nu	mber of exons	6	8	5	6	7
mRNA a	ccession number	KU310911	KU310910	NM_0011095	NM_0011305	KU310912.1
				23.1	07.1	
Length o	of mRNA (nt)	1498	1980	822	1026	1158
Coding s	sequence (CDS)	215988	1811044	61615	29892	1821009
Protein a	ccession number	AMB20857.1	AMB20856.1	NP_0011029	NP_0011239	AMB43178
				93.1	79.1	
Number	of amino acids	257	287	184	287	275
Molecula	ar Weight (kDa)	28.90	33.10	19.5	30.19	30.22
Localiza	tion	transmembra	transmembra	transmembra	transmembra	transmembran
		ne	ne	ne	ne	e
Isoelectr	ic point (pI)	5.14	5.22	10.28	5.54	6.05
O-glycos	sylation sites	171,172,178,	160. 200, 207	NIL	32,80,81,86,8	254,258
		193			7,88,92,97,18	
					8,192,268	
GRAVY	index	0.500	0.0700	0.519	0.071	-0.064
Phosph	Serine	12,54,115,16	33, 65, 69,	3,31,33,37,43	27,56,69,72,7	24,51,64,65,1
orylati		2, 227	110, 160,	,68,88,102,11	6,80,86,115,1	09,122,148,15
on sites			171, 200,	8,126,129,13	83,192,205,2	3,194,214,269
			207, 242, 283	0,164	17,239,240,2	
					48,265,268,2	
					82,	
	Threonine	4, 6, 133,	13, 34, 138,	4,9,97,110,11	38,39,87,88,9	37,87,99,169,
		139, 178, 214	176, 278	3,133,	2,108,123,16	243
				137,160	0,180,188,24	
					4,245,251	
	Tyrosine	119, 228	172, 198,	115,116	100,132,166,	103,141,241,
			211, 239		266,	
Signal peptide		No	No	Yes (1-25)	Yes (1-18)	Yes (1-26)
(amino acid range)						
Disulfide	bonds	69-86, 107-	37-133, 52-	51-80	12–142, 15–	57 - 136, 115
		158, 110-189,	217, 60-218,		47, 110-152	- 142, 196 -
		159-217, 192-	95-232, 98-			263
		204	186. 187-245			

Depending on their organization in the plasma membrane, UPK1a and UPK1b belong to tetraspanin family, whereas the other UPKs are included in the monospanin family. Analyzing sequence similarity among a group of proteins provides information on the possible functional roles. Such an analyses is lacking for the rat UPK proteins. To determine the similarity among the rat UPKs, their sequences were aligned using T-coffee program (Figures. 4 and 5). Among UPK1A and UPK1B, the sequence similarity was about 53% (Table 4). The similarity score of UPK2 with UPK3A and UPK3B was 23 and 24 respectively. UPK3A and UPK3B had a similarity score of 39 (Table 4). The rat, mouse and human UPK sequences were aligned to determine the homology of

each of the UPK among these species (Figures 6). Rat UPK1A displayed 98 and 70% similarity with the mouse and human counterparts respectively (Table 4). Similarly, UPK1B, UPK2 and UPK3A and UPK3B displayed a very high similarity with the mouse and human counterparts. (Table 4).

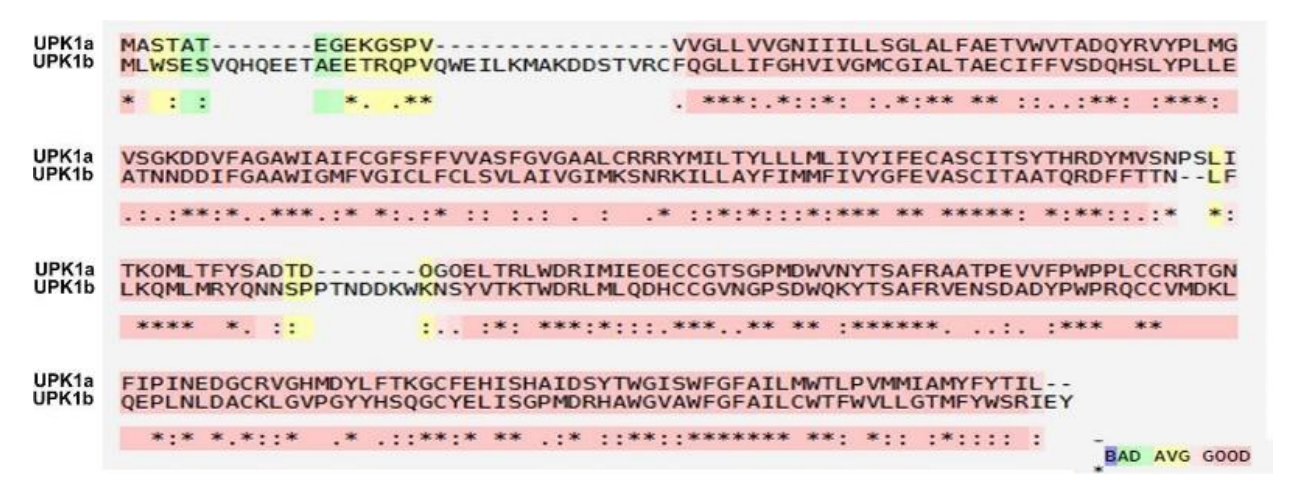


Figure 4. Multiple sequence alignment of UPK1a and UPK1b proteins. Alignment of rat UPK1a and UPK1b protein sequences. Identical and similar amino acids are indicated by (*) and (: and.) respectively. Color coding indicates agreement between all the various pairwise structural alignments. Pink brick regions are in perfect agreement across all the methods, while blue regions have a very poor agreement.

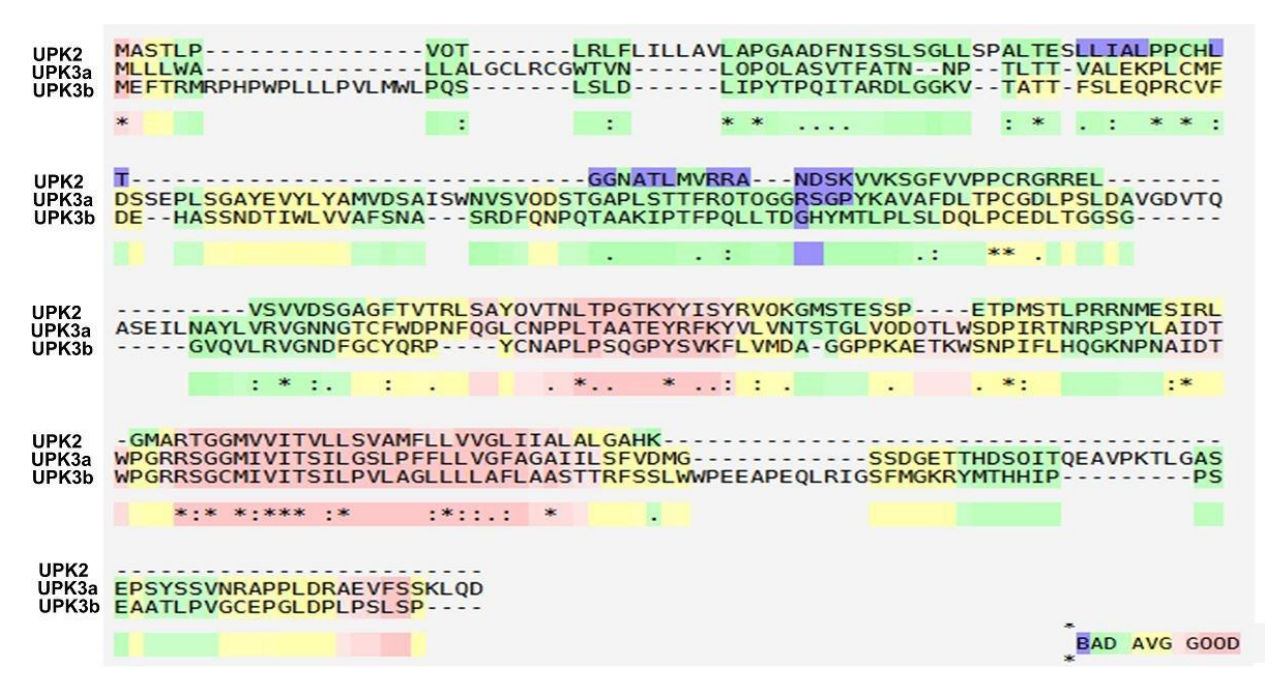
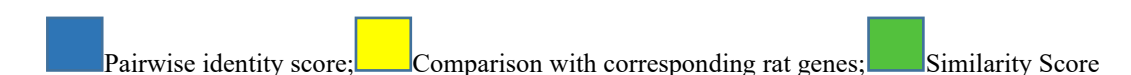


Figure 5. Multiple sequence alignment of UPK2, UPK3a and UPK3b proteins. Alignment of rat UPK2 and UPK3a and UPK3b protein sequences. Identical and similar amino acids are indicated by (*) and (: and .) respectively. Color coding indicates agreement between all the various pairwise structural alignments. Pink brick regions are in perfect agreement across all the methods, while blue regions have a very poor agreement.

Table 4. Pairwise identity and similarity analysis of rat, mouse and human uroplakin proteins

	Rat			Mouse				Human							
	UPK1a	UPK1b	UPK2	UPK3a	UPK3b	UPK1a	UPK1b	UPK2	UPK3a	UPK3b	UPK1a	UPK1b	UPK2	UPK3a	UPK3b
UPK1a	100	53	03	15	07	98	56	03	16	08	70	43	20	04	03
UPK1b	35	100	06	18	03	36	88	10	15	02	30	80	10	14	02
UPK2	03	04	100	23	24	02	05	94	26	24	13	06	87	25	17
UPK3a	08	12	16	100	39	10	10	18	95	39	02	08	18	84	28
UPK3b	03	02	14	28	100	04	02	15	27	92	02	01	17	21	82



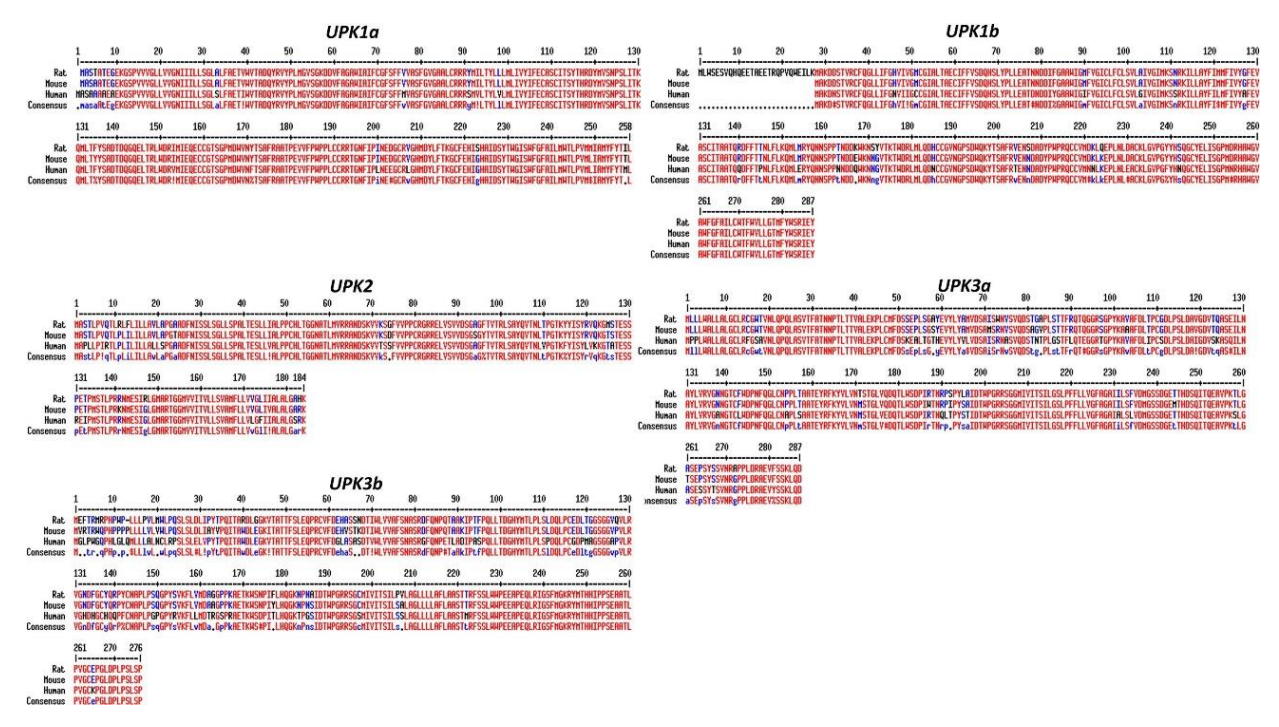


Figure 6. Alignment of rat, mouse and human UPK proteins. Amino acids indicated in blue indicate a match among two of the three species, whereas those indicated in black indicate a mismatch in one of the species or in all three species. A dot in the consensus sequence indicates a mismatch (amino acids in black color font) in all the three species.

Gene expression is influenced by the nature of genes present in its vicinity and this can be determined by neighbourhood analyses. *Upk* genes are located on different chromosomes and such an analyses to determine the nature of genes that flank them in the rat and the comparison with the mouse and human genomes is not reported. We show *that Psenen*, *U2af114*, *Igflr1*, *Zptb32*, *Cox6b1* and *Rbm42* genes were found to be commonly present in the rat, mouse and human chromosomal regions where *Upk1a* was located (Figure 7). In the case of *Upk1b*, the *genes Igs11*, *B4galt4*, *Tmem39a and Poglut1* were present in the neighbourhood region in all the three species (Figure 7). Genes that were commonly present in the neighbourhood of *Upk2* were *S1c37a4*, *Trappc4*, *Bcl91 and Cxcr5* (Figure 8). *Smc1b*, *Ribc2*, *Fam118a and Fbln1* were the genes commonly present in the *Upk3a* neighbourhood in all the three species (Figure 8). Genes that were commonly present in the neighbourhood of *Upk3b* were *Dtx2*, *Zp3*, *Ssc4d*, *Ywhag* and *Hspb1* (Figure 8).

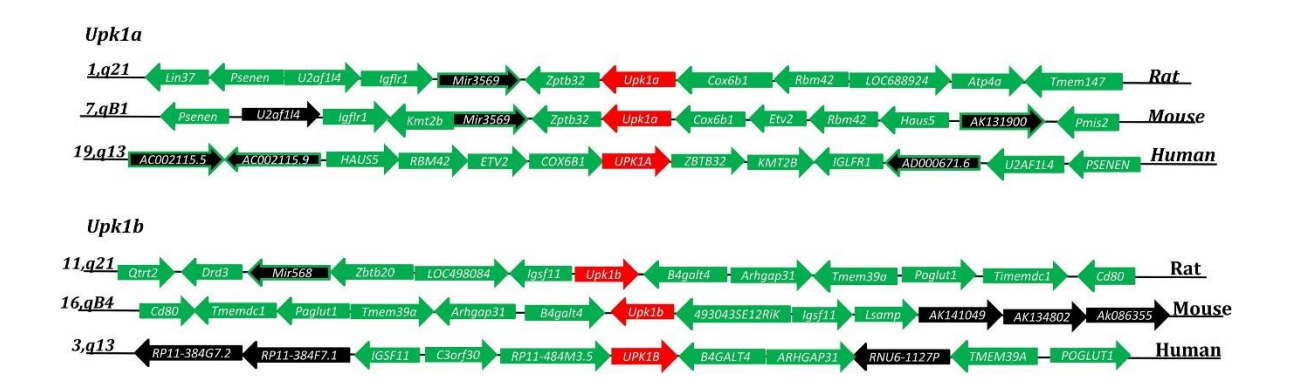


Figure 7. Genomic neighborhood analysis of rat, mouse and human Upkla and UPklb genes. Green arrows with names represent the genes and directions of the arrow represent the direction of sense strand. Red arrow indicates Upk gene. Black arrows indicate noncoding/pseudo/hypothetical genes. Alpha numericals on the left of each row indicates chromosomal region. The order of chromosomal regions is rat, mouse and human.

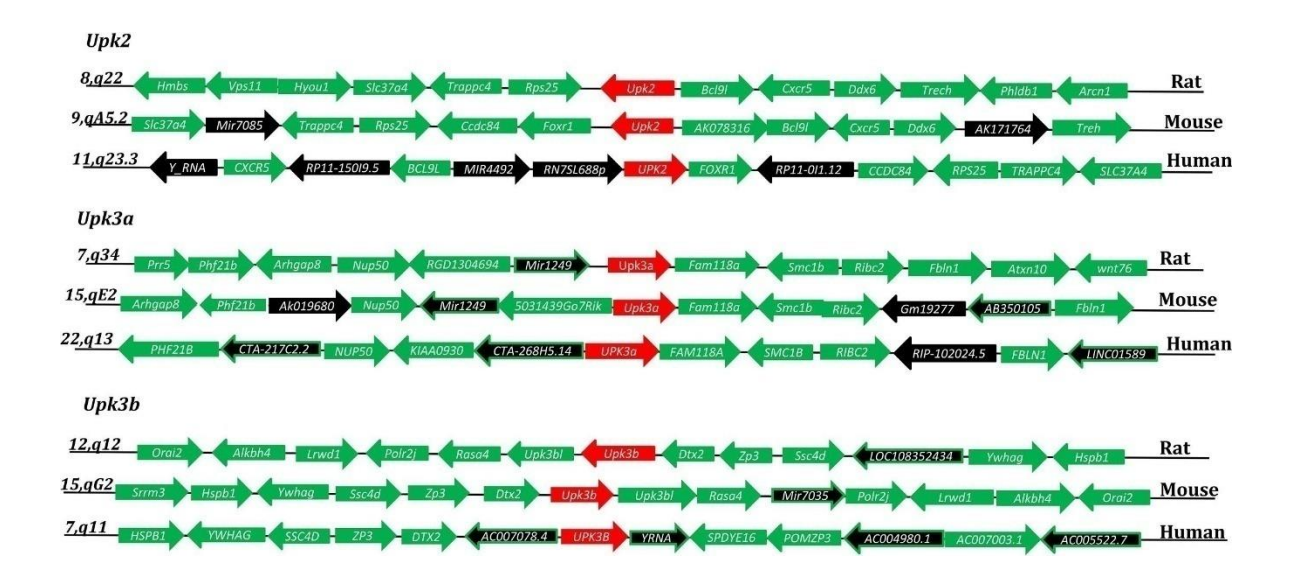


Figure 8. Genomic neighborhood analysis of rat, mouse and human Upk2, Upk3a and Upk3b genes. Green arrows with names represent the genes and directions of the arrow represent the direction of sense strand. Red arrow indicates Upk gene. Black arrows indicate noncoding/pseudo/hypothetical genes. Alpha numericals on the left of each row indicates chromosomal region. The order of chromosomal regions is rat, mouse and human.

Though the three dimensional structures for UPKs in some species are reported, such an attempt was not made for rat UPKs. Because of the differences in the amino acid sequence homology of these proteins among the species, the three dimensional structure of rat UPKs may

vary. Hence, to gain further insight into the structural aspects of UPKs, their three dimensional structure was obtained (Figure 9). The templates used for generating the three dimensional structures of UPKs varied significantly (Table 5). Ramachandran plots generated for each of the UPKs indicated that majority of the amino acids are in the allowed regions and the structures predicted are valid (Table 5). UPK1a and UPK1b that belong to tetraspanin family display more of alpha-helix, whereas UPK2, UPK3a and UPK3b that belong to monospanin family tend to have more random coil (Figure 9). To correlate the observations made in the three dimensional structure, the percentage of different structural features were determined by Self-Optimized Prediction Method with Alignment (SOPMA). UPK1a was found to have 40.07, 23.34, 8.17 and 28.40% of alpha-helix, extended strand, beta-turn and random coil respectively (Table 6). UPK2 also showed such a similar distribution wherein the percentage of alpha-helix, extended strand, beta-turn and random coil were 42.85, 18.11, 7.31 and 31.70 respectively (Table 6). It appears that UPK1a and UPK1b have higher content of alpha-helix followed by random coil, extended strand and betaturn. In UPK2, the percentage of alpha-helix, extended strand, beta-helix and random coil content was 32.06, 22.28, 10.32 and 35.32 (Table 6). UPK3a is predicted to have 19.51, 26.82, 10.45 and 43.20 percent of alpha-helix, extended strand, beta-helix and random coil (Table 6). UPK3b contains 12.72, 22.18, 5.45 and 59.63 percentage of alpha-helix, extended strand, beta-helix and random coil respectively (Table 6). From these analyses it appears that the percentage of random coil was higher followed by extended strand, alpha helix and beta-turn in the case of members belonging to monospanin family (UPK2, UPK3a and UPK3b).

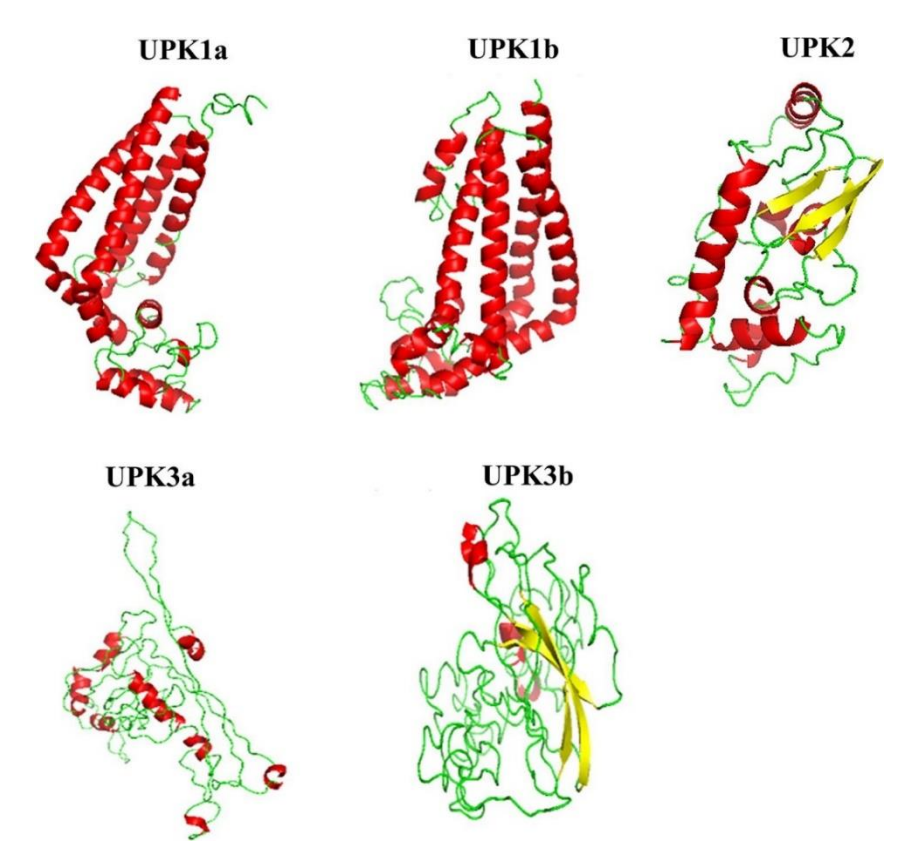


Figure 9. Three dimensional structure of rat UPK proteins. Amino acid sequences of UPK1a, UPK1b, UPK2, UPK3a and UPK3b were submitted to the GPCR-I-TASSER server and models with high confidence score (C-score; (-5 to 2) were selected. Structural validation was performed using PROCHECK and Ramachandran plot analysis and models with 90% and above residues in the most favored or allowed or additionally allowed regions were considered for further analysis. PyMOL based visualization showing β - sheets in yellow, helices in red and loop regions in green.

Table 5. Ramachandran plot analysis for the 3D structure of rat uroplakins.

Name of the	UPK1a	UPK1b	UPK2	UPK3a	UPK3b
model					
Crystal ID of	CD81, 3RKO	CD81, 3QNQ	5L75, 5FMV,	4BML, 5E7L,	5E7L, 5C2V,
template used for			5L75, 5C17,	4NL6, 2EDY,	5E52, 4LDU,
generating 3D			4I18, 5N8P,	5GAO, 4MGU,	4LDV, 2EDY,
model			2PFF, 4KG7,	4LDU, 2EYZ,	2EYZ, 4NL6,
			2COV	1TIA, 3L5H	1TIA
Residues in most	174, 77.3%	183, 71.2%	98, 62.8%	129, 53.1%	92, 41.4%
favored regions,					
%					
Residues in	39, 17.3%	53, 20.6%	51, 32.7%	95, 39.1%	83, 37.4%
additional allowed					
regions, %					
Residues in	7, 3.1%	15, 5.8%	3, 1.9%	10, 4.1%	28, 12.6%
generously		•			•
allowed regions,					
%					
Residues in	5, 2.2%	6, 2.3%	4, 2.6%	9, 3.7%	19, 8.6%
disallowed	,	,	,	,	,
regions, %					
Number of non-	225	257	156	243	222
glycine and non-					
proline residues					
Number of end-	2	2	2	2	1
residues (excl. Gly					
and Pro)					
Number of	20	18	15	22	20
glycine residues	-		-		
	10	10	1.1	20	22
Number of proline	10	10	11	20	32
residues					
Total number of	257	287	184	287	275
residues					

Table 6. Secondary structure prediction by Self-Optimized Prediction Method with Alignment (SOPMA)

Protein name	Alpha helix (%)	Extended strand (%)	Beta turn (%)	Random coil (%)
UPK1a	40.07	23.34	8.17	28.40
UPK1b	42.85	18.11	7.31	31.70
UPK2	32.06	22.28	10.32	35.32
UPK3a	19.51	26.82	10.45	43.20
UPK3b	12.72	22.18	5.45	59.63

1.3.2. Uroplakin expression in the rat

Analyzing *Upk* gene and protein expression pattern in the male reproductive tract and their possible contribution to this organ system has gained importance in the recent past. In this study, to gain an in depth understanding of *Upk* expression in the male reproductive system of rats, their mRNA expression pattern was analyzed using PCR. *Upk1a* and *Upk1b* were expressed in the caput, cauda, testis, seminal vesicle and prostate (Figure 10A). *Upk2* was predominantly expressed in the testis with lower level of expression in the caput, cauda, seminal vesicle and prostate. *Upk3a* mRNA was not detected in all the male reproductive tract tissues. *Upk3b* expression was evident in the caput, cauda, testis and seminal vesicle with no expression in the prostate (Figure 10A). All *Upks* were expressed abundantly in the bladder, which was used as a positive control. Western blotting indicated the expression of UPK1a, UPK1b and UPK2 and UPK3b proteins in the caput, cauda, testis, seminal vesicle and prostate (Figure 10B).

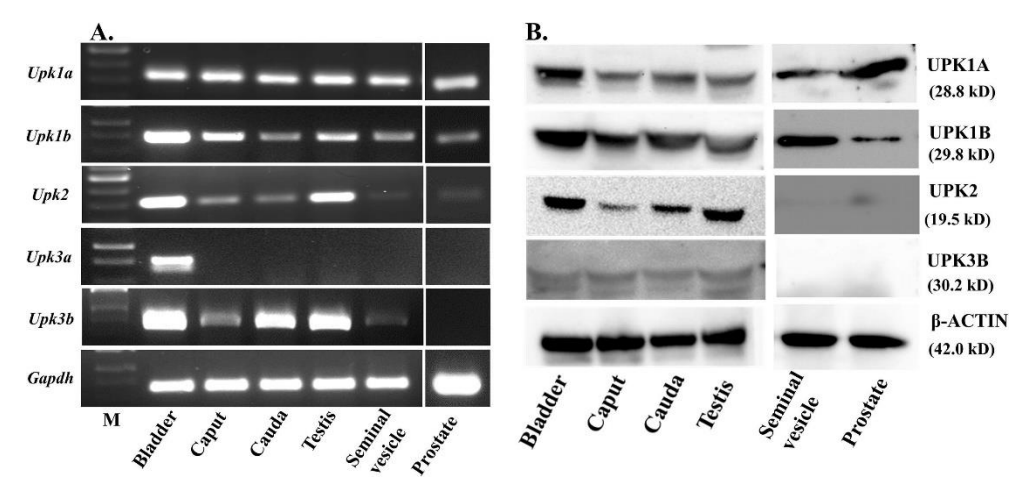


Figure 10. Expression of Upk mRNA and protein in the rat male reproductive tissues. (A) Upk mRNA expression. Total RNA isolated from bladder, caput, cauda, testis, seminal vesicle and prostate was reverse transcribed and the cDNA obtained was used as template for amplifying the Upk1a, Upk1b, Upk2, Upk3a and Upk3b by gene specific PCR. Gapdh expression was analyzed to serve as internal control. (B) UPK protein expression. 100 µg of the protein obtained from bladder, caput, cauda and testis homogenates were electrophoresed on 15% SDS-PAG and transferred to nitrocellulose membrane. The immunoblots were probed with UPK1a or UPK1b antibody (raised in rabbit) or UPK2 antibody (raised in goat) or UPK3b antibody (raised in goat); followed by incubation with labelled anti-rabbit secondary antibody raised in goat or anti-goat secondary antibody raised in rabbit.

To further confirm whether *Upks* are male reproductive specific, their expression was analyzed in other tissues of male rats and in the reproductive tissues of female rats. *Upk1a*, *Upk1b*, *Upk2* and *Upk3b* were found to be expressed in all the tissues analyzed, whereas *Upk3a* was restricted to lung, kidney and cervix (Figure 11).

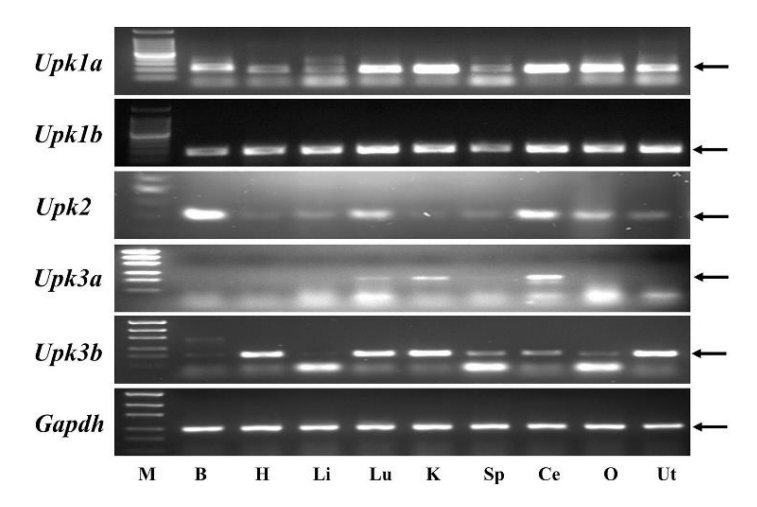


Figure 11. Tissue distribution of Upks. Total RNA isolated from Brain (B), Heart (H), Lungs (Lu), Liver (Li), Kidney (K), Spleen (Sp), Cervix (Ce), Ovary (O) and Uterus (Ut) was reverse transcribed and the cDNA obtained was used as template for amplifying the Upkla, Upklb, Upk2, Upk3a and Upk3b by gene specific PCR. Gapdh expression was analyzed to serve as internal control. M indicates DNA ladder. Arrow indicates the amplicon of interest.

Since gene regulation in the testis and epididymis is highly regulated by androgens during development, Upk mRNA expression pattern in the epididymis and testis during different stages of development was analyzed (Figure 12). In the epididymis, Upk1a and Upk2 expression was evident from 20 days of postnatal development, where as Upk1b and Upk3b were detected in all the stages. Upk3a was not detected at all the stages analyzed (Figure 12). In the testis, except for Upk3a, other Upks were found to be expressed at all the developmental stages analyzed (Figure 12).

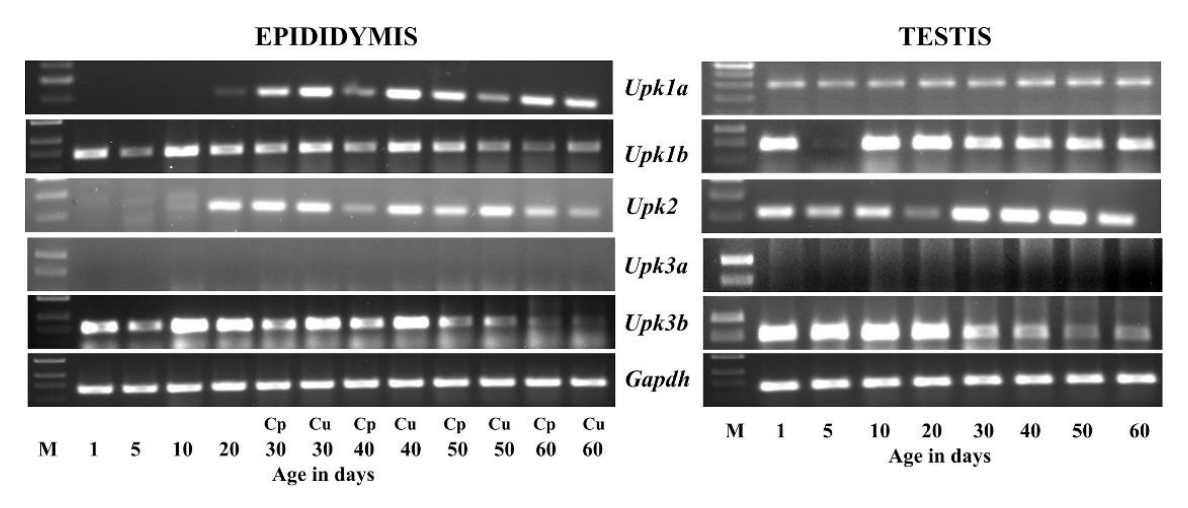


Figure 12. Developmental regulation of Upk genes in epididymis and testes. RNA from epididymis and testes collected from 1, 5, 10, 20, 30, 40, 50 and 60 day old rats was reverse transcribed and the cDNA obtained was used as template for amplifying the Upk1a, Upk1b, Upk2, Upk3a and Upk3b by gene specific PCR. Gapdh expression was analyzed to serve as internal control. Cp- caput, Cu-cauda.

To determine if UPKs may have a role in male reproductive physiology, sperm function and fertilization, we examined their localization in the caput, cauda, testis and male gametes by immunofluorescence microscopy using a trinocular fluorescent microscope. Prior to the localization analyses in the tissues, the specificity of the antibodies were tested by including positive and negative controls. We put our best efforts for recombinant expression of UPK proteins to be used in peptide controls. However, we met with little success. Alternatively, HEK cells were transfected with pcDNA vector encoding either one of the UPK proteins and incubated with the respective primary and secondary antibodies (positive control). Further, untransfected HEK cells were incubated with primary and secondary antibody served as negative controls. HEK cells transfected with the vector encoding the UPK protein showed abundant fluorescence (Figure 13), whereas such a fluorescence was not observed in untransfected cells (Figure 14). Further, we also checked for the non-specific binding of the secondary antibody by incubating the tissue sections only with FITC-labelled secondary antibody. The negative controls (incubated only with the secondary antibody) did not shown any fluorescence (Figure 15). These observations suggest that the antibodies used were specific to the respective UPK protein.

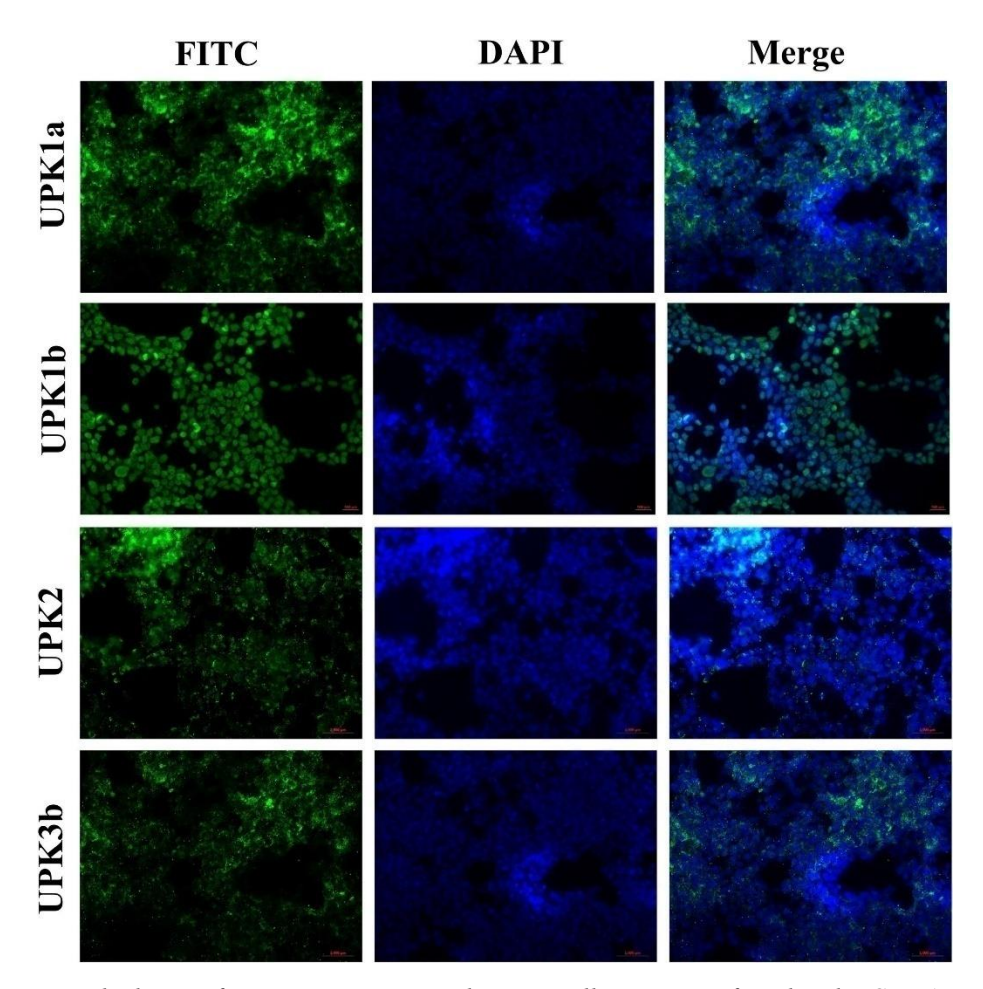


Figure 13. UPK antibody specificity in positive controls. HEK cells were transfected with pCDNA vector encoding UPK1a or UPK1b or UPK2 or UPK3b. 24 hours after transfection, the cells were fixed on glass cover slips. They were incubated with UPK1a or UPK1b antibody (raised in rabbit) or UPK2 antibody (raised in goat) or UPK3b antibody (raised in goat); followed by incubation with FITC labelled anti-rabbit secondary antibody raised in goat or anti-goat secondary antibody raised in rabbit. Nucleus was stained with 4', 6-diamidino-2-phenylindole and images taken using fluorescence microscope with excitation and emission at 495 nm and 519 nm respectively.

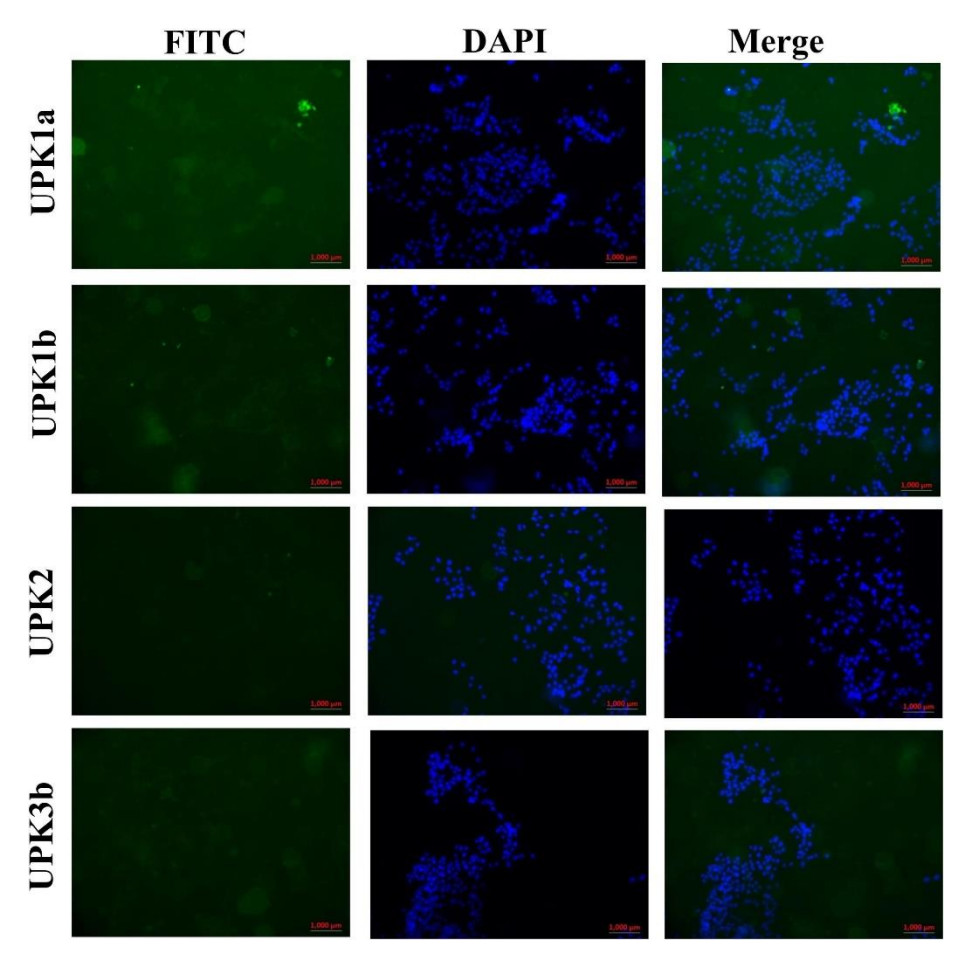


Figure 14. UPK antibody specificity in negative controls. Untransfected HEK cells were incubated with UPK1a or UPK1b antibody (raised in rabbit) or UPK2 antibody (raised in goat) or UPK3b antibody (raised in goat); followed by incubation with FITC labelled anti-rabbit secondary antibody raised in goat or anti-goat secondary antibody raised in rabbit. Nucleus was stained with 4', 6-diamidino-2-phenylindole and images taken using fluorescence microscope with excitation and emission at 495 nm and 519 nm respectively.

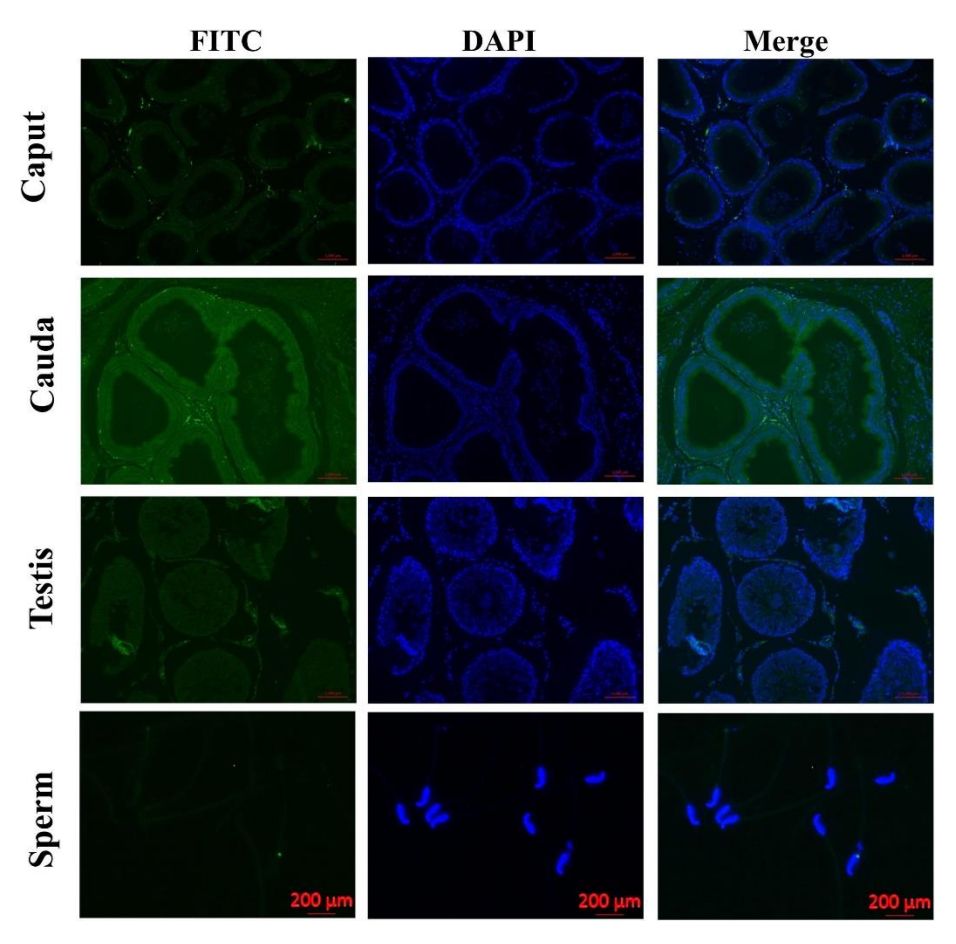


Figure 15. Immunofluorescence detection in negative control. Testis, Caput, Cauda and Spermatozoa were incubated with FITC labelled anti-rabbit secondary antibody raised in goat or anti-goat secondary antibody raised in rabbit. Nucleus was stained with 4', 6-diamidino-2-phenylindole and images taken using fluorescence microscope with excitation and emission at 495 nm and 519 nm respectively.

UPK1a was localized in majority of the cells that are closer to the basement in the caput and cauda. In the testis, the localization was observed throughout the seminiferous tubules and also in the interstitial cells. Further, it was localized in all the regions of the sperm (Figure 16). Similar staining pattern was observed for UPK1b (Figure 17), UPK2 (Figure 18) and UPK3b (Figure 19). In the sperm, all the UPKs were localized in the head, mid piece and tail regions (Figures 16–19).

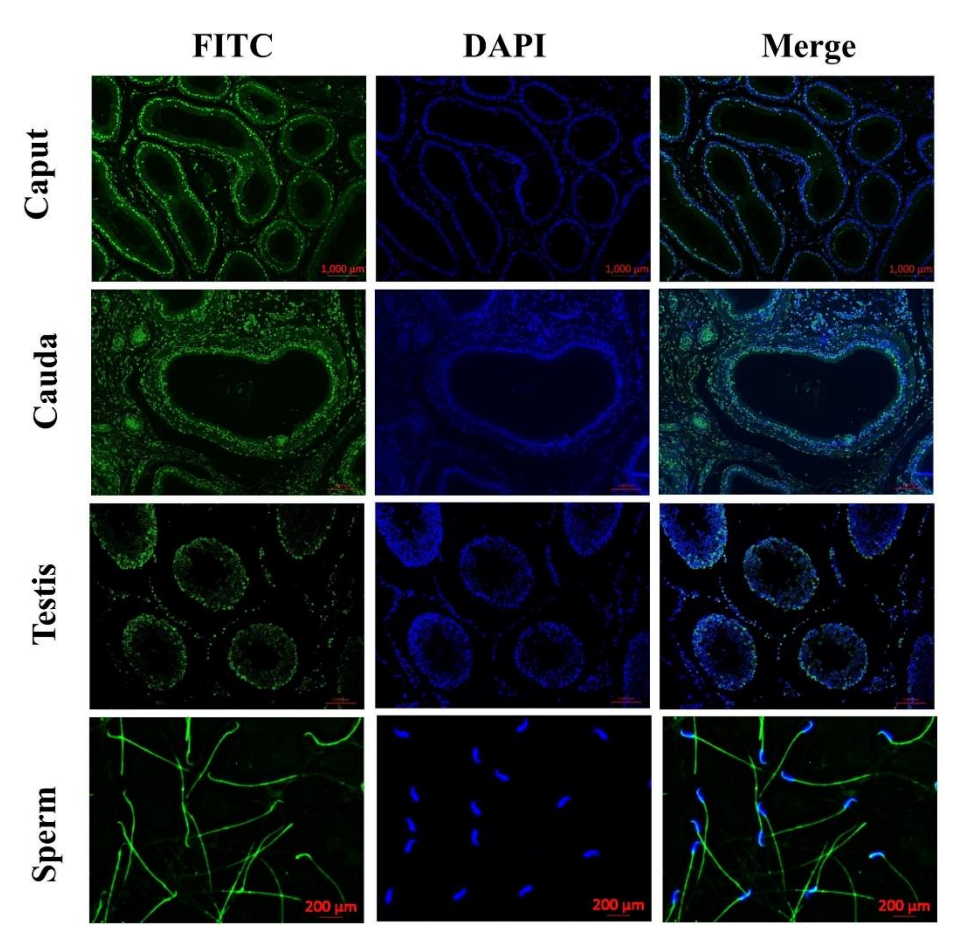


Figure 16. Immunolocalization of UPK1a. Serial sections (5 µm thickness) of the rat testes and epididymides and smears of spermatozoa were fixed and incubated for one hour with UPK1a antibody (raised in rabbit) followed by incubation with FITC labelled anti-rabbit secondary antibody raised in goat. Nucleus was stained with 4', 6-diamidino-2-phenylindole and images taken using fluorescence microscope with excitation and emission at 495 nm and 519 nm respectively. Magnification: 10X.

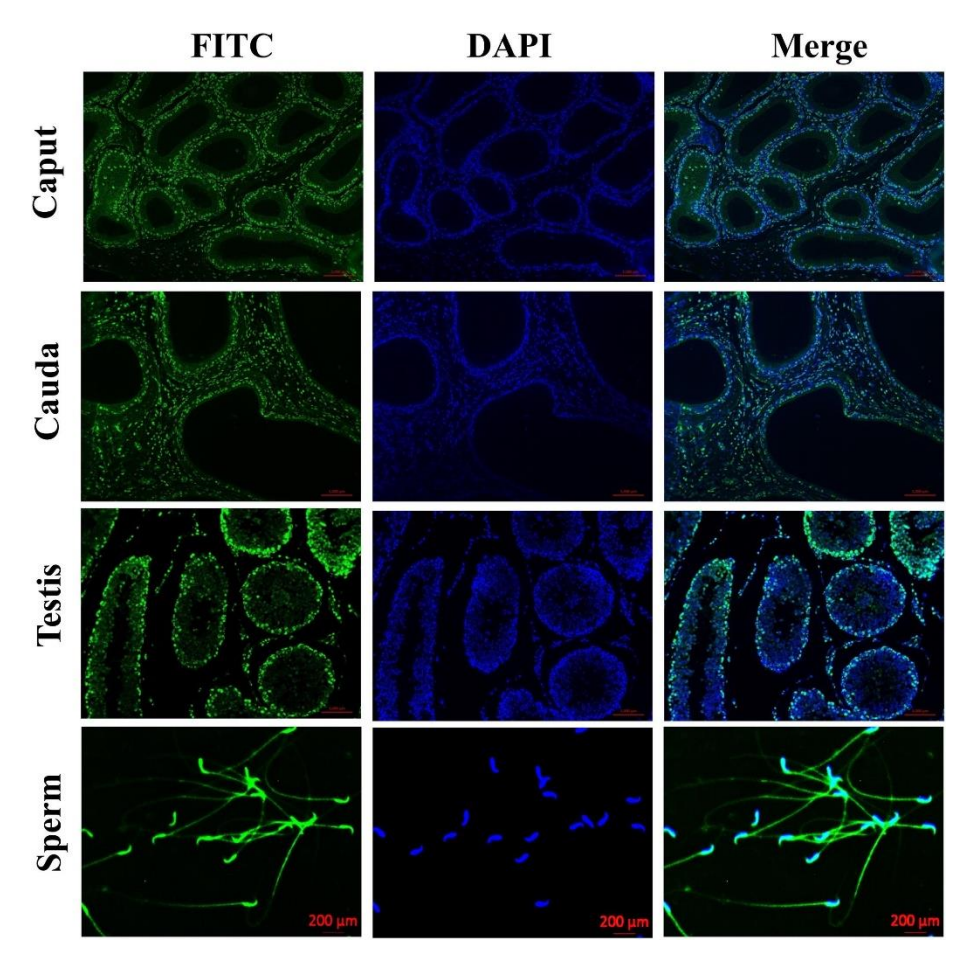


Figure 17. Immunolocalization of UPK1b. Serial sections (5 µm thickness) of the rat testes and epididymides and smears of spermatozoa were fixed and incubated for one hour with UPK1b antibody (raised in rabbit) followed by incubation with FITC labelled anti-rabbit secondary antibody raised in goat. Nucleus was stained with 4', 6-diamidino-2-phenylindole and images taken using fluorescence microscope with excitation and emission at 495 nm and 519 nm respectively. Magnification: 10X.

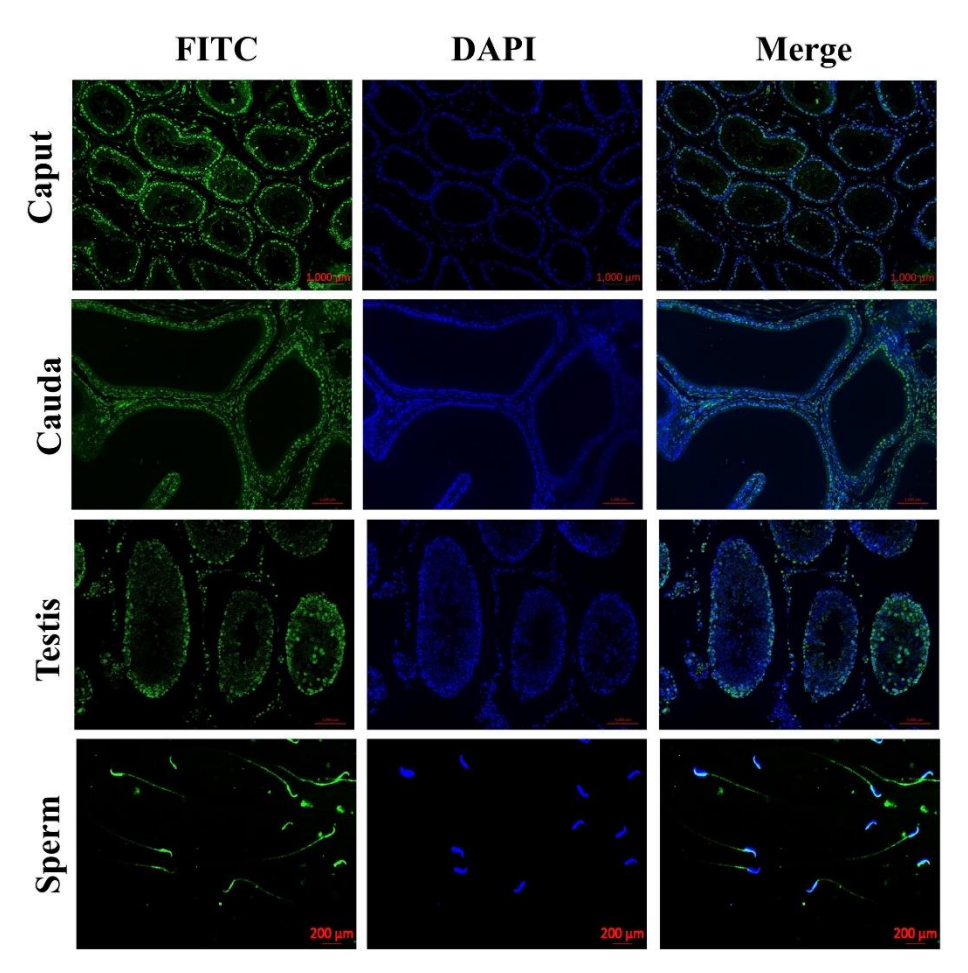


Figure 18. Immunolocalization of UPK2. Serial sections (5 μm thickness) of the rat testes and epididymides and smears of spermatozoa were fixed and incubated for one hour with UPK2 antibody (raised in goat) followed by incubation with FITC labelled anti-goat secondary antibody raised in rabbit. Nucleus was stained with 4', 6-diamidino-2-phenylindole and images taken using fluorescence microscope with excitation and emission at 495 nm and 519 nm respectively. Magnification: 10X.

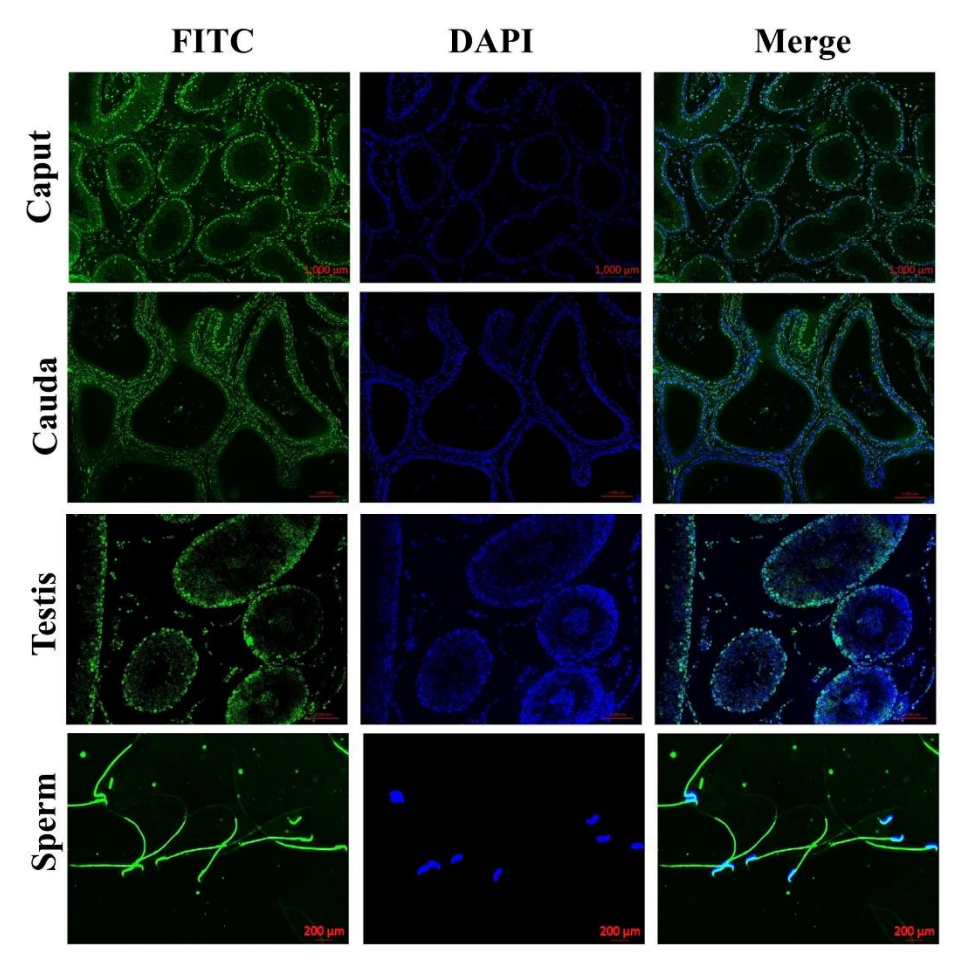


Figure 19. Immunolocalization of UPK3b. Serial sections (5 μ m thickness) of the rat testes and epididymides and smears of spermatozoa were fixed and incubated for one hour with UPK3b antibody (raised in goat) followed by incubation with FITC labelled anti-goat secondary antibody raised in rabbit. Nucleus was stained with 4', 6-diamidino-2-phenylindole and images taken using fluorescence microscope with excitation and emission at 495 nm and 519 nm respectively. Magnification: $10\times$.

1.3.3. Modulation of *Upk* gene expression by LPS

Male reproductive tract proteins are known to have roles in innate immunity besides sperm function. Since we observed that *Upks* are abundantly expressed in the male reproductive tract tissues, we anticipate that they may have additional role in innate immune responses and this could be a novel function of UPKs that has not been reported till now. In order to understand the possible functional role of UPKs in the male reproductive system immune responses, we analyzed the dynamics of their mRNA levels during endotoxin challenge using *in vitro* and *in vivo* model

systems. Since *Upk1a*, *Upk1b* and *Upk3b* were expressed in LC540 and RCE cells, further analyses were carried out on only these genes. In LC540 cells, *Upk1a* expression increased significantly up to 12 h after treatment, whereas such an increased expression of *Upk1b* was observed only up to 3 h. However, *Upk3b* expression was decreased 24 h after LPS challenge (Figure 20). In the RCE cells, *Upk1a*, *Upk1b* and *Upk3b* expression increased significantly up to 6 h after LPS treatment followed by a decline below the control levels at the later time points (Figure 20).

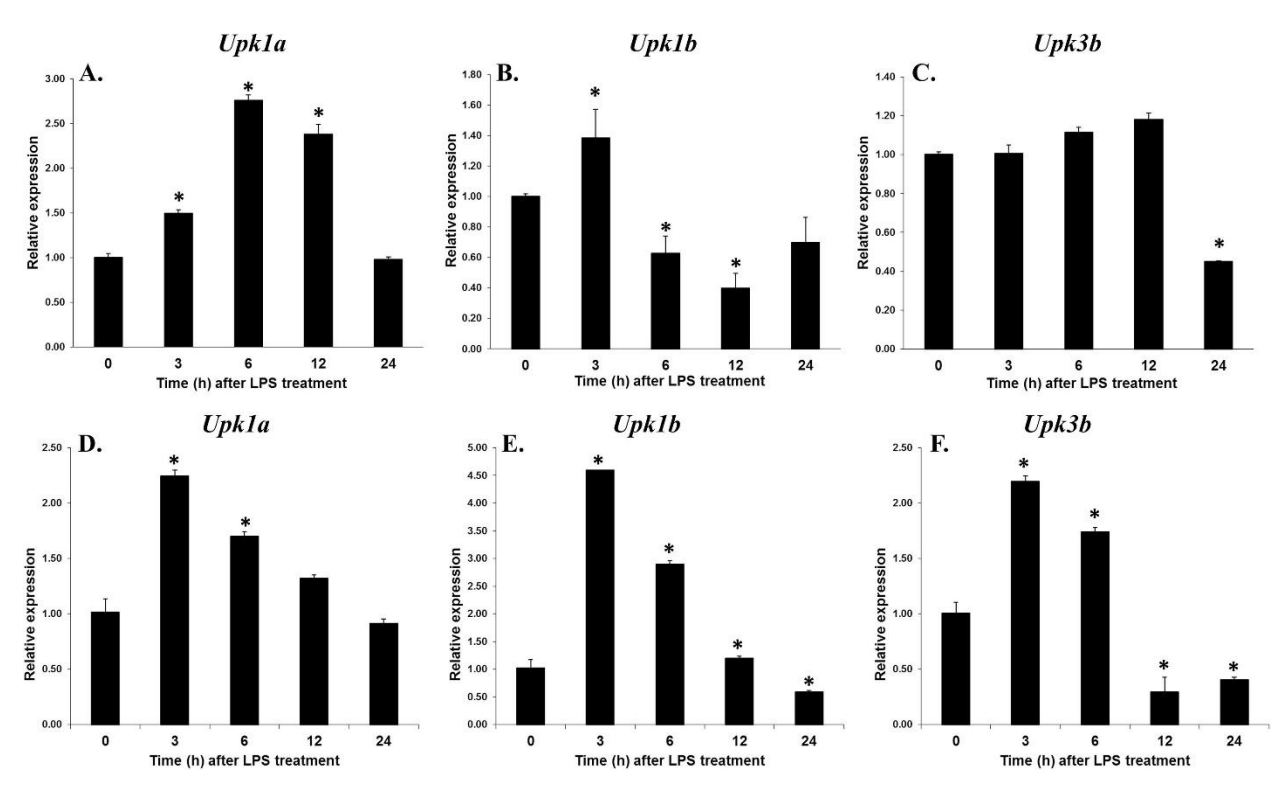


Figure 20. Immunolocalization of UPK3b. 1×106 cells were plated in each well of a 24 well plate and treated with 100 ng/ml LPS. RNA isolated from cells were collected at 3, 6, 12 and 24 h after LPS treatment was reverse transcribed and the resulting cDNA was used to analyze Upk1a, Upk1b and Upk3a gene expression by real time PCR. A-C, LC540 cells; D-F, RCE cells Values shown are Mean \pm S.D. * denotes p < 0.05 compared to 0 h control.

The effect of endotoxin challenge was also evaluated *in vivo* using rat as the model system. In the caput obtained from rats challenged with LPS, the mRNA levels of *Upk1a*, *Upk2* were not altered; whereas, a time dependent significant decline in *Upk1b* and *Upk3b* was observed (Figure 21). In the cauda, the mRNA levels of all the *Upks* were found to be significantly decreased following LPS administration (Figure 21). Testicular *Upk1a* and *Upk1b* expression was decreased at all the time points after LPS treatment. *Upk2* though increased at the 3 h time point was found

to be decreased at the later time points. *Upk3b* expression remained unchanged. (Figure 21). *Upk1a, Upk1b, Upk2* mRNA levels were significantly reduced in the seminal vesicles. *Upk3b* mRNA levels were down regulated at 6 and 24 h after LPS challenge, (Figure 21). In the prostate, though *Upk1a* and *Upk2* mRNA levels increased in a time dependent manner after LPS challenge up to 12 h followed by a decline, the mRNA levels of *Upk1b* was significantly reduced at all the time points analyzed (Figure 21).

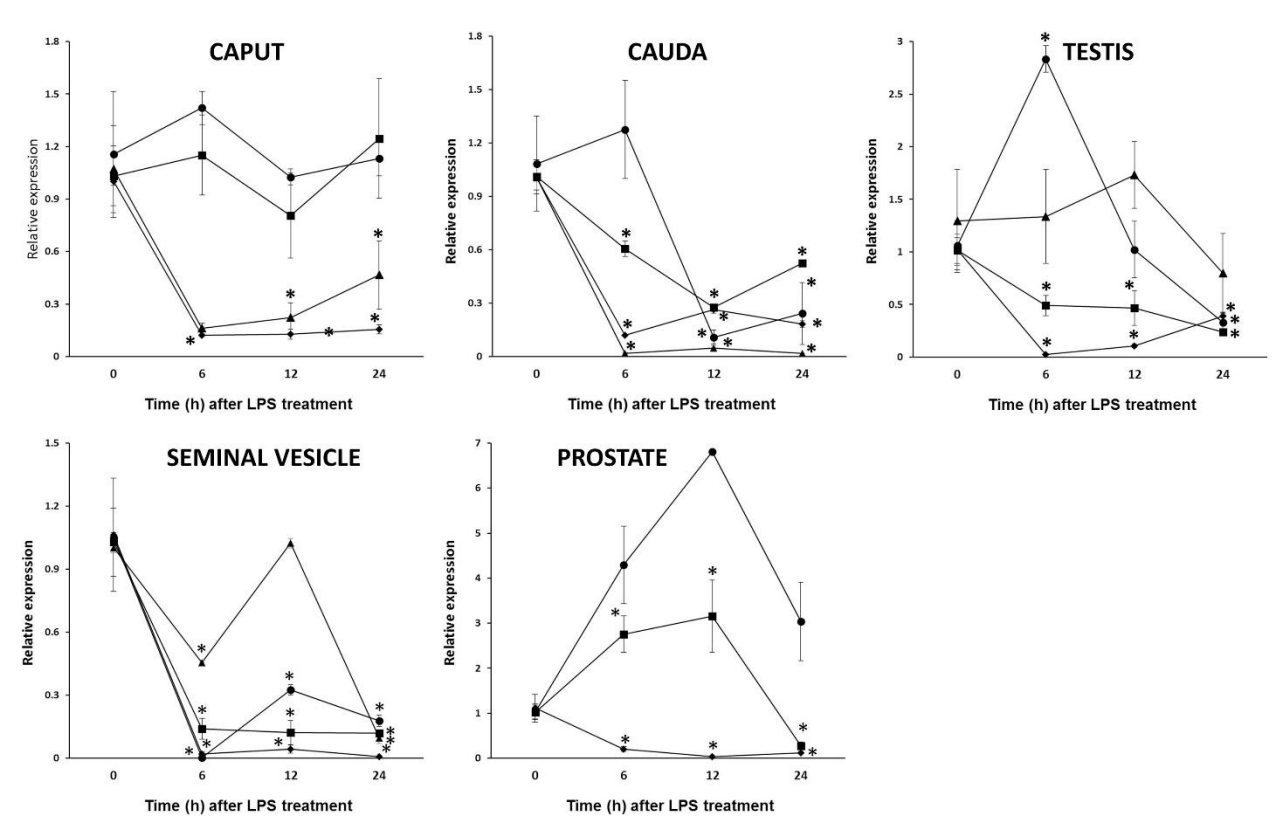


Figure 21.Upk gene expression in the male reproductive tract upon endotoxin challenge. Rats were challenged with a single intraperitoneal dose (1 mg/kg body weight) of LPS. Caput, cauda, testis, seminal vesicle and prostate were collected at 0, 6, 12 and 24 h after LPS treatment. RNA isolated from these tissues was reverse transcribed and the resulting cDNA was used for analyzingUpk gene expression by real time PCR. \blacksquare – Upk1a; \blacklozenge – Upk1b; \bigcirc – Upk2; \blacktriangle – Upk3b. Values shown are Mean \pm S.D. \ast denotes p < 0.05 compared to 0 h control.

1.4. Discussion

UPKs are implicated to play a crucial role in urothelial physiology and pathogenesis (Carpenter *et al.*, 2016, Wu *et al.*, 2009, Liao *et al.*, 2018, Zupancic and Romih 2013). They have been projected as key factors to indicate urothelial infections and cancers of the urothelial system (Lee 2011). However, their expression beyond the urothelial systems was proposed (Lee 2011). *Upk* expression was reported in the human female genital tract (Shapiro *et al.*, 2000) and may have a role in the developmental process (Cunha *et al.*, 2017) and pathophysiology (Ogawa *et al.*, 1999). Reduced *Upk* gene expression is associated with poor prognosis in colorectal and adenocarcinoma patients (He *et al.*, 2014, Zheng *et al.*, 2014). UPKs were implicated to be crucial in the fertilization process (Liao *et al.*, 2018). Analyzing the role of UPKs in other organ system has been an emerging area of research in the recent past. This study aims at investigating the possible functions of UPKs in the male reproductive system using rat as the model system. The rationale is based on the fact that male reproductive system and urothelium are of same embryonic origin and thus UPKs may play a crucial role in many cellular and tissue processes.

UPKs first emerged in cartilaginous fish, which could be a common ancestor of vertebrates (Garcia-Espanaet al., 2006). Over a period of time UPKs were identified in many species and are found to be highly conserved and have common evolutionary ancestors (Desalle et al., 2014, Wu et al., 1994). Recently three new UPKs were identified and this demonstrates the continued interest to study the role of UPKs in mammalian physiology (Desalle et al., 2014). Rat genome wide search indicated the presence of five Upk genes, namely, Upk1a, Upk1b, Upk2, Upk3a and Upk3b, of which *Upk3b* sequence is predicted. Sequence analyses revealed that the rat *Upk3b* is located on chromosome 12. Similar to the rat, the mouse and human *Upks* identified till date are located on different chromosomes, suggesting that they are not clustered though they contribute to the common function. We identified and reported the rat *Upk3b* gene and this is a novel aspect of this study. Upk3b gene contains seven exons and is transcribed to an 1158 nucleotide mRNA that encodes a protein with 275 amino acids. Rat UPK3b contains a single transmembrane domain similar to that of mouse and human monospanins. However, its sequence similarity with UPK2 and UPK3a was found to be only 14 and 28 percent respectively. Rat UPK3b shows 92 and 82 percent homology with its mouse and human counterparts respectively. Though the rat UPK3b is classified as a monospanin and displays similarities to that of human in terms of localization of the

gene on a separate chromosome and the predicted function in urothelium, sequence homology reveals that it appears to be closely related only to the mouse UPK3b. Gene neighborhood analyses for rat *Upk*genes indicated similarities in the nature of genes present in the vicinity of *Upk* genes of mouse and human. A number of genes were commonly present in the vicinity of *Upks* in all the three species. It is possible that the location of *Upk* genes in relation to the other genes is conserved through evolutionary process across the species. Three dimensional structure analyses of rat UPKs indicate that UPK1a and UPK1b (tetraspanin family members) and UPK2, UPK3a and UPK3b (monospanin family members) are similar in appearance. The high content of alpha-helix in the tetraspanin family members and that of random coil in the monospanin family members appears to correlate with the number of spans they make in the plasma membrane. The 3D structure of UPKs proposed in this study are indicative and whether the proposed structures can fit into the existing models of asymmetric unit membrane particles needs to be validated using advanced methods such as nuclear magnetic resonance spectroscopy. Information presented on the sequence similarity among rat UPKs and between UPKs of different species, genome neighborhood and three dimensional structure are relatively less reported for UPKs of rat and other species; and thus contributes to the further understanding of the functional role of these proteins.

Though, UPKs were predicted to be expressed in other tissues (Lee 2011), their presence and importance in the male reproductive tract is gaining importance in the recent years. The importance of UPKs in fertilization was recently demonstrated in the mouse (Liao *et al.*, 2018). In the rat model system, characterization of UPKs still remains to be explored. Determination of expression pattern and functional role of UPKs may vary from species to species and hence this study aimed to understand the contribution of UPKs in the rat male reproductive tract. *Upk1a*, *Upk1b*, *Upk2* and *Upk3b* mRNA was detected in the caput, cauda, testis, seminal vesicle and prostate, whereas *Upk3a* was not detected in any of the tissues. Presence of UPK1a, UPK1b, UPK2 and UPK3b in the caput, cauda and testis as detected by immunoblotting further confirmed the expression of UPKs in male reproductive tract. The expression of *Upk* mRNAs in other tissues of the rat suggest that these genes are ubiquitously expressed and may have functions beyond the urinary system. In the rat, UPK expression in the urethra and vaginal introitus was associated with the developmental process (Cunha *et al.*, 2017). Such a correlation between *Upk* gene expression and postnatal development was not studied in the male reproductive tract. Developmental

regulation of the male reproductive tract in many species is governed by dynamic changes in gene expression pattern, which in turn is determined by the fluctuating levels of androgens (Rodriguez et al., 2001, Harris and Bartke 1974). Our results indicate that, in the epididymis, Upk1b and Upk3b are constitutively expressed starting from early stages of development, whereas *Upk1a* and *Upk2* are detected at later stages. In the testis, except for *Upk3a*, all other *Upks* seem to be expressed in all the stages of development. It appears that some *Upks* are essential at all stages of development whereas some are governed byandrogen levels. Testosterone levels vary greatly during the developmental process. A steady increase in testosterone levels occurs in the rete testis of 30–130 day old rats (Harris and Bartke 1974, Harris and Bartke 1981). Androgen levels in the epididymis of rat decline from birth until 20 days and a normal level of 10 ng/g tissue (35 nM) is maintained until approximately 40 days after which, the levels begin to increase to that of the adult, between 15 and 20 ng/g (Charest et al., 1989). Serum testosterone levels in the young rat remain low and do not begin to increase to adult levels until 35-40 days of age (Nayfehet al., 1966). It can be hypothesized that the androgens may influence the expression of *Upk* genes directly by binding to their promotor elements or through modulation of other transcription factors. Immunofluorescence microscopy revealed the localization of UPKs in the rat male reproductive tract tissues and on the spermatozoa. We previously demonstrated the localization of proteins that play an important role in spermatogenesis and sperm maturation. They were found to be abundant in the epithelial lining of caput, cauda and testis and on spermatozoa (Rajesh and Yenugu 2012, Rajesh and Yenugu 2015, Narmadhaet al., 2011, Narmadha and Yenugu 2016). In this study, we show that UPKs are predominantly localized in the epithelial lining of caput, cauda and testis, suggesting that they may a play a crucial role in spermatogenesis and sperm maturation. A recent study reported the localization of UPK1b in the apical region of the cauda epididymis (Liao et al., 2018). Since the tetraspanin UPKs are expected to be localized in the vesicles, they should be detected in the apical regions. However, the localization pattern we demonstrate is different from that is reported by Liao et al. This could be due to variation in the species being studied. Further, imaging using high resolution microscopy are warranted to demonstrate the subcellular localization of UPKs in the tissues analysed in this study. All the UPKs analyzed were localized throughout the sperm. Liao et al reported that all UPK proteins were localized only to the head region of the mouse sperm (Liao et al., 2018). The pattern of localization of UPKs i.e. throughout the rat sperm could be due to species variation. The presence of these proteins on the sperm indicates their possible role in

many functions such as capacitation, acrosome reaction, sperm egg recognition and fertilization. Since the urothelial and reproductive tract tissues originate from the same embryonic origin, this could be an important reason for the presence of UPKs in both these organ systems. The exact role of UPKs in the male reproductive tract and their contribution to sperm function needs further investigation.

Proteins in the male reproductive tract have been demonstrated to have functions beyond spermatogenesis and sperm maturation. Ample evidence exists that some of them play a crucial role in innate immunity. For example, members belonging to defensin, Sperm Associated Antigen 11 (SPAG11), Prostate and Testis expressed (PATE), Lysozyme like (LYZL) families were found to be altered in response to endotoxin challenge or in model systems that mimic an infection (Biswas and Yenugu 2011, Rajesh and Yenugu 2012, Narmadhaet al., 2011). Their expression was epigenetically regulated (Biswas and Yenugu 2014). Since UPKs were found to be expressed abundantly in the male reproductive tract, it is possible that may also contribute to innate immunity. Implicating UPKs for their multiple roles in the same organ system has not been demonstrated earlier and our approach in this direction is novel. We observed that *Upk* expression was in generally down regulated when challenged with LPS both in vitro and in vivo. It is well established that Uropathogenic bacteria use UPKs as an advantage to infect the urothelial tissues (Mulvey et al., 1998, Martinez et al., 2000). UPK3a signaling is very crucial for bladder response during bacterial infection (Thumbikatet al., 2009). Presence of surfactant D protein acted as a competitor to FimH (fimbrial tip-positioned adhesive protein) of UPEC because of its ability to bind to UPK1a and thereby reducing the available levels of UPK1a and thus the bacteria induced inflammation (Kurimuraet al., 2012). In view of the above evidences, it is possible that UPKs may have a significant role during endotoxin or bacterial induced responses in the male reproductive system. Since LPS is a component of the capsule of Uropathogenic bacteria, the down regulation of Upk mRNAs in the male reproductive tract tissues during LPS challenge could be a protective mechanism. It is possible that down regulation of UPKs may result in non-availability of UPKs for Uropathogenic bacterial binding and thereby lowering the infection severity. We previously demonstrated that LPS induced changes in the defensin expression involved TLR (toll-like receptor) mediated NF-kB (nuclear factor kappa-light-chain-enhancer of activated B cells) activation and epigenetic changes such as DNA methylation and histone acetylation / methylation (Biswas and Yenugu 2014, Biswas *et al.*, 2015). UP1a promoter methylation is implicated in bladder carcinoma (Cunha *et al.*, 2017), suggesting that the promoters of *Upks*could be modulated by epigenetic changes under altered physiological conditions. It would be very interesting to study the molecular mechanisms (signaling pathways and epigenetic changes) by which LPS modulates *Upk* gene expression and also the interaction of Uropathogenic bacteria with UPKs of male reproductive system.

We conclude that UPKs are abundantly expressed in the male reproductive tract of rat and may contribute to the general physiology of this organ system, spermatogenesis, sperm function and immune responses.

1.5. References

- 1. Desalle, R., Chicote, J.U., Sun, T.T., Garcia-Espana, A., 2014. Generation of divergent uroplakin tetraspanins and their partners during vertebrate evolution: identification of novel uroplakins. BMC Evol. Biol. 14, 13.
- 2. Garcia-Espana, A., Chung, P.J., Zhao, X., Lee, A., Pellicer, A., Yu, J., et al., 2006. Origin of the tetraspanin uroplakins and their co-evolution with associated proteins: implications for uroplakin structure and function. Mol. Phylogenet. Evol. 41, 355–367.
- 3. Wu, X.R., Lin, J.H., Walz, T., Haner, M., Yu, J., Aebi, U., et al., 1994. Mammalian uroplakins. A group of highly conserved urothelial differentiation-related membrane proteins. J. Biol. Chem. 269, 13716–13724.
- 4. Yu, J., Lin, J.H., Wu, X.R., Sun, T.T., 1994. Uroplakins Ia and Ib, two major differentiation products of bladder epithelium, belong to a family of four transmembrane domain (4TM) proteins. J. Cell Biol. 125, 171–182.
- 5. Lin, J.H., Wu, X.R., Kreibich, G., Sun, T.T., 1994. Precursor sequence, processing, and urothelium-specific expression of a major 15-kDa protein subunit of asymmetric unit membrane. J. Biol. Chem. 269, 1775–1784.
- 6. Wu, X.R., Sun, T.T., 1993. Molecular cloning of a 47 kDa tissue-specific and differentiation- dependent urothelial cell surface glycoprotein. J. Cell Sci. 106 (Pt 1), 31–43.

- 7. Hu, C.C., Liang, F.X., Zhou, G., Tu, L., Tang, C.H., Zhou, J., et al., 2005. Assembly of urothelial plaques: tetraspanin function in membrane protein trafficking. Mol. Biol. Cell 16, 3937–3950.
- 8. Tu, L., Kong, X.P., Sun, T.T., Kreibich, G., 2006. Integrity of all four transmembrane domains of the tetraspanin uroplakin Ib is required for its exit from the ER. J. Cell Sci. 119, 5077–5086.
- 9. Tu, L., Sun, T.T., Kreibich, G., 2002. Specific heterodimer formation is a prerequisite for uroplakins to exit from the endoplasmic reticulum. Mol. Biol. Cell 13, 4221–4230.
- 10. Carpenter, A.R., Becknell, M.B., Ching, C.B., Cuaresma, E.J., Chen, X., Hains, D.S., et al., 2016. Uroplakin 1b is critical in urinary tract development and urothelial differentiation and homeostasis. Kidney Int. 89, 612–624.
- 11. Sakakibara, K., Sato, K., Yoshino, K., Oshiro, N., Hirahara, S., Mahbub Hasan, A.K., et al., 2005. Molecular identification and characterization of Xenopus egg uroplakin III, an egg raft-associated transmembrane protein that is tyrosine-phosphorylated upon fertilization. J. Biol. Chem. 280, 15029–15037.
- 12. Hasan, A.K., Fukami, Y., Sato, K., 2011. Gamete membrane microdomains and their associated molecules in fertilization signaling. Mol. Reprod. Dev. 78, 814–830.
- 13. Mahbub Hasan, A.K., Sato, K., Sakakibara, K., Ou, Z., Iwasaki, T., Ueda, Y., et al., 2005. Uroplakin III, a novel Src substrate in Xenopus egg rafts, is a target for sperm protease essential for fertilization. Dev. Biol. 286, 483–492.
- 14. Chicote, J.U., DeSalle, R., Segarra, J., Sun, T.T., Garcia-Espana, A., 2017. The Tetraspanin-Associated Uroplakins Family (UPK2/3) Is Evolutionarily Related to PTPRQ, a Phosphotyrosine Phosphatase Receptor. PLoS ONE 12, e0170196.
- 15. Kong, X.T., Deng, F.M., Hu, P., Liang, F.X., Zhou, G., Auerbach, A.B., et al., 2004. Roles of uroplakins in plaque formation, umbrella cell enlargement, and urinary tract diseases. J. Cell Biol. 167, 1195–1204.
- 16. Hu, P., Deng, F.M., Liang, F.X., Hu, C.M., Auerbach, A.B., Shapiro, E., et al., 2000. Ablation of uroplakin III gene results in small urothelial plaques, urothelial leakage, and vesicoureteral reflux. J. Cell Biol. 151, 961–972.

- 17. Jenkins, D., Bitner-Glindzicz, M., Malcolm, S., Hu, C.C., Allison, J., Winyard, P.J., et al., 2005. De novo Uroplakin IIIa heterozygous mutations cause human renal adysplasia leading to severe kidney failure. J. Am. Soc. Nephrol. 16, 2141–2149.
- Schonfelder, E.M., Knuppel, T., Tasic, V., Miljkovic, P., Konrad, M., Wuhl, E., et al.,
 2006. Mutations in Uroplakin IIIA are a rare cause of renal hypodysplasia in humans. Am.
 J. Kidney Dis. 47, 1004–1012.
- 19. Wu, X.R., Kong, X.P., Pellicer, A., Kreibich, G., Sun, T.T., 2009. Uroplakins in urothelial biology, function, and disease. Kidney Int. 75, 1153–1165.
- 20. Wu, X.R., Sun, T.T., Medina, J.J., 1996. *In vitro* binding of type 1-fimbriated Escherichia coli to uroplakins Ia and Ib: relation to urinary tract infections. Proc. Natl. Acad. Sci. U.S.A. 93, 9630–9635.
- 21. Mulvey, M.A., Lopez-Boado, Y.S., Wilson, C.L., Roth, R., Parks, W.C., Heuser, J., et al., 1998. Induction and evasion of host defenses by type 1-piliated uropathogenic Escherichia coli. Science 282, 1494–1497.
- 22. Martinez, J.J., Mulvey, M.A., Schilling, J.D., Pinkner, J.S., Hultgren, S.J., 2000. Type 1 pilus-mediated bacterial invasion of bladder epithelial cells. EMBO J. 19, 2803–2812.
- 23. Huang, H.Y., Shariat, S.F., Sun, T.T., Lepor, H., Shapiro, E., Hsieh, J.T., et al., 2007. Persistent uroplakin expression in advanced urothelial carcinomas: implications in urothelial tumor progression and clinical outcome. Hum. Pathol. 38, 1703–1713.
- 24. Zupancic, D., Zakrajsek, M., Zhou, G., Romih, R., 2011. Expression and localization of four uroplakins in urothelial preneoplastic lesions. Histochem. Cell Biol. 136, 491–500.
- 25. Hemler, M.E., 2003. Tetraspanin proteins mediate cellular penetration, invasion, and fusion events and define a novel type of membrane microdomain. Annu. Rev. Cell Dev. Biol. 19, 397–422.
- 26. Levy, S., Shoham, T., 2005. The tetraspanin web modulates immune-signalling complexes. Nat. Rev. Immunol. 5, 136–148.
- 27. Adachi, W., Okubo, K., Kinoshita, S., 2000. Human uroplakin Ib in ocular surface epithelium. Invest. Ophthalmol. Vis. Sci. 41, 2900–2905.
- 28. Olsburgh, J., Harnden, P., Weeks, R., Smith, B., Joyce, A., Hall, G., et al., 2003. Uroplakin gene expression in normal human tissues and locally advanced bladder cancer. J. Pathol. 199, 41–49.

- 29. Kuriyama, S., Tamiya, Y., Tanaka, M., 2017. Spatiotemporal expression of UPK3B and its promoter activity during embryogenesis and spermatogenesis. Histochem. Cell Biol. 147, 17–26.
- 30. Liao, Y., Chang, H.C., Liang, F.X., Chung, P.J., Wei, Y., Nguyen, T.P., et al., 2018. Uroplakins play conserved roles in egg fertilization and acquired additional urothelial functions during mammalian divergence. Mol. Biol. Cell mbcE18080496.
- 31. Geourjon, C., Deléage, G., 1995. SOPMA: significant improvements in protein secondary structure prediction by consensus prediction from multiple alignments. Computer Appl. Biosci.: CABIOS 11, 681–684.
- 32. Frishman, D., Argos, P., 1995. Knowledge-based protein secondary structure assignment. Proteins 23, 566–579.
- 33. Zhang, J., Yang, J., Jang, R., Zhang, Y., 2015. GPCR-I-TASSER: A hybrid approach to g protein-coupled receptor structure modeling and the application to the human genome. Structure 23, 1538–1549.
- 34. Laskowski, R.A., MacArthur, M.W., Moss, D.S., Thornton, J.M., 1993. PROCHECK: a program to check the stereochemical quality of protein structures. J. Appl. Crystallogr. 26, 283–291.
- 35. Ramachandran, G.N., Ramakrishnan, C., Sasisekharan, V., 1963. Stereochemistry of polypeptide chain configurations. J. Mol. Biol. 7, 95–99.
- 36. Biswas, B., Yenugu, S., 2013. Lipopolysaccharide induces epididymal and testicular antimicrobial gene expression *in vitro*: insights into the epigenetic regulation of spermassociated antigen 11e gene. Immunogenetics 65, 239–253.
- 37. Biswas, B., Yenugu, S., 2011. Antimicrobial responses in the male reproductive tract of lipopolysaccharide challenged rats. Am. J. Reprod. Immunol. 65, 557–568.
- 38. Zupancic, D., Romih, R., 2013. Heterogeneity of uroplakin localization in human normal urothelium, papilloma and papillary carcinoma. Radiol. Oncol. 47, 338–345.
- 39. Lee, G., 2011. Uroplakins in the lower urinary tract. Int. Neurourol. J. 15, 4–12.
- 40. Shapiro, E., Huang, H.Y., Wu, X.R., 2000. Uroplakin and androgen receptor expression in the human fetal genital tract: insights into the development of the vagina. J. Urol. 164, 1048–1051.

- 41. Cunha, G.R., Kurita, T., Cao, M., Shen, J., Robboy, S., Baskin, L., 2017. Molecular mechanisms of development of the human fetal female reproductive tract. Differentiation 97, 54–72.
- 42. Ogawa, K., Johansson, S.L., Cohen, S.M., 1999. Immunohistochemical analysis of uroplakins, urothelial specific proteins, in ovarian Brenner tumors, normal tissues, and benign and neoplastic lesions of the female genital tract. Am. J. Pathol. 155, 1047–1050.
- 43. He, Y., Kong, F., Du, H., Wu, M., 2014. Decreased expression of uroplakin Ia is associated with colorectal cancer progression and poor survival of patients. Int. J. Clin. Exp. Pathol. 7, 5031–5037.
- 44. Zheng, Y., Wang, D.D., Wang, W., Pan, K., Huang, C.Y., Li, Y.F., et al., 2014. Reduced expression of uroplakin 1A is associated with the poor prognosis of gastric adenocarcinoma patients. PLoS ONE 9, e93073.
- 45. Rodriguez, C.M., Kirby, J.L., Hinton, B.T., 2001. Regulation of gene transcription in the epididymis. Reproduction 122, 41–48.
- 46. Harris, M.E., Bartke, A., 1974. Concentration of testosterone in testis fluid of the rat. Endocrinology 95, 701–706.
- 47. Harris, M.E., Bartke, A., 1981. Androgen levels in the rete testis fluid during sexual development. Experientia 37, 426–427.
- 48. Charest, N.J., Petrusz, P., Ordronneau, P., Joseph, D.R., Wilson, E.M., French, F.S., 1989. Developmental expression of an androgen-regulated epididymal protein. Endocrinology 125, 942–947.
- 49. Nayfeh, S.N., Barefoot Jr., S.W., Baggett, B., 1966. Metabolism of progesterone by rat testicular homogenates. II. Changes with age. Endocrinology. 78, 1041–1048.
- 50. Rajesh, A., Yenugu, S., 2012. Genomic organization, tissue distribution and functional characterization of the rat Pate gene cluster. PLoS ONE 7, e32633.
- 51. Rajesh, A., Yenugu, S., 2015. Effect of immunization against prostate- and testis-expressed (PATE) proteins on sperm function and fecundity in the rat. J. Reprod. Immunol. 110, 117–129.
- 52. Narmadha, G., Muneswararao, K., Rajesh, A., Yenugu, S., 2011. Characterization of a novel lysozyme-like 4 gene in the rat. PLoS ONE 6, e27659.

- 53. Narmadha, G., Yenugu, S., 2016. Immunization against lysozyme-like proteins affect sperm function and fertility in the rat. J. Reprod. Immunol. 118, 100–108.
- 54. Biswas, B., Yenugu, S., 2014. Transcriptional regulation of the rat sperm-associated antigen 11e (Spag 11e) gene during endotoxin challenge. Mol. Genet. Genomics 289, 837–845.
- 55. Thumbikat, P., Berry, R.E., Zhou, G., Billips, B.K., Yaggie, R.E., Zaichuk, T., et al., 2009. Bacteria-induced uroplakin signaling mediates bladder response to infection. PLoSPathog. 5, e1000415.
- 56. Kurimura, Y., Nishitani, C., Ariki, S., Saito, A., Hasegawa, Y., Takahashi, M., et al., 2012. Surfactant protein D inhibits adherence of uropathogenic Escherichia coli to the bladder epithelial cells and the bacterium-induced cytotoxicity: a possible function in urinary tract. J. Biol. Chem. 287, 39578–39588.
- 57. Biswas, B., Bhushan, S., Meinhardt, A., Yenugu, S., 2015. Uropathogenic Escherichia coli (UPEC) induced antimicrobial gene expression in the male reproductive tract of rat: evaluation of the potential of Defensin 21 to limit infection. Andrology. 3, 368–375.

Chapter-2

Functional characterization of Uroplakin1a (*Upk1a*) using knock-out model

2.1. Introduction

The barrier permeability and structural stability of urothelium in the bladder is conferred by uroplakins (UPKs), which form plaques to generate an asymmetric unit membrane (AUM). Depending on the number of times they span the plasma membrane, two classes of them have been identified, namely monospanins and tetraspanins. UPKs identified in different species are UPK1a, UPK1b, UPK2, UPK2b, UPK3a, UPK3b (a slight isoform of UPK3a), UPK3c and UPK3d (Desalle, Chicote, Sun, & Garcia-Espana, 2014; Garcia-Espana et al., 2006; X. R. Wu et al., 1994). The plaque formation stems out of specific interaction among the UPKs (UPK1a interacts with UPK2, while UPK1b interconnects with UPK3a) (C. C. Hu et al., 2005; Tu, Kong, Sun, & Kreibich, 2006; Tu, Sun, & Kreibich, 2002; X. R. Wu et al., 1994). Besides their primary role in protecting the urothelium, they are implicated in a variety of physiological and pathological processes. Elevated levels of UPKs in benign urological diseases (Szymańska, Matuszewski, Dembowski, & Piwowar, 2021), implication of Upk2a as a potential biomarker for the detection of lung carcinoma (Leivo, Tacha, & Hansel, 2021; J. Zhu et al., 2021), up regulation of Upkla and anti-sense RNA to *Upk1a* in lung cancer (Byun, Choi, Jeong, Yoon, & Baek, 2020), promotion of glycolysis and proliferation in liver cancer (Song et al., 2020) and Upk1b as a novel prognostic marker for gastric cancer (Z. Zhu et al., 2020) are some of the roles of UPKs reported in the last two years.

The significance of UPKs in male reproductive physiology is gaining importance. UPK3a and UPK11b forms a complex to mediate sperm-egg interaction and fertilization in *Xenopus* oocytes (Hasan, Fukami, & Sato, 2011; Mahbub Hasan *et al.*, 2005; Sakakibara *et al.*, 2005). The time and location dependent expression of UPK3b in the sperm, epididymis and ovarian follicles (Kuriyama, Tamiya, & Tanaka, 2017) their expression in oocytes and association with multivesicular bodies and reduced fecundity of UPII/IIIa knock out provides further evidence on their role in reproductive physiology (Liao, Chang, Liang, Chung, Wei, Nguyen, Zhou, Talebian, Krey, Deng, Wong, Chicote, Grifo, Keefe, Shapiro, Lepor, Wu, DeSalle, Garcia-Espana, *et al.*, 2018). The sperm-egg membrane fusion signal is mediated by the oocyte/egg membrane microdomain (MD)-associated uroplakin III-Src system to kick start the embryonic and zygotic development *Xenopus laevis*(Sato & Tokmakov, 2019). We demonstrated the expression of

Upk1a, Upk1b, Upk2 and Upk3b mRNA and protein in the male reproductive tract of rat (Babu Munipalli & Yenugu, 2019). During uropathogenic E. coli (UPEC) infection, UPKs serve as anchors and this is mediated by the binding of the type-1 fimbriae to initiate a series of events that favour bacterial infection in a variety of tissues (Martinez, Mulvey, Schilling, Pinkner, & Hultgren, 2000; Mulvey et al., 1998; X. R. Wu, Kong, Pellicer, Kreibich, & Sun, 2009; X. R. Wu, Sun, & Medina, 1996). We also demonstrated that the expression of UPKs in the epididymis, testis seminal vesicle and prostate was altered under conditions of endotoxin challenge (Babu Munipalli & Yenugu, 2019). However, in depth studies that explored the involvement of UPKs at the molecular level in the male reproductive tract are not yet reported. In order to further understand the functional significance of UPKs in male reproductive tract, we generated *Upkla* knockout mice and analyzed their fecundity, sperm function and responsiveness of the male reproductive tract tissues to UPEC infection. Further, the testicular transcriptome profile of *Upkla* knockout mice was obtained by next generation sequencing. We report that the *Upkla* male mice are sub fertile with reduced sperm count, displayed normal sperm function (capacitation and acrosome reaction) and lacked the ability to clear the UPEC efficiently. Transcriptome analyses of the testis of knockout mice revealed that genes associated with a wide variety of biological, cellular and molecular function were differentially expressed, indicating the multifunctional roles of UPKs in testicular function.

2.2. Materials and methods

2.2.1. Generation of *Upk1a* knockout mice

Upk1aknockout mice (B6NJ: C57BL/6NJNcbs-Upk1Aem2MGEF) generated by using Cas9 / sgRNA, at Mouse Genome Engineering Facility, NCBS (National Centre for Biological Sciences), Bangalore, India. The strategy used for generation of the knockout mice is depicted (Figure 1). Specific guide RNAs were designed to target the mouse Upk1a gene (NM_026815.2) to facilitate deletion of the region between 392 to 557 (166 bp) that spans a part of intron 1 and exon 2 and part of intron 2 (Figure 2). The 5' → 3'sequence of the guide RNAs used are: sgRNA#34 (on plus strand): 5'- TTTGGTGAGACGCGGAATAA [TGG-PAM] -3' and sgRNA#38 (on minus strand): 5'- TACTTCAGACCCCATCTACC [AGG-PAM] -3'. B6/NJNcbs mice zygotes were microinjected in the pronuclear region with a solution containing Cas9 protein

(50 ng/μl final), sgRNA#34 (12.5 ng/μl final) and sgRNA#38 (12.5 ng/μl final). Resulting founders were back crossed twice with wild type mice (B6/NJNcbs). After two successive B6/NJNcbs backcrosses, the animals obtained were heterozygote *Upkla*^{+/-} N2 mice. Homozygote (*Upkla*^{-/-}) knockout animals that had a deleted sequence (part of intron 1 and exon 2 and part of intron 2) were generated by crossing *Upkla*^{+/-} N2 with *Upkla*^{+/-} N2. DNA of male and female mice from tail regions were subjected to genomic PCR to confirm the deletion using PCR primers that flanked the targeted region (Figure 2). The PCR amplicons (wild type and *Upkla*^{-/-} 536 and 360 bp respectively) were sequenced. Knockout mice used for further studies were obtained from the same founder and age matched.

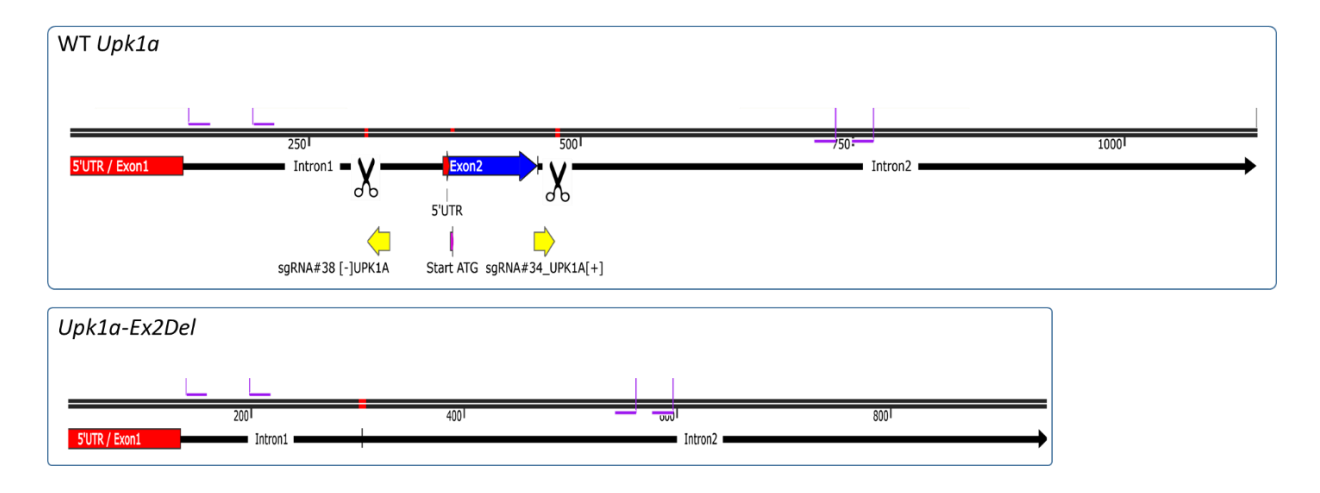


Figure 1:Strategy to generate Upk1a knockout mice. Upper panel shows the gene structure of mouse Upk1a (5'UTR, exon1, intron 1, exon2 and intron 2). Scissors indicate the targeted regions to generate the knockout mice. sgRNA#38 and sgRNA34 were used to target the minus and plus strands. FP and RP are genotyping primers. Lower panel indicates the structure of exon1 deleted Upk1a gene mediated by CRISPR-Cas9 editing.

B6NJ: C57BL/6NJNcbs-Upk1A^{em2MGEF}

AGATCACCTTGCCCCAGTGGCCAGTCAGGAGCACAATCCTGAATTTCAGGTCTGTAAATCACTTGAGTGTCAAGGAGCTCATAAAAATCTATCATGGTCAGTCTGCAACTCCTGCCCCCTCCTCTCTGAGACTGGCTCAAGGAGGGGTTTGGCATATATAGGGAGCTGCTGTAGCTGGGGCTGACCAGAGAGGGCTTCTGTAGAAAGGTGAGGAGGTGTTCTGGGGGTTTGACAGGGCCAAGGGGCTGCTCGGGAGGGCCTGCTCTGTAGAA

(FP)

sgRNA#38 [-]UPK1A

TTCTGCAGCGACAGAGGGAGAAGAGGGTCTCCTGTGGTGGTGGGGCTGCTGGTCGTGGCAACATCATTATTTTGGTGAGACGCGGAATAATGGGAGCGGGAAAGTGTGGTGGGGGAGGTGGCAGCTGAGATCCCAGGTCTATGAGCTGCAGGC

sgRNA#34_UPK1A[+]

(RP)

Figure 2. Gene sequence of mouse Upk1a. Exon 1 and Exon 2 sequences are indicated in red colored font, while the red colored and underlined sequence is the CDS. 5'UTR and intronic sequences are in black colored font. Yellow highlighted sequences are the targets for the guide RNAs. The 166 bp region targeted for deletion (392 to 557) indicated in bold font lies within the yellow highlighted sequences. Grey highlighted sequences are identified to design forward primer (FP) and reverse primer (RP) for genotyping. The expected amplicon size for wild type and knockout is 536 and 370 bp respectively.

2.2.2. RT-PCR

RNA was isolated to generate cDNA by using commercially available kits (Promega) and PCR analyses carried out with *Upk1a* gene specific primers. The typical condition for a PCR reaction was: 94°C for 1 min; 30-32 cycles at 94°C for 30 sec, 58°C for 30 sec and 72°C for 30 sec and the termination stage of extension at 72°C for 10 min. Electrophoresed the PCR amplicons on 2% agarose gels. Using SYBR master mix kit (Applied Biosystems, Warrington, UK), real-time PCR was performed with standard cycling conditions by in a thermal cycler (Applied

Biosystems). For calculating the fold change in expression, *Gapdh* levels were measured to serve as internal control.

2.2.3. Assessment of fecundity

Wild type and $Upkla^{-/-}$ mice (aged 90 days; n = 6 for each group) were subjected to natural mating to assess fecundity. Each male mice was housed with two female mice and monitored for detection of pregnancy. Further females were separated and noted the litter sizes.

2.2.4. Assessment of capacitation and acrosome reaction

Capacitation and acrosome reaction in the spermatozoa was measured as reported previously (Rajesh & Yenugu, 2015, 2017). Filipin, the cholesterol-binding dye (Cat no. F9765, Sigma Aldrich, USA), was used to assess capacitation. During capacitation, cholesterol loss is evident, which can be monitored using a specific fluorescent dye, filipin. Capacitated spermatozoa display reduced fluorescence intensity compared to their uncapacitated counterparts (Bou Khalil *et al.*, 2006). Spermatozoa (from mice aged 90 days) incubated with 25 μM filipin for 1 hr and extensively washed with PBS were permitted to capacitate in M2 medium for 4 hours. Uncapacitated spermatozoa were also included in the assay. A flow cytometer (BD Biosciences) was used to measure the fluorescence with excitation (340 nm) and emission wavelengths (425 nm).

The acrosome reaction is characterized by an enhancement in the levels of intracellular calcium concentration ([Ca2+]i). The same was assessed using Fluo-3-AM (a calcium-binding fluorescent dye). To initiate an acrosome reaction, the ionophore, A23187 (10 μM; (Sigma Aldrich, USA) was added to spermatozoa (from mice aged 90 days), and put the reaction in the incubator should be maintained at 37°C, 5% CO₂ and 95% air about one hour. After the incubation, Fluo 3-AM (10 mM) was added, and the fluorescence intensity was measured in a flow cytometer with excitation and emission wavelengths set at 488 nm and 515–540 nm, respectively. Fluorescence intensity was measured for 10,000 individual sperm cells. Linear and logarithmic modes were used to collect Forward scatter (FSC) and side scatters (SSC). The intensity of fluorescence of capacitated / acrosome reacted spermatozoa is demonstrated as percent relative to the fluorescence intensity noticed in the uncapacitated / acrosome intact spermatozoa.

2.2.5. Histological evaluation

Different tissues of wild-type and *Upk1a* knockout mice (aged 90 days) were placed for 24 hr in 4% paraformaldehyde (PFA) and washed with 70% ethanol. Sequential tissue dehydration was carried out with graded ethanol (80, 90, and 100%) and isopropanol overnight at 60°C. The processed tissues were embedded in paraffin wax, and five-micron sections were prepared for histological staining. Xylene-based deparaffinization and rehydration in graded ethanol (100, 90, 80, 70, and 50 %) were carried out, followed by staining for 10 mins duration with Harris hematoxylin solution. Consequently, sections were handled by washing with distilled water in 1% hydrochloric acid for 30 sec for differentiation and immersion in 0.2% ammonia water for 1 min. Staining was also carried out for 1 min with 0.2% eosin Y solution. The sections were then dehydrated by placing them consecutively in 50, 70, 80, 90, and 100% alcohol. Washed with xylene and mounted using a xylene-based mounting medium. For histopathological evaluation in multiple fields images Captured for each section was conducted by a board-certified histopathologist. The histopathologist reported histopathological changes as per the established principles (KN, AK, & DK, 2013; R., 2013).

2.2.6. UPEC infection and assessment

Briefly, 30,000 UPEC suspended in 100 µl PBS was injected intraperitoneally into wild-type and knockout mice (aged 90 days), and the animals were constantly monitored. Animals were sacrificed 1, 3, and 5 days after injection. Caput, cauda, testis, seminal vesicle, prostate, bladder, liver, and kidney were collected and homogenized in sterile PBS. To resolve the number of UPEC present in the tissues. Real-time PCR was carried out for papC, a UPEC-specific gene. Initially, serial dilutions (1:10 to 1: 1,00,00,000 containing 33000000 to 33 *E. coli*) of UPEC were prepared, and 10 µl of each was subjected to real-time PCR. A graph plotted with Ct value and *E. coli* number on the X and Y axes, respectively. The bacterial count in each tissue was determined by correlating the Ct value on the graph.

2.2.7. Gene chip hybridization, data collection, and enrichment analysis.

The quality of RNA isolated from the testis of wild-type and knockout mice (aged 90 days) was checked with Agilent TapeStation system, and RNA-seq was carried out using Illumina HiSeq platform. FastQC and MultiQC software are used for the data quality check (de Sena Brandine & Smith, 2019). The data was checked for base call quality distribution, % bases above Q20,

Q30, %GC, and sequencing adapter contamination. All the samples passed the QC threshold (Q30>90%). Raw sequence reads were processed to remove adapter sequences and low-quality bases using fastp(S. Chen, Zhou, Chen, & Gu, 2018). QC passed reads were mapped onto *Mus musculus* (GCF_000001635.27_GRCm39_genomic.fna) reference genome using STAR v2 aligner (Dobin *et al.*, 2013). On average, 99.86% of the reads aligned onto the reference genome. Gene level expression values were obtained as reading counts using feature Counts software (Liao, Smyth, & Shi, 2014). Differential expression analysis was carried out using the DESeq2 (Love, Huber, & Anders, 2014). The read counts were normalized (variance stabilized normalized counts) using DESeq2, and differential enrichment analysis was performed. Genes with absolute log2 fold change ≥ 1 and ≤ -1 with a p-value ≤ 0.05 were considered significant. The genes that displayed unique differential expression were used for Gene Ontology (GO) and trail improvement analysis by DAVID software.

2.2.8. Statistical analyses

Holm-Sidak test is used for statistical analyses using Sigma Plot software (SPSS Inc., Chicago, IL, USA). The values revealed are Mean \pm S.D. * indicates p < 0.05 compared with the respective control.

2.2.9. Ethics approval statement

The *Upk1a*-/- mice were generated under the NCBS-IAEC project (No. #AJ-1/2015(R1-E). The University of Hyderabad Institutional Animal Ethics Committee approved the animal studies (UH/IAEC/SY/2021-1/20)

2.3. Results

2.3.1. Genotypic characterization of knockout mice

Heterozygote *Upk1a*^{+/-} N2 mice obtained from NCBS, Bangalore were crossed to generate *Upk1a*^{-/-} mice. Genotyping was performed using primers that are flanked on either sides of the targeted sequence of *Upk1a* gene. An amplicon with a size of 536 bp was obtained by genomic PCR with DNA from wild type animals, whereas the amplicon size was 370 bp in *Upk1a*^{-/-} mice (Figure 3A). In the heterozygote mice, two PCR amplicons of sizes 536 bp and 370 bp were observed. The effect of *Upk1a* gene knockout on the expression of its mRNA was analyzed by RT-PCR in the bladder. *Upk1a* mRNA expression was completely absent in the knockoutmice as demonstrated by PCR analyses (Figure 3B).

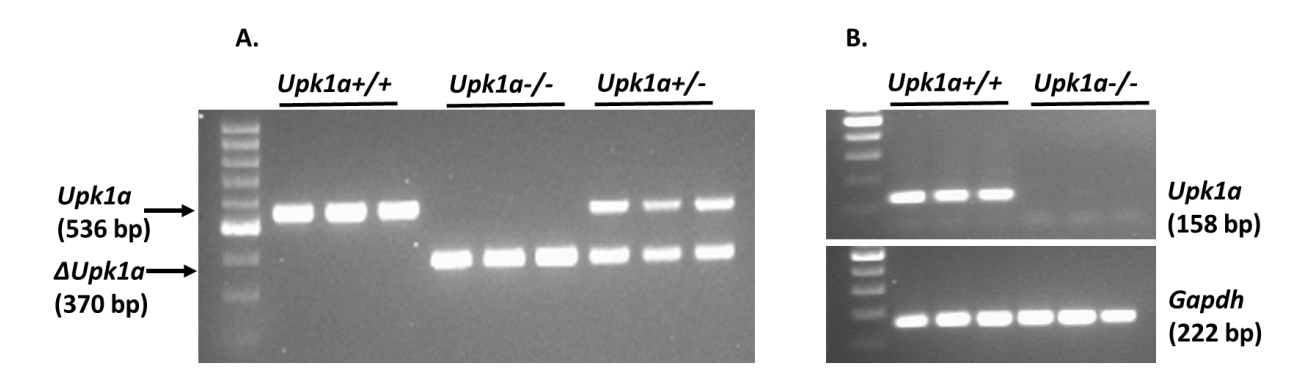


Figure 3. Genotyping and Upk1a gene expression. (A). Genotyping of wild type, Upk1a heterozygous and Upk1a knockout mice. DNA was isolated from the tail piece and subjected to genomic PCR using primers that flank the regions of the targeted region. Wild type amplicon size: 536; Knockout amplicon size: 370 bp. (B). Upk1a mRNA expression in bladder of wild type and knockout mice. RNA isolated from the bladder was reverse transcribed and Upk1 mRNA expression was assessed by PCR using gene specific primers.

2.3.2. Body and organ weights

There was no difference in the average body weight of wild type and knockout male mice (Table 1). However, significant increase in the relative organ weight of bladder, kidney and prostate was evident. On the contrary significant decrease was observed for caput epididymis and testis. Pictures of the organs that showed changes in the size / weight are presented in figure 4.

Table 1. Relative organ weights of wild type and knockout mice.

Tissues	Wild type	Knockout
Bladder	0.0136 ± 00019	$0.0028 \pm 0.00103*$
Caput	0.0012 ± 00007	$0.0009 \pm 0.00012*$
Testis	0.0041 ± 0.00012	$0.0031 \pm 0.00015*$
Prostate	0.00088 ± 0.00007	0.0018 ± 0.00056 *
Seminal vesicle	0.0119 ± 0.00145	0.0134 ± 0.00161
Pancreas	0.007 ± 0.00057	0.0066 ± 0.00078
Spleen	0.0029 ± 0.00022	0.0031 ± 0.00025
Kidney	0.0078 ± 0.00024	$0.0434 \pm 0.00304*$
Liver	0.0482 ± 0.0060	0.0080 ± 0.00612
Lung	0.0093 0.00103	0.0059 ± 0.00209
Heart	0.00631 0.00062	0.0124 ± 0.00094
Brain	0.0177 0.00027	0.0183 ± 0.00205

^{*} Indicates p < 0.05.

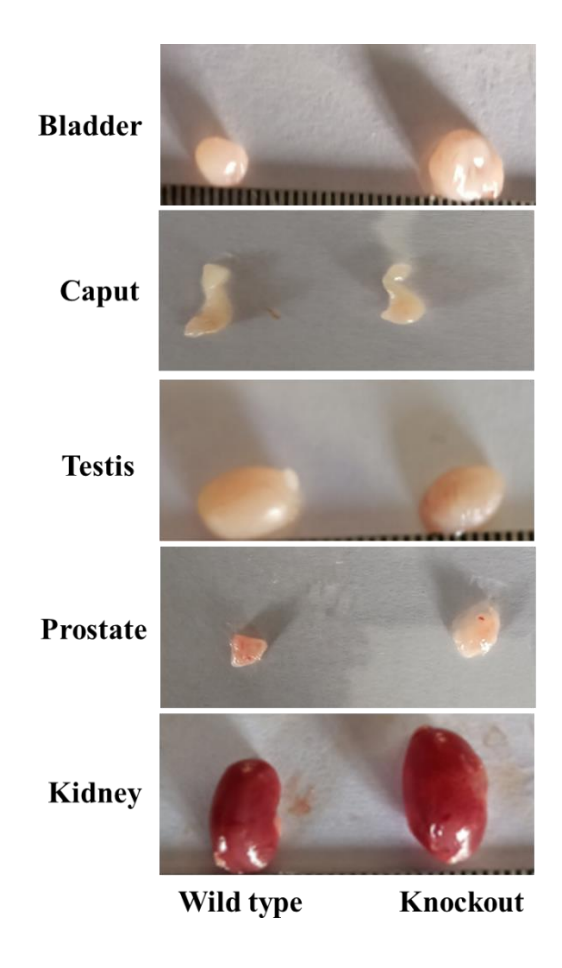


Figure 4. Representative images of organs that displayed change in weight. Bladder, caput, testis, prostate and kidney were taken out from wild type and Upkla knockout mice and photographed.

2.3.3. Fecundity, sperm count and sperm function

The effect of Upkla mRNA ablation on the male reproductive function was evaluated in terms of fecundity, sperm count and sperm function. Fecundity (litter size obtained after natural mating) of Upkla knockout male mice was significantly decreased when compared to their wild type counterparts (Figure 5) The average number of pups in ten litters each for wild type and knock mice was 9.81 ± 1.55 and that of Upkla knockout mice was 6.1 ± 1.28 . Concomitant with the decreased litter size, sperm count was also found to significantly less in the Upkla knockout mice (Figure 5). The sperm count (in millions; mean \pm S.D.) in the wild type and Upkla knockout mice was 16.32 ± 1.66 and 12.27 ± 0.67 respectively. Sperm function (capacitation and acrosome reaction) was assessed to determine whether this could also contributed to the decreased litter size.

In the wild type capacitated sperm, a decrease in fluorescence intensity was observed, indicating the occurrence of capacitation (Figure 6). In the sperm of knockout mice, there was no significant decrease in fluorescence intensity, indicating that spermatozoa of knockout mice failed to undergo capacitation. In the sperm of wild type mice increased fluorescence of Fluo-3AM was evident, indicating the occurrence of acrosome reaction (Figure 6). Similar increase in the fluorescence intensity was also observed in the sperm of knockout mice, suggesting that acrosome reaction may not be affected in *Upk1a* ablated mice.

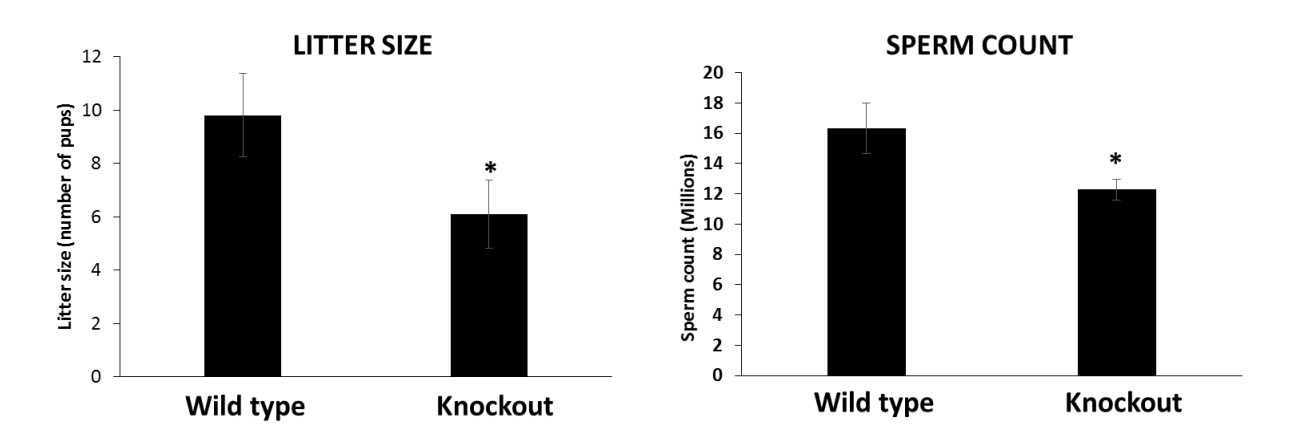


Figure 5. Fecundity in wild type and Upk1a knockout mice. **A.** Litter size. Adult wild type and knockout mice (n=6 each) were mated with females of proven fertility for a week. The number of pups born were noted. **B.** Caudal spermatozoa were collected in phosphate buffered saline (pH 7.0) and counted in a hemocytometer. Values expressed are mean \pm S.D. * indicates p < 0.05 compared to the wild type control.

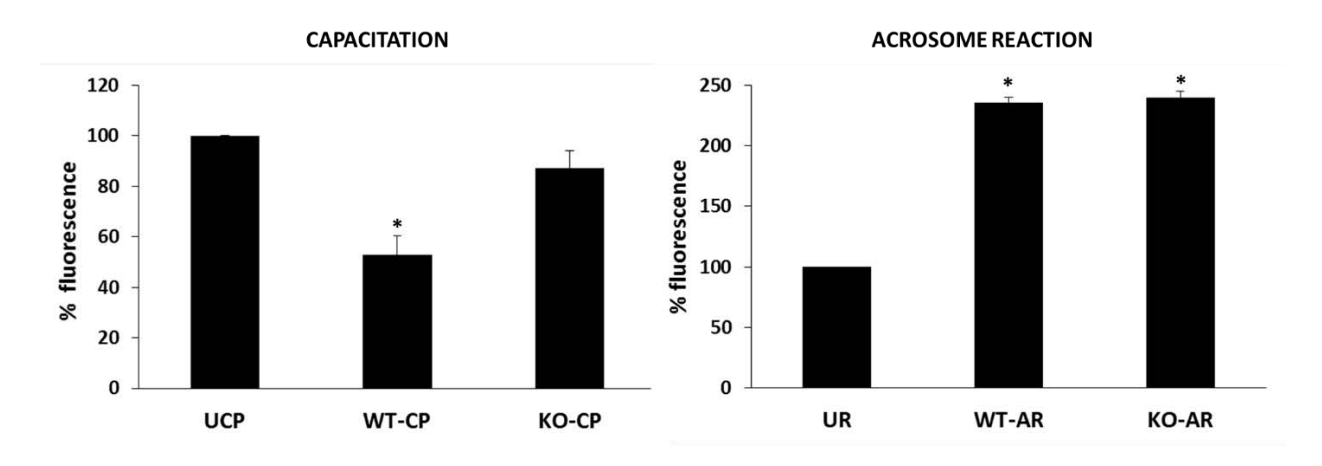


Figure 6. Sperm function in wild type and Upk1a knockout mice. (A). Capacitation. Caudal sperm were incubated with the cholesterol binding dye fillipin (25 μ M) and allowed to capacitate. Fluorescence intensity was measured in a flow cytometer with excitation and emission wavelengths at 340 and 425 nm respectively. (B). Acrosome reaction. Spermatozoa collected from the cauda were subjected to spontaneous acrosome reaction using the ionophone (A23187;10 μ M). They were then stained with Fluo 3-AM (10 mM) and the fluorescence intensity measured in a flow

cytometer with excitation and emission wavelengths set at 488 nm and 515–540 nm respectively. The fluorescence intensity of capacitated / acrosome reacted spermatozoa is expressed as percent relative to the fluorescence intensity observed in the uncapacitated / acrosome intact spermatozoa. UCP – uncapacitated; WT-CP – wild type capacitated; KO-CP – knockout capacitated; UR – unreacted; WT-AR – wild type acrosome reacted; KO-AR – knockout acrosome reacted; VA and VA indicates VA indicates VA compared to VA indicates VA indi

2.3.4. Histopathology

Anatomical changes that may occur in the *Upkla* knockout mice was evaluated by subjecting different tissues to histopathological evaluation (Table 2 / Figure 7, 8, 9 and 10). Moderate inflammation in tubules along with mild hyperplasia of tubular epithelial cells was observed in the caput epididymis (Figure 7). In the cauda epididymis severe ductular atrophy characterized by mucosal epithelial cells surrounded by dense thickened fibrosis / connective tissue was observed (Figure 7). Testes were characterized with foci of seminiferous tubular edema, mild degenerative changes, mild hyperplasia of Leydig cells and mild edema / accumulation of fluids in between tubules (Figure 7). Prostate was characterized with severe atrophy of tubular glands in which massive proliferation of fibrous/ connective tissue surrounding the mucosal epithelial of tubular glands and atrophy of mucosal epithelial cells /glands with infiltration of multinucleated giant cells (Figure 7). Foci of mild degenerative changes in mucosal epithelial cells was evident in the seminal vesicle (Figure 8). In the bladder, severe mucosal transitional epithelial (urothelium) hyperplasia and severe sub mucosal fibrosis; accumulation of inflammatory exudate with dead debris and inflammatory cells in lumen was evident (Figure 8). In the kidney, atrophy of glomerulus, severe tubular nephritis in associated with tubular/ interstitial inflammation, degeneration and fibrosis, while some of the tubules were in dysplastic or pre neoplastic stages (Figure 8). Liver was characterized by mild foci of infiltration of inflammatory cells in centri lobular region, whereas normal portal region with portal vein, bile duct and hepatic artery was observed (Figure 8). Lungs displayed moderate alveolar/interstitial edema with inflammation and fibrosis (Figure 9). The brain was characterized with multiple foci of apoptotic neurons while morphology of frontal cortex, hippocampus and cerebral cortex was normal (Figure 9). Though normal morphology of acinar cells was observed in the pancreas, atrophy of islets was evident (Figure 9). Normal morphology of the heart and spleen was evident (Figure 10).

 Table 2. Histopathological changes in wild type and Upkla knock out mice

Tissue	Wild type	Upk1a knockout
Caput	Normal morphology	Moderate inflammation in tubules [red arrow] along with mild hyperplasia of tubular epithelial cells [green arrow]
Cauda	Normal morphology	Severe ductular atrophy characterized by mucosal epithelial cells surrounded by dense thickened fibrosis / connective tissue.
Testis	Mild interstitial edema/ accumulation of fluids in between seminiferous tubules. Mild proliferation of Leydig cells.	Foci of seminiferous tubular edema and mild degenerative changes. Mild hyperplasia of Leydig cells. Mild edema / accumulation of fluids in between tubules
Seminal vesicle	Normal morphology	Foci of mild degenerative changes in mucosal epithelial cells.
Prostate	Normal morphology of mucosal glands.	Severe atrophy of tubular glands in which massive proliferation of fibrous/ connective tissue surrounding the mucosal epithelial of tubular glands. Atrophy of mucosal epithelial cells /glands with infiltration of multinucleated giant cells.
Bladder	Moderate sub mucosal inflammation and fibrosis.	Severe mucosal transitional epithelial [urothelial] hyperplasia [Red arrow] and severe sub mucosal fibrosis [green arrow]. Accumulation of inflammatory exudate with dead debris and inflammatory cells in lumen.
Pancreas	Normal morphology of islets.	Normal morphology of acinar cells of pancreas. Atrophy of islets of pancreas with apoptosis of beta cells.
Spleen	Normal morphology of lymphatic follicles	Normal morphology of lymphatic follicles were observed
Kidney	Normal morphology.	Atrophy of glomerulus, severe tubular nephritis is associated with tubular/ interstitial inflammation, degeneration and fibrosis [Red arrow]. Some of the tubules are in dysplastic or pre neoplastic stages [green arrow].
Liver	Normal morphology.	Mild foci of infiltration of inflammatory cells found in centri lobular region. Normal portal region with portal vein, bile duct and hepatic artery.
Heart	Normal morphology.	Normal morphology
Lungs	Normal morphology.	Moderate alveolar/ interstitial edemawith inflammation and fibrosis.
Brain	Normal morphology.	Multiple foci of apoptotic neurons. Normal morphology of frontal cortex, hippocampus and cerebral cortex.

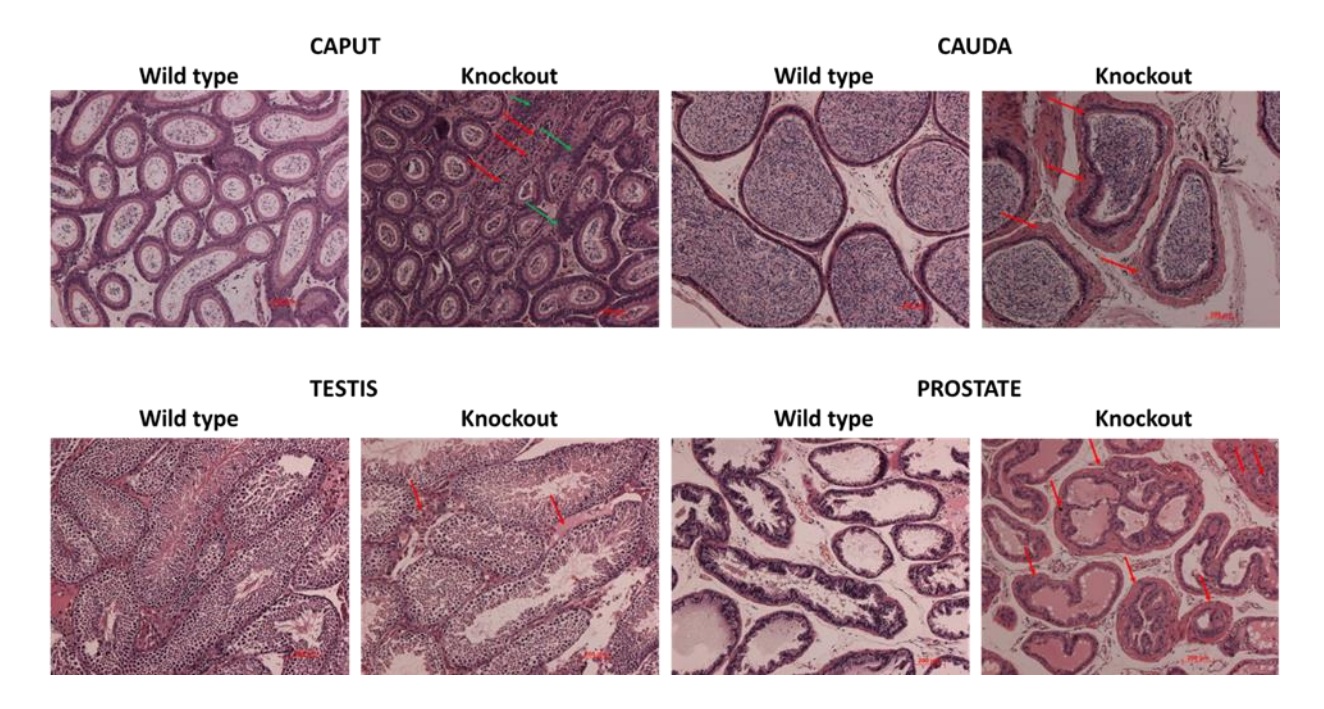


Figure 7. Histopathological analyses of caput, cauda, testis and prostate in wild type and Upkla knockout mice. Five micron sections of the tissues were made and stained with Hematoxylin and Eosin and observed for histopathological changes under a light microscope (magnification: 200 µm). Arrows indicate the histological damage. Caput: Moderate inflammation in tubules [red arrow], mild hyperplasia of tubular epithelial cells [green arrow]. Cauda: Severe ductular atrophy and dense thickened fibrosis / connective tissue. Testis: Seminiferous tubular edema, mild hyperplasia of Leydig cells and accumulation of fluids in between tubules. Prostate: Severe atrophy of tubular glands, massive proliferation of fibrous/ connective tissue, atrophy of mucosal epithelial cells /glands and infiltration of multinucleated giant cells.

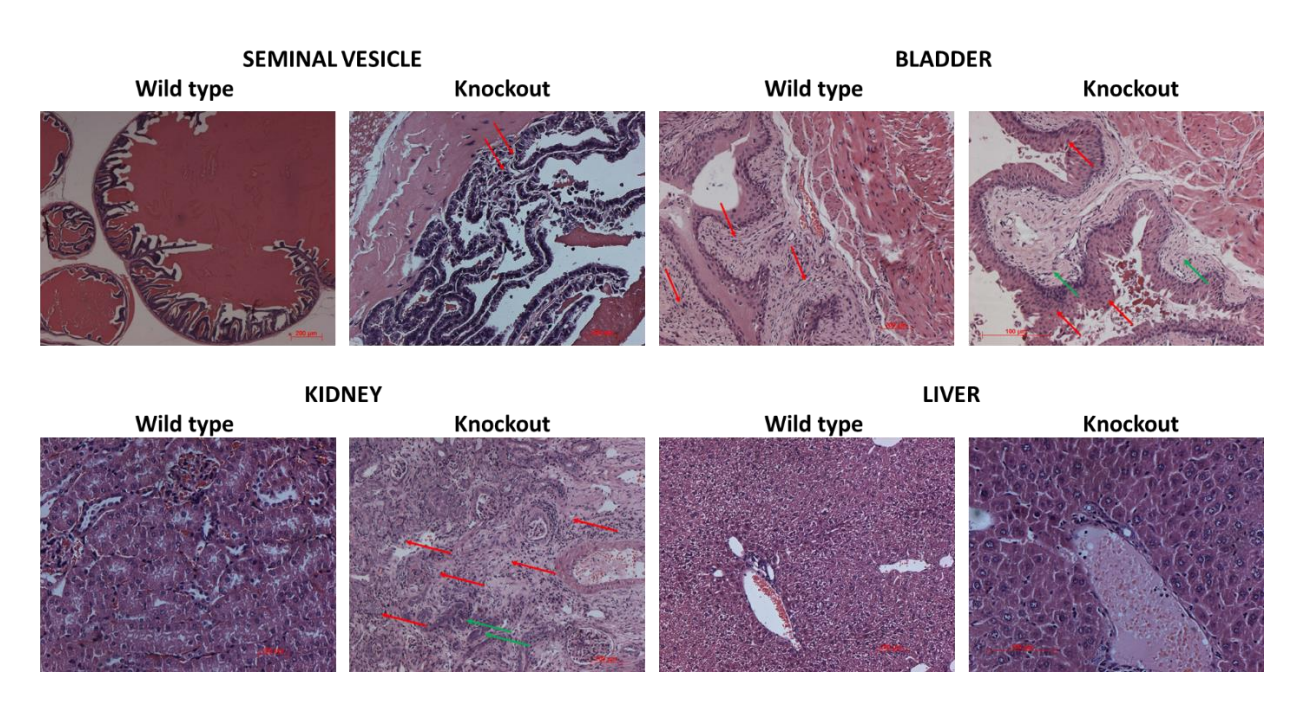


Figure 8. Histopathological analyses of seminal vesicle, bladder, kidney and liver in wild type and Upkla knockout mice. Five micron sections of the tissues were made and stained with Hematoxylin and Eosin and observed for histopathological changes under a light microscope (magnification: 200 µm; bladder and liver of knockout 100 µm). Arrows indicate the histological damage. Seminal Vesicle: Foci of mild degenerative changes in mucosal epithelial cells. Bladder: Severe mucosal transitional epithelial [urothelial] hyperplasia [Red arrow] and severe sub mucosal fibrosis [green arrow]. Accumulation of inflammatory exudate and inflammatory cells in lumen. Kidney: Atrophy of glomerulus, severe tubular nephritis and tubular/interstitial inflammation, degeneration and fibrosis [Red arrow]. Dysplastic or pre neoplastic stages of tubules [green arrow]. Liver: Infiltration of inflammatory cells in centri lobular region.

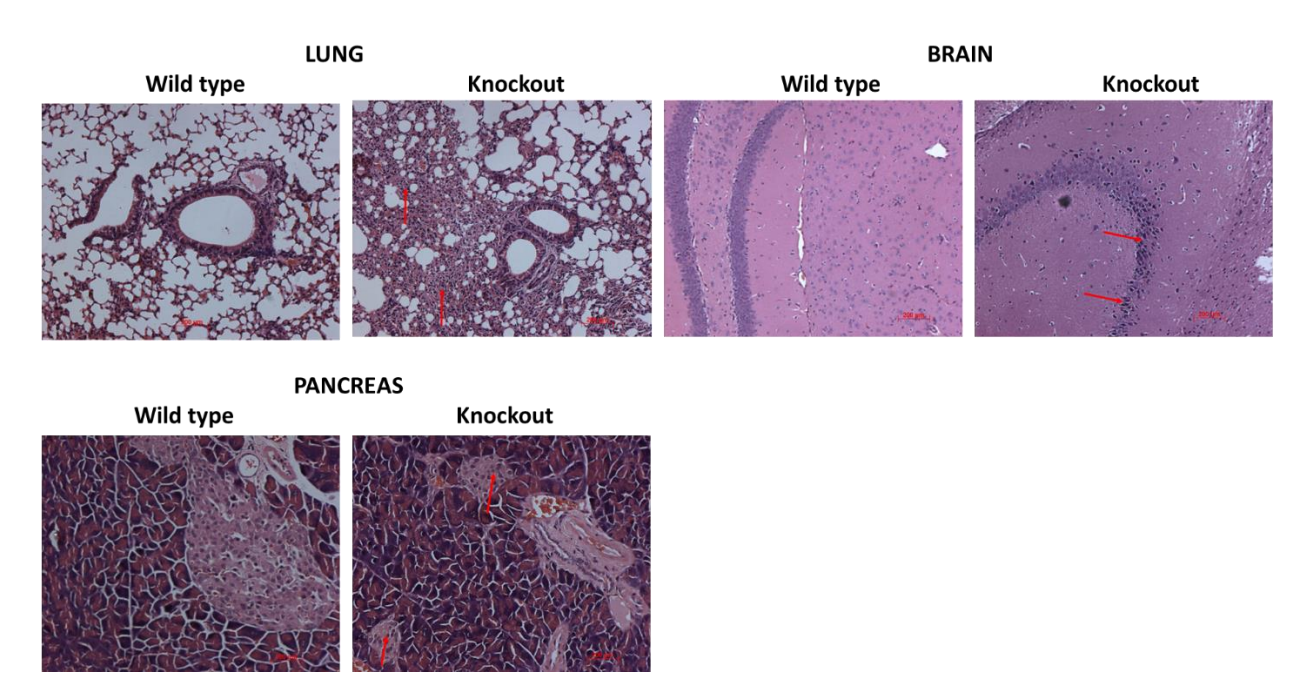


Figure 9. Histopathological analyses of lung, brain and pancreas in wild type and Upk1a knockout mice. Five micron sections of the tissues were made and stained with Hematoxylin and Eosin and observed for histopathological changes under a light microscope (magnification: 200 μm). Arrows indicate the histological damage. Lung: Moderate alveolar/ interstitial edema with inflammation and fibrosis. Brain: Multiple foci of apoptotic neurons. Pancreas: Atrophy of islets of pancreas with apoptosis of beta cells.

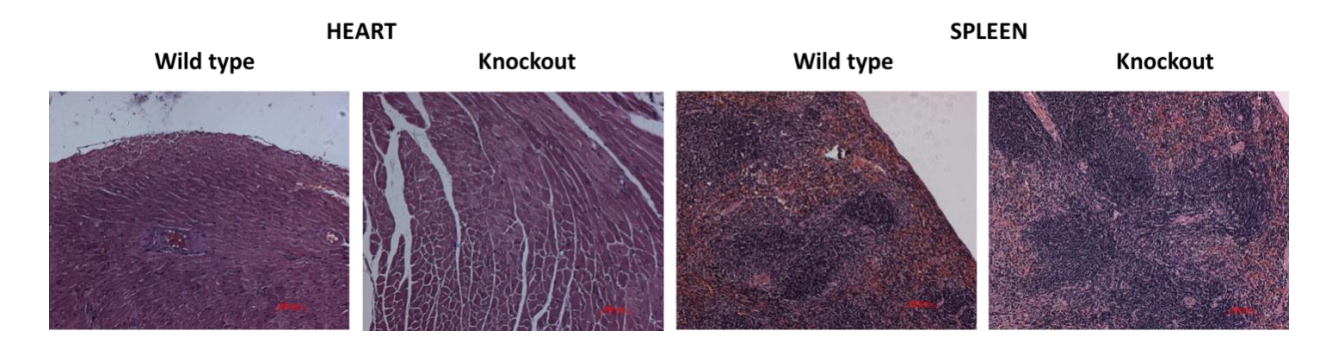


Figure 10. Histopathological analyses of heart and spleen in wild type and Upk1a knockout mice. Five micron sections of the tissues were made and stained with Hematoxylin and Eosin and observed for histopathological changes under a light microscope (magnification: 200 μm).

2.3.5. UPEC infection and bacterial clearance

Since UPK1A is a crucial component of the plaques that protect the urothelium, we analyzed the effect of ablation of this protein on UPEC infection and time dependent efficacy of clearance of the bacterial cells. After day 1 of infection, no significant difference in the number of UPEC was observed in the caput, cauda, testes, seminal vesicle, prostate, bladder, kidney and liver of *Upk1a* knockout mice, when compared to the wild type (Figures 11 and 12). The number of UPEC continued to remain significantly high in all the tissues of knockout mice at 3 days after infection, when compared to the tissues of wild type mice. Similar trend was observed at the 5 day time point (Figures 11 and 12).

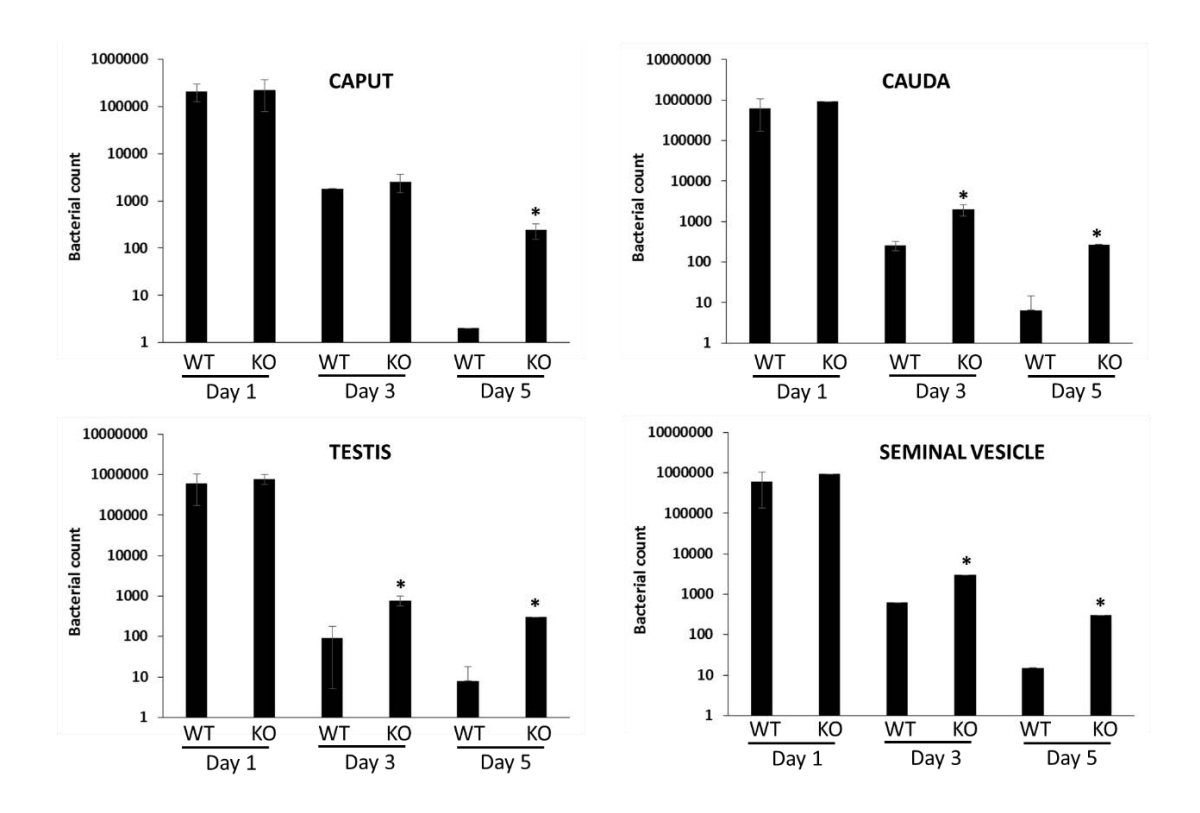


Figure 11. Bacterial clearance in UPEC injected wild type and Upk1a knockout mice. Adult wild type and Upk1a knockout mice were intraperitoneally injected with 30,000 cfu of UPEC suspended in 100 ul PBS. Caput, cauda, testis and seminal vesicle were collected at 1, 3 and 5 days after injection. Real time PCR was performed for the UPEC specific gene papC to determine the number of UPEC present in the tissues. * indicates p < 0.05 compared to the wild type at each time point.

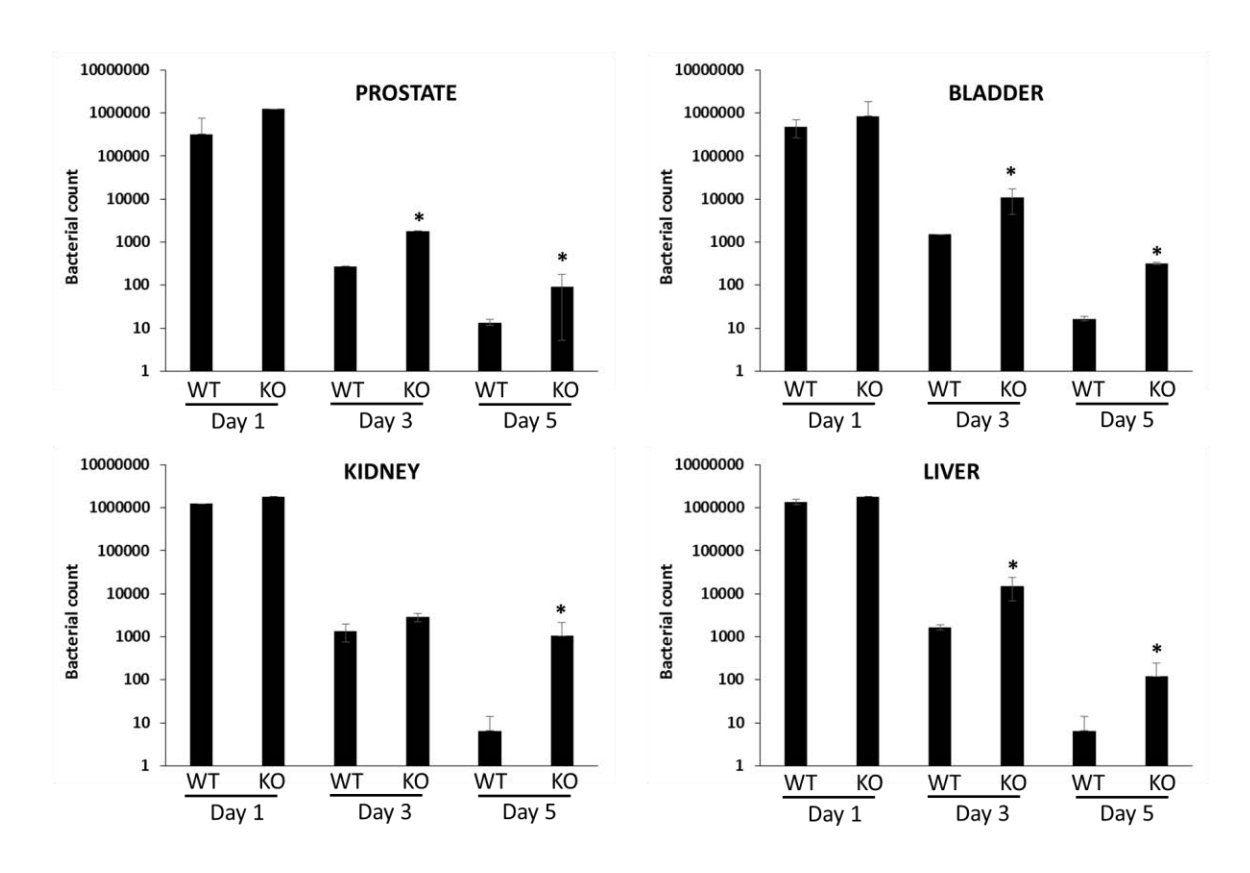


Figure 12. Bacterial clearance in UPEC injected wild type and Upk1a knockout mice. Adult wild type and Upk1a knockout mice were intraperitoneally injected with 30,000 cfu of UPEC suspended in 100 ul PBS. Prostate, bladder, kidney and liver were collected at 1, 3 and 5 days after injection. Real time PCR was performed for the UPEC specific gene papC to determine the number of UPEC present in the tissues. * indicates p < 0.05 compared to the wild type at each time point.

2.3.6. Transcriptome analyses

Since the reduced fecundity observed in knockout mice was found to be concomitant with reduced sperm count, we analyzed the differential global transcriptome changes in the testis of these mice in comparison to the wild type mice. Details of the different types of genes that are differentially expressed are presented (Table 3). Among the 34503 genes analyzed, 148 of them were differentially expressed (67 up regulated and 81 down regulated). The list of up and down regulated genes are provided in <u>supplementary table 1 and 2</u> respectively (*Please click on the link provided to access supplementary data*). Surprisingly, we observed that 1128 genes that are expressed in the testis of wild type mice were completely absent in the knockout mice (<u>Supplementary table 3</u>). On the contrary, 2330 genes were found to be expressed only in the testis

of knockout mice, but absent in the wild type (supplementary table 4). Gene ontology using DAVID software was evaluated to understand the possible physiological processes that could be affected by the genes that are unique in the testis of wild type and knockout mice (supplementary tables 5 and 6). The processes in which at least 20 genes were implicated are listed (Tables 4 and 5). The set of genes that were absent in the testis of *Upk1a* knockout mice (uniquely expressed in wild type) primarily affected the integral components of membrane (plasma membrane), G-protein receptor activity and signaling, olfactory receptor activity and perception of smell and in organization of extracellular space / region (Table 4). The set of genes that were uniquely expressed in *Upk1a* knockout mice (absent in wild type mice) predominantly affected the integral components of membrane (plasma membrane), G-protein receptor activity and signaling, olfactory receptor activity and perception of smell, organization of extracellular space / region, immune and inflammatory responses to pathogens (Table 5). We also conducted gene ontology analyses for genes that were differentially expressed (Supplementary table 7). Interestingly, we observed that genes involved in spermatid development, meiotic cell cycle, regulation of gene expression and synaptonemal complex were differentially regulated (Table 6).

Table 3. Distribution of genes in the testis of Upkla knockout vs wild type Mice

	Coding	Noncoding (IncRNA, snoRNA, snRNA)	Unassigned	sRNA	Ribosomal	tRNA	Others	TOTAL
Genes analyzed (in number)	19421	4934	8499	0	2	0	1647	34503
Differentially expressed	58	30	52	0	0	0	8	148
Up regulated*	29	13	21	0	0	0	4	67
Down regulated#	29	17	31	0	0	0	4	81

^{*}Log2FC > 1.0 and p <0.05; #Log2FC < -1.0 and p < 0.05;

Table 4. Processes influenced by genes that are absent in the testis of Upkla knockout mice (unique to wild type)

Category	ID and Description	Count
CC	GO:0016021- Integral component of membrane	173
CC	GO:0005886- Plasma membrane	153
MF	GO:0004930- G-protein coupled receptor activity	122
BP	GO:0007186- G-protein coupled receptor signalling pathway	104
MF	GO:0004984- Olfactory receptor activity	91
BP	GO:0007608- Sensory perception of smell	84
CC	GO:0005615- Extracellular space	57
CC	GO:0005576- Extracellular region	49
CC	GO:0005887- Integral component of plasma membrane	40
BP	GO:0007165- Signal transduction	31
MF	GO:0005549- Odorant binding	31

Table 5. Processes influenced by genes that are uniquely expressed in the testis of Upkla knockout mice (absent in wild type)

Category	ID and Description	Count
CC	GO:0016021- Integral component of membrane	309
CC	GO:0005886- Plasma membrane	258
BP	GO:0007186- G-protein coupled receptor signalling pathway	159
MF	GO:0004930- G-protein coupled receptor activity	157
CC	GO:0005615- Extracellular space	147
BP	GO:0007608- Sensory perception of smell	114
MF	GO:0004984- Olfactory receptor activity	114
CC	GO:0005576- Extracellular region	102
BP	GO:0007165- Signal transduction	56
CC	GO:0005887- integral component of plasma membrane	54
CC	GO:0009897- Eexternal side of plasma membrane	42
BP	GO:0045087- Iinnate immune response	41
BP	GO:0006955- Immune response	35
MF	GO:0005549- Odorant binding	35
BP	GO:1990830- Cellular response to leukemia inhibitory factor	34
BP	GO:0042742- Defense response to bacterium	31
BP	GO:0019236- Response to pheromone	30
MF	GO:0016503- Pheromone receptor activity	30
BP	GO:0071222- Cellular response to lipopolysaccharide	23
MF	GO:0005125- Cytokine activity	22

BP	GO:0006954- Inflammatory response	21
----	-----------------------------------	----

Table 6. Processes influenced by genes that are differentially expressed in the testis of Upkla knockout vs wild type mice.

Category	ID and Description	
BP	GO:0007186- G-protein coupled receptor signalling pathway	9
MF	GO:0004930- G-protein coupled receptor activity	9
BP	GO:0007286- Spermatid development	5
BP	GO:0051321- Meiotic cell cycle	5
BP	GO:0010468- Regulation of gene expression	5
CC	GO:0000795- Synaptonemal complex	5

2.4. Discussion

UPKs initially thought to play a critical role in protecting the urothelium have increasingly been reported for their multifunctional role in many normal physiological processes besides their implication in pathological conditions. The functional role of UPKs have been evaluated in transgenic animal model systems. *Upk2* and *Upk3a* knockout mice exhibit significant alterations in bladder function (Aboushwareb *et al.*, 2009). Abnormal targeting and defective glycosylation of *Upk1b* was reported in *Upk3* knockout mice (P. Hu *et al.*, 2000). Using Upk1b knock mice, the importance of this protein in urinary tract development, urothelial differentiation and homeostasis was demonstrated (Carpenter *et al.*, 2016). In terms of reproductive function, Upk2/3a double knockout mice were sub fertile (Liao, Chang, Liang, Chung, Wei, Nguyen, Zhou, Talebian, Krey, Deng, Wong, Chicote, Grifo, Keefe, Shapiro, Lepor, Wu, DeSalle, Garcia-España, *et al.*, 2018). In view the limited information on the role of UPKs in male reproductive function, we used *Upk1a* knockout mice to gain further insights.

The relative organ weights of caput epididymis and testis were significantly reduced in the *Upk1a* knockout mice indicates the importance of this protein in developmental processes of these organs. Alterations in the maturation of gametes and gamete delivery organs and the implication of *Upk3b* was demonstrated (Kuriyama *et al.*, 2017). The decreased weight of epididymis and testis could have contributed to the decreased fecundity observed in this study. On the other hand, significant increase in the relative organ weight of bladder, kidney and prostate was observed.

UPKs have been implicated in a variety of cancers (Matuszewski et al., 2016). The increase in the weight of bladder, kidney and prostate could be due to the loss of controlling mechanisms of *Upk1a* both at developmental and in adult stages. However, in depth investigations are required to determine the role of *Upk1a* in controlling the mechanisms that govern organ development and cellular homeostasis. Histopathological analyses revealed inflammation, hypertrophy and degenerative changes in the epididymis, testis, prostate and seminal vesicle of *Upk1a* knockout mice. Such histopathological changes in the male reproductive tract tissues implicated with loss of *Upk1a* were not reported previously. It is possible that the histological damages in the male reproductive tract tissues could have contributed to deficiency in spermatogenesis (due to altered composition of seminal secretions of seminal vesicles and prostate) there by resulting in reduced fecundity observed in this study. Anatomical damages were also observed in the bladder, kidney, liver, lungs and brain. Limited information is available on the histopathological changes that occur under conditions of *Upk* knockdown. Loss of *Upk3* was associated with urothelial barrier defect (Zwaans et al., 2021). Accelerated renal parenchymal loss was evident in Upkla knockout mice (Jackson et al., 2018). The damage to liver, lung and brain observed in the Upkla knockout mice indicate a far reaching role of this protein in multiple organ systems. Further studies are warranted to decipher the physiological, cellular and molecular aspects in these organs in *Upk1a* knockout mice.

The role of UPKs in mammalian reproductive physiology is not well reported. In this study, the male reproductive function in terms of fecundity and spermatogenesis appear to be hampered in Upk1a knockout mice, though capacitation and acrosome reaction was not affected. Reduced fertilization rates and decreased fecundity was previously reported in Upk3a knockout mice (Liao, Chang, Liang, Chung, Wei, Nguyen, Zhou, Talebian, Krey, Deng, Wong, Chicote, Grifo, Keefe, Shapiro, Lepor, Wu, DeSalle, Garcia-Espana, $et\ al.$, 2018). It is established that the average litter size of C57BL/6J mice strain is 5 to 11 and it depended on the maternal weight gain (Finlay, Liu, Ermel, & Adamson, 2015). Our results indicate that the average litter size litter size of wild type mice was 9.81 ± 1.55 and that Upk3a knockout mice was 6.1 ± 1.28 and the difference was statistically significant. It appears that the knockout mice are producing average litter size. However, the average maternal weight gain was not noted in this study. Thus, with the current results with us, it appears to be ambiguous whether the Upk1a knockout mice show reduced fertility. We demonstrated the localization of UPKs in male reproductive tract and on spermatozoa

(Babu Munipalli & Yenugu, 2019) and predicted a crucial role for these proteins in this organ system. Results of this study provided evidence that *Upkla* may govern events in spermatogenesis; and it would be interesting to explore further studies in this direction. It is a very well establishedfact that *Upk1a* acts as an anchor for UPEC adherence to urothelium. The binding of UPKs to the type I pili of the bacteria induces signaling in bladder cells and play a vital role in urinary tract infections (Thumbikat, Berry, Schaeffer, & Klumpp, 2009; Thumbikat, Berry, Zhou, et al., 2009). In this study, we observed that the number of UPEC continued to remain higher in *Upk1a* knockout mice up to 5 days after challenge, when compared to wild type mice. The absence of *Upk1a* does not allow binding of UPEC to urothelial cells thereby lacking initiate signaling cascades for innate responses to clear the bacterium. Further, a variety of factors such as cytokines play an important role in bacterial clearance (Muñoz-Carrillo et al., 2018). In the transcriptome analyses of this study, we observed that immune and inflammatory responses to pathogens were also affected due to differential expression of genes in *Upk1a* knockout mice. It is possible that the key factors of inflammation, especially cytokines may have a role in the decreased bacterial clearance in this study. Studies directed to evaluate the role of cytokines in bacterial clearance in *Upk1a* knockout mice are warranted.

Extensive transcriptome analysis under conditions of *Upk* gene ablation are not yet reported. Since reduced fecundity was associated with compromised spermatogenesis in this study, we conducted high throughput transcriptome analyses using RNA isolated from the testis. Though differential expression of many genes was observed, an interesting aspect is the unique expression of 2330 genes and absence of 1128 genes in the testis of *Upk1a* knockout mice. Gene ontology analyses indicated that these genes are involved in integral components of membrane (plasma membrane), G-protein receptor activity and signaling, olfactory receptor activity and perception of smell, organization of extracellular space / region, immune and inflammatory responses to pathogens. It is well established that UPKs are trans membrane proteins and form an integral part of the urothelium not only in the bladder but in other urinary tract tissues (Matuszewski *et al.*, 2016). The perturbations in the processes related to plasma membrane, G-protein signaling and receptor activity are in line with the aspects of UPK localization and function. The implication of odorant receptors in sperm chemotaxis is gaining importance (Ali *et al.*, 2021). It is possible that an interplay may exist between *Upk1a* and olfactory receptors. Significant reduction in the levels of UPK3 was associated with inflammation in observed in patients with chronic spinal cord Injury

and recurrent urinary tract infections (S. Y. Wu et al., 2022). Inflammation in bladder tissues after irradiation in mice was associated with decreased UPK3 expression (Zwaans et al., 2021). The differential expression of genes that play role in inflammation due to *Upk1a* knock down reinforces the role of UPKs in many disease processes. In the set of genes that were differentially expressed in the testis of *Upk1a* knockout vs wild type mice, processes that belonged to spermatid development, meiotic cell cycle, regulation of gene expression and synaptonemal complex were affected; all of which are crucial in spermatogenesis. Knockdown of cyclin-dependent kinase 7 (CDK7) resulted in failure of meiosis initiation, DNA repair and synaptonemal complex formation in the spermatogonia of mice (X. Chen et al., 2021). Similarly, Transactive response DNA-binding protein of 43 kDa (TDP-43) knockout mice displayed synaptonemal defects and failure of meiosis in spermatocytes (Thumbikat, Berry, Schaeffer, et al., 2009). Thus, the differential expression of genes that govern meiosis and synaptonemal complex formation in *Upk1a* knockout mice indicates the role of this gene in spermatogenesis and this could be one of the reasons for the decreased sperm count observed in this study. We observed that large number of genes were exclusively expressed in the testis of knockout mice and at the same time many genes that were expressed in the testes of wild type mice were absent in the knockout mice. Gene ontology analyses revealed that some of the pathways were commonly affected in both these conditionsi.e. genes specifically expressed in either WT or KO mice testis. However, the number of genes that are involved vary a lot in each of the pathway under these two different conditions. As a matter of caution, it is to be stated that whether the enrichment or absence of these genes in the knockout mice will affect the pathways in an enhanced or downgraded responses needs in depth investigation.

In conclusion, we report that *Upk1a* knockout mice are sub-fertile with compromised sperm count, and displayed impaired capacitation but normal acrosome reaction. Anatomical damage to the male reproductive tissues (caput, cauda, testis, prostate and seminal vesicle) as well as non-reproductive tissues (bladder, pancreas, kidney, liver and brain) were evident, suggesting that this gene plays role in the functioning of multiple organs. The lower efficiency of bacterial clearance in the tissues of *Upk1a* mice indicates the failure of initiating signaling mechanisms of the urothelium to sense and clear the invading pathogens. Differential expression of genes involved in a variety of physiological process due to *Upk1a* ablation further reinforces the crucial role of this gene in normal and disease processes.

2.5. References

- Aboushwareb, T., Zhou, G., Deng, F. M., Turner, C., Andersson, K. E., Tar, M., . . . Christ, G. J. (2009). Alterations in bladder function associated with urothelial defects in uroplakin II and IIIa knockout mice. *Neurourology and Urodynamics*, 28(8), 1028-1033. doi:10.1002/nau.20688
- 2. Ali, M. A., Wang, Y., Qin, Z., Yuan, X., Zhang, Y., & Zeng, C. (2021). Odorant and Taste Receptors in Sperm Chemotaxis and Cryopreservation: Roles and Implications in Sperm Capacitation, Motility and Fertility. *Genes (Basel)*, 12(4). doi:10.3390/genes12040488
- 3. Babu Munipalli, S., & Yenugu, S. (2019). Uroplakin expression in the male reproductive tract of rat. *General and Comparative Endocrinology*, 281, 153-163. doi:10.1016/j.ygcen.2019.06.003
- 4. Bou Khalil, M., Chakrabandhu, K., Xu, H., Weerachatyanukul, W., Buhr, M., Berger, T., . . . Tanphaichitr, N. (2006). Sperm capacitation induces an increase in lipid rafts having zona pellucida binding ability and containing sulfogalactosylglycerolipid. *Developmental Biology*, 290(1), 220-235. doi:10.1016/j.ydbio.2005.11.030
- Byun, Y., Choi, Y. C., Jeong, Y., Yoon, J., & Baek, K. (2020). Long Noncoding RNA Expression Profiling Reveals Upregulation of Uroplakin 1A and Uroplakin 1A Antisense RNA 1 under Hypoxic Conditions in Lung Cancer Cells. *Molecules and Cells*, 43(12), 975-988. doi:10.14348/molcells.2020.0126
- Carpenter, A. R., Becknell, M. B., Ching, C. B., Cuaresma, E. J., Chen, X., Hains, D. S., & McHugh, K. M. (2016). Uroplakin 1b is critical in urinary tract development and urothelial differentiation and homeostasis. *Kidney International*, 89(3), 612-624. doi:10.1016/j.kint.2015.11.017
- 7. Chen, S., Zhou, Y., Chen, Y., & Gu, J. (2018). fastp: an ultra-fast all-in-one FASTQ preprocessor. *Bioinformatics*, 34(17), i884-i890. doi:10.1093/bioinformatics/bty560
- 8. Chen, X., Li, Y., Dai, H., Zhang, H., Wan, D., Zhou, X., . . . Zhu, H. (2021). Cyclin-dependent kinase 7 is essential for spermatogenesis by regulating retinoic acid signaling

- pathways and the STAT3 molecular pathway. *IUBMB Life*, 73(12), 1446-1459. doi:10.1002/iub.2574
- 9. de Sena Brandine, G., & Smith, A. D. (2019). Falco: high-speed FastQC emulation for quality control of sequencing data. *F1000Res*, 8, 1874. doi:10.12688/f1000research.21142.2
- 10. Desalle, R., Chicote, J. U., Sun, T. T., & Garcia-Espana, A. (2014). Generation of divergent uroplakin tetraspanins and their partners during vertebrate evolution: identification of novel uroplakins. *BMC Evol Biol*, *14*, 13. doi:10.1186/1471-2148-14-13
- Dobin, A., Davis, C. A., Schlesinger, F., Drenkow, J., Zaleski, C., Jha, S., . . . Gingeras, T.
 R. (2013). STAR: ultrafast universal RNA-seq aligner. *Bioinformatics*, 29(1), 15-21. doi:10.1093/bioinformatics/bts635
- 12. Finlay, J. B., Liu, X., Ermel, R. W., & Adamson, T. W. (2015). Maternal Weight Gain as a Predictor of Litter Size in Swiss Webster, C57BL/6J, and BALB/cJ mice. *J Am Assoc Lab Anim Sci*, 54(6), 694-699.
- 13. Garcia-Espana, A., Chung, P. J., Zhao, X., Lee, A., Pellicer, A., Yu, J., . . . Desalle, R. (2006). Origin of the tetraspanin uroplakins and their co-evolution with associated proteins: implications for uroplakin structure and function. *Molecular Phylogenetics and Evolution*, 41(2), 355-367. doi:10.1016/j.ympev.2006.04.023
- 14. Hasan, A. K., Fukami, Y., & Sato, K. (2011). Gamete membrane microdomains and their associated molecules in fertilization signaling. *Molecular Reproduction and Development*, 78(10-11), 814-830. doi:10.1002/mrd.21336
- 15. Hu, C. C., Liang, F. X., Zhou, G., Tu, L., Tang, C. H., Zhou, J., . . . Sun, T. T. (2005). Assembly of urothelial plaques: tetraspanin function in membrane protein trafficking. *Molecular Biology of the Cell*, 16(9), 3937-3950. doi:10.1091/mbc.e05-02-0136
- Hu, P., Deng, F. M., Liang, F. X., Hu, C. M., Auerbach, A. B., Shapiro, E., . . . Sun, T. T. (2000). Ablation of uroplakin III gene results in small urothelial plaques, urothelial leakage, and vesicoureteral reflux. *Journal of Cell Biology*, 151(5), 961-972. doi:10.1083/jcb.151.5.961
- 17. Jackson, A. R., Li, B., Cohen, S. H., Ching, C. B., McHugh, K. M., & Becknell, B. (2018). The uroplakin plaque promotes renal structural integrity during congenital and acquired

- urinary tract obstruction. *American Journal of Physiology. Renal Physiology, 315*(4), F1019-f1031. doi:10.1152/ajprenal.00173.2018
- 18. KN, G.-C., AK, O., & DK, M. (2013). Principles for valid histopathologic scoring in research. *Veterinary Pathology*, *50*, 1007-1015.
- 19. Kuriyama, S., Tamiya, Y., & Tanaka, M. (2017). Spatiotemporal expression of UPK3B and its promoter activity during embryogenesis and spermatogenesis. *Histochemistry and Cell Biology*, *147*(1), 17-26. doi:10.1007/s00418-016-1486-8
- 20. Leivo, M. Z., Tacha, D. E., & Hansel, D. E. (2021). Expression of uroplakin II and GATA-3 in bladder cancer mimickers: caveats in the use of a limited panel to determine cell of origin in bladder lesions. *Human Pathology*, 113, 28-33. doi:10.1016/j.humpath.2021.04.005
- 21. Liao, Y., Chang, H. C., Liang, F. X., Chung, P. J., Wei, Y., Nguyen, T. P., . . . Sun, T. T. (2018). Uroplakins play conserved roles in egg fertilization and acquired additional urothelial functions during mammalian divergence. *Molecular Biology of the Cell*, mbcE18080496. doi:10.1091/mbc.E18-08-0496
- 22. Liao, Y., Chang, H. C., Liang, F. X., Chung, P. J., Wei, Y., Nguyen, T. P., . . . Sun, T. T. (2018). Uroplakins play conserved roles in egg fertilization and acquired additional urothelial functions during mammalian divergence. *Molecular Biology of the Cell*, 29(26), 3128-3143. doi:10.1091/mbc.E18-08-0496
- 23. Liao, Y., Smyth, G. K., & Shi, W. (2014). featureCounts: an efficient general purpose program for assigning sequence reads to genomic features. *Bioinformatics*, 30(7), 923-930. doi:10.1093/bioinformatics/btt656
- 24. Love, M. I., Huber, W., & Anders, S. (2014). Moderated estimation of fold change and dispersion for RNA-seq data with DESeq2. *Genome Biology*, 15(12), 550. doi:10.1186/s13059-014-0550-8
- 25. Mahbub Hasan, A. K., Sato, K., Sakakibara, K., Ou, Z., Iwasaki, T., Ueda, Y., & Fukami, Y. (2005). Uroplakin III, a novel Src substrate in Xenopus egg rafts, is a target for sperm protease essential for fertilization. *Developmental Biology*, 286(2), 483-492. doi:10.1016/j.ydbio.2005.08.020

- 26. Martinez, J. J., Mulvey, M. A., Schilling, J. D., Pinkner, J. S., & Hultgren, S. J. (2000). Type 1 pilus-mediated bacterial invasion of bladder epithelial cells. *EMBO Journal*, 19(12), 2803-2812. doi:10.1093/emboj/19.12.2803
- 27. Matuszewski, M. A., Tupikowski, K., Dołowy, Ł., Szymańska, B., Dembowski, J., & Zdrojowy, R. (2016). Uroplakins and their potential applications in urology. *Cent European J Urol*, 69(3), 252-257. doi:10.5173/ceju.2016.638
- 28. Mulvey, M. A., Lopez-Boado, Y. S., Wilson, C. L., Roth, R., Parks, W. C., Heuser, J., & Hultgren, S. J. (1998). Induction and evasion of host defenses by type 1-piliated uropathogenic Escherichia coli. *Science*, 282(5393), 1494-1497. Retrieved from https://www.ncbi.nlm.nih.gov/pubmed/9822381
- 29. Muñoz-Carrillo, J. L., Contreras-Cordero, J. F., Gutiérrez-Coronado, O., Villalobos-Gutiérrez, P. T., Ramos-Gracia, L. G., & Hernández-Reyes, V. E. (2018). Cytokine Profiling Plays a Crucial Role in Activating Immune System to Clear Infectious Pathogens. In R. K. T. a. P. S. Bisen (Ed.), *Immune Response Activation and Immunomodulation*.
- 30. R., K. (2013). Multiparametric and semi-quantitative scoring systems for the evaluation of mouse modelhistopathology—A systematic review. *BMC Veterinary Research*, *9*, 123.
- 31. Rajesh, A., & Yenugu, S. (2015). Effect of immunization against prostate- and testis-expressed (PATE) proteins on sperm function and fecundity in the rat. *Journal of Reproductive Immunology*, 110, 117-129. doi:10.1016/j.jri.2015.02.009
- 32. Rajesh, A., & Yenugu, S. (2017). shRNA mediated ablation of prostate and testis expressed (Pate) messenger RNA results in impaired sperm function and fertility. *Andrology*, *5*(3), 541-547. doi:10.1111/andr.12321
- 33. Sakakibara, K., Sato, K., Yoshino, K., Oshiro, N., Hirahara, S., Mahbub Hasan, A. K., . . . Fukami, Y. (2005). Molecular identification and characterization of Xenopus egg uroplakin III, an egg raft-associated transmembrane protein that is tyrosine-phosphorylated upon fertilization. *Journal of Biological Chemistry*, 280(15), 15029-15037. doi:10.1074/jbc.M410538200
- 34. Sato, K. I., & Tokmakov, A. A. (2019). Membrane Microdomains as Platform to Study Membrane-Associated Events During Oogenesis, Meiotic Maturation, and Fertilization in Xenopus laevis. *Methods in Molecular Biology*, 1920, 59-73. doi:10.1007/978-1-4939-9009-2 5

- 35. Song, Y., Wang, H., Zou, X. J., Zhang, Y. X., Guo, Z. Q., Liu, L., . . . Zhang, D. Y. (2020). Reciprocal regulation of HIF-1α and Uroplakin 1A promotes glycolysis and proliferation in Hepatocellular Carcinoma. *J Cancer*, 11(22), 6737-6747. doi:10.7150/jca.48132
- 36. Szymańska, B., Matuszewski, M., Dembowski, J., & Piwowar, A. (2021). Initial Evaluation of Uroplakins UPIIIa and UPII in Selected Benign Urological Diseases. *Biomolecules*, 11(12). doi:10.3390/biom11121816
- 37. Thumbikat, P., Berry, R. E., Schaeffer, A. J., & Klumpp, D. J. (2009). Differentiation-induced uroplakin III expression promotes urothelial cell death in response to uropathogenic E. coli. *Microbes and Infection*, 11(1), 57-65. doi:10.1016/j.micinf.2008.10.008
- 38. Thumbikat, P., Berry, R. E., Zhou, G., Billips, B. K., Yaggie, R. E., Zaichuk, T., . . . Klumpp, D. J. (2009). Bacteria-induced uroplakin signaling mediates bladder response to infection. *PLoS Pathog*, *5*(5), e1000415. doi:10.1371/journal.ppat.1000415
- 39. Tu, L., Kong, X. P., Sun, T. T., & Kreibich, G. (2006). Integrity of all four transmembrane domains of the tetraspanin uroplakin Ib is required for its exit from the ER. *Journal of Cell Science*, 119(Pt 24), 5077-5086. doi:10.1242/jcs.03285
- 40. Tu, L., Sun, T. T., & Kreibich, G. (2002). Specific heterodimer formation is a prerequisite for uroplakins to exit from the endoplasmic reticulum. *Molecular Biology of the Cell,* 13(12), 4221-4230. doi:10.1091/mbc.e02-04-0211
- 41. Wu, S. Y., Jiang, Y. H., Jhang, J. F., Hsu, Y. H., Ho, H. C., & Kuo, H. C. (2022). Inflammation and Barrier Function Deficits in the Bladder Urothelium of Patients with Chronic Spinal Cord Injury and Recurrent Urinary Tract Infections. *Biomedicines*, 10(2). doi:10.3390/biomedicines10020220
- 42. Wu, X. R., Kong, X. P., Pellicer, A., Kreibich, G., & Sun, T. T. (2009). Uroplakins in urothelial biology, function, and disease. *Kidney International*, 75(11), 1153-1165. doi:10.1038/ki.2009.73
- 43. Wu, X. R., Lin, J. H., Walz, T., Haner, M., Yu, J., Aebi, U., & Sun, T. T. (1994). Mammalian uroplakins. A group of highly conserved urothelial differentiation-related membrane proteins. *Journal of Biological Chemistry*, 269(18), 13716-13724. Retrieved from https://www.ncbi.nlm.nih.gov/pubmed/8175808

- 44. Wu, X. R., Sun, T. T., & Medina, J. J. (1996). In vitro binding of type 1-fimbriated Escherichia coli to uroplakins Ia and Ib: relation to urinary tract infections. *Proceedings of the National Academy of Sciences of the United States of America*, 93(18), 9630-9635. Retrieved from https://www.ncbi.nlm.nih.gov/pubmed/8790381
- 45. Zhu, J., Lu, Q., Li, B., Li, H., Wu, C., Li, C., & Jin, H. (2021). Potential of the cell-free blood-based biomarker uroplakin 2 RNA to detect recurrence after surgical resection of lung adenocarcinoma. *Oncol Lett*, 22(1), 520. doi:10.3892/ol.2021.12781
- 46. Zhu, Z., Xu, J., Li, L., Ye, W., Chen, B., Zeng, J., & Huang, Z. (2020). Comprehensive analysis reveals CTHRC1, SERPINE1, VCAN and UPK1B as the novel prognostic markers in gastric cancer. *Transl Cancer Res*, 9(7), 4093-4110. doi:10.21037/tcr-20-211
- 47. Zwaans, B. M. M., Carabulea, A. L., Bartolone, S. N., Ward, E. P., Chancellor, M. B., & Lamb, L. E. (2021). Voiding defects in acute radiation cystitis driven by urothelial barrier defect through loss of E-cadherin, ZO-1 and Uroplakin III. *Sci Rep*, 11(1), 19277. doi:10.1038/s41598-021-98303-2

Chapter-3

Evaluating the functional role of Uroplakin1a at the molecular level using Yeast Two Hybrid Screening

3.1. Introduction

Protein-protein interactions (PPIs) are crucial in many cellular and sub-cellular processes, such as signaling, ion transport, metabolite trafficking, protein folding, etc. Determination of PPIs is initially accomplished by in silico methods, which involves phylogenetic profiling, identifying structural patterns and homologous pairs, intracellular localization, and post-translational modifications (Barh *et al.*, 2014). The information thus obtained is deposited in PPI databases generated by large-scale integration efforts, including curating the large number of research papers and reports and creating a controlled vocabulary for describing PPI experiments (Kotlyar, Pastrello, Rossos, & Jurisica, 2018). Mutations in the amino acid sequence of the proteins affect PPIs. Identification of such mutations by computational approaches is very important in understanding the consequences effected by the PPIs in the biological system (DK, P, Uppin, S, & CPD, 2018). Further, PPIs have been implicated in a variety of diseases and validated as potential drug targets. For example, the inhibitors of PPIs are developed as therapeutic targets for the treatment of cancer (Hardcastle, 2016).

Production and maturation of male germ cells involve the interaction of a diverse nature of proteins to mediate structural, biochemical and molecular events that are crucial in this process. The etiology of spermatogenic failure involves Testis-Specific Y-Centric Protein-Protein Interaction Network (Ansari-Pour, Razaghi-Moghadam, Barneh, & Jafari, 2016). Human testis-specific protein TEX101, interactome indicated the interactions between proteins that are essential for spermatogenesis and seminal plasma composition (Schiza et al., 2018). Similarly, the amyloid precursor protein interaction network in human testis entails a large number of sentinel proteins crucial for male reproduction (Silva et al., 2015). A combination of RNA and protein profiling data when combined with network interactions identified a large set of genes associated with spermatogenesis in humans and mice (Petit et al., 2015). Interaction of epididymal proteins with sperm proteins has been an active area of study for many decades and continues to be an active area of investigation. For example, rat specific epididymal proteins interaction with sperm was demonstrated in 1980 (Adrina, Fernanda, Gonzalez, Lucrecia, & Jorge, 1980) Interaction of proteins of epididymal origin with spermatozoa.). The sperm proteins are extensively modified due to interaction with the epididymal luminal proteins and these interactions are crucial for sperm function and fertilization (Björkgren & Sipilä, 2019). The protein interactome of Human

Epididymis protein 4 (HE4) plays a crucial role in fertilization, specifically in sperm maturation, motility and capacitation (Kant *et al.*, 2019). The interaction of EPPIN, an epididymis specific protein with proteins in the seminal fluid presented the diversity of PPIs of different organs (Mariani *et al.*, 2020). The interaction of cystic fibrosis transmembrane conductance regulator (CFTR) with fibroblast growth factor (FGF) and luteinizing hormone (LH) are implicated in azoospermia and epididymal maldevelopment caused by cryptorchidism (Hadziselimovic, Verkauskas, & Stadler, 2022).

In the previous chapters, we demonstrated that UPKs are abundantly expressed in the male reproductive tract tissues and on sperm. Ablation of Upk1a by knockout strategy resulted in subfertility in the mice. Further, their expression was modulated during endotoxin / bacterial challenge. It is thus pertinent that these proteins may govern a variety of physiological, cellular, biochemical and molecular processes. The possibility of UPK interaction with proteins that are involved in male gametogenesis and sperm function is worth investigating. Hence, in this part of the study, we report the interacting partners of UPK1A and UPK2 using yeast two hybrid screening technique.

3.2. Materials and methods

3.2.1. Yeast two hybrid screening

The yeast two hybrid screening(Y2H) was performed using Matchmaker Gold Yeast Two-Hybrid System (Takara Cat. No. 630489) to identify the possible interacting partners of UPK1A. It is based on the principle that when the DNA binding domain and activation domain that are expressed as fusion proteins with the bait and prey proteins respectively are in close proximity, transcription of ADE2 and HIS occurs which allows the survival of the yeast on synthetically defined medium that is devoid of certain amino acids (Figure 1).

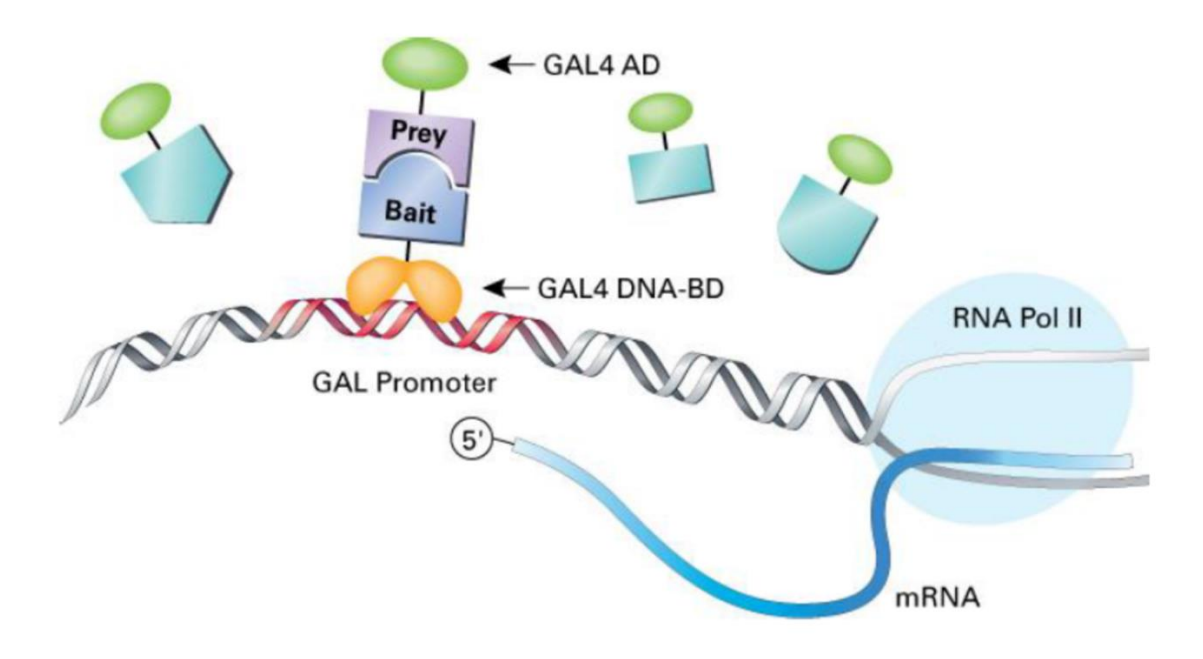


Figure 1. Principle of the yeast two hybrid screening.

The entire procedure consisted of the following basic steps (Figure 2)

- Validation of control plasmids
- Auto-activation and toxicity determination
- Identification of UPK1A interacting partners in the testis cDNA library
- Confirmation of interaction between the partners

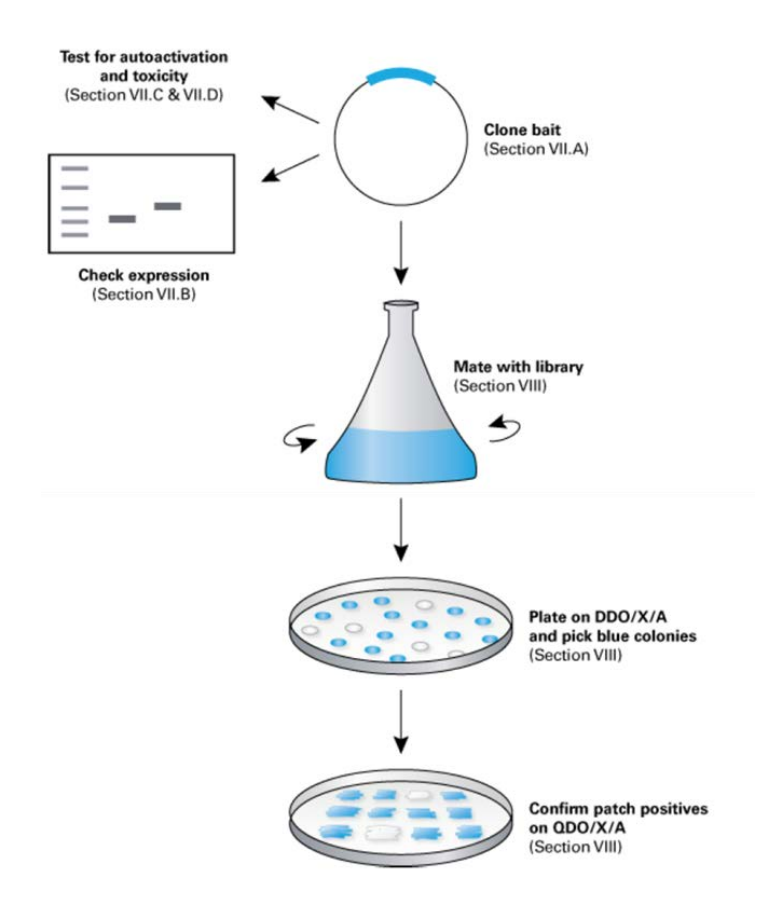


Figure 2. Over view of the yeast 2 hybrid screening procedure.

3.2.2. Performing control experiments for validation

Yeast strains and plasmids

- Y2H Gold *Saccharomyces cerevisiae strain* Y2H Gold detects interactions between the proteins through four reporter gene expressions (*AUR1-C, ADE2, HIS3, and MEL1*).
- Y187 Saccharomyces cerevisiae strain Y187 for prey vector construct transformation and library preparation.
- pGBKT7-BD Vector that encodes the Gal4 DNA binding domain.
- pGADT7-AD Vector that encodes the DNA activation domain.
- pGBKT7-53 Gal4 DNA-BD fused with murine p53
- pGBKT7-Lam Vector that encodes lamin linked with the DNA binding domain
- pGADT7-T Vector that encodes large T-antigen SV40 linked with the activation domain.

Preparation of yeast culture medium and plates

A mixture of yeast extract, peptone, and dextrose was mixed to prepare YPD media essential for the growth of Saccharomyces cerevisiae strains (Y2H Gold and Y187 strains). The synthetically defined (SD) medium is frequently used to cultivate S. cerevisiae that satisfies all yeast cells' nutritional requirements supplemented with carbon and nitrogen. Minimum medium is prepared by adding essential amino acids to the SD medium. Which plasmids and activated reporters are chosen will depend on the specific minimum medium that is used. Leucine and tryptophan are left out of the formulation (or "Dropped Out"), which is why the medium is known as SD/-Trp/-Leu dropout. The SD/-Trp/-Lue dropout medium is employed for choosing pGBKT7, the bait, and pGADT7, the prey plasmids. The other essential amino acids, such as glycine and aspartic acid are present in the medium. Since the plasmids encode genes for biosynthesis of tryptophan, and leucine, the cells carrying Matchmaker bait and prey plasmids can thrive. As part of the two-hybrid assay's confirmation step, the SD/-Trp/-Lue/-His/-Ade dropout nourishment is used to choose the bait and prey plasmids to activate the Gal-responsive HIS3 and ADE2 genes. The colonies that develop on it likewise produce proteins that interact to trigger HIS3 and ADE2 and contain both bait and prey plasmids. After the two-hybrid screen, this medium is used to verify interactions.

Culture of yeast strains and transformation with control plasmids

As an initial step, the yeast strains Y2H Gold and Y187 were grown on YPD plates for use in further experiments (Figure 3). The yeast strains were then transformed with control plasmids (pGBKT7-53, pGBKT7-Lam and pGADT7-T) to test their ability to grow on selection media plates (SD/-Trp and SD/-Lue). The transformation procedure, in brief, is the method followed for transforming the control plasmids into competent yeast cells by polyethylene glycol (PEG)/ lithium acetate (LiAc) (Takara. YeastmakerTM Yeast Transformation System Cat. Nos. 630439). 5 x 10⁶ cells from the overnight incubated primary culture were added to 250 ml of YPD broth and incubated for 4-5 hours at 30°C with constant rotation. 1 x 10⁸ cells from the secondary culture were used for small-scale transformation. The cell pellet was resuspended with 500 μl of PEG/LiAc. The carrier DNA 50 μg and 100 ng plasmid DNA were added to the competence cells. Briefly, vortexed cells were incubated for 40 minutes at 42°C, centrifuged at 13,000 rpm for 15

sec, resuspended in 200 μ l of sterile water and plated the cell suspension on selective dropout media.

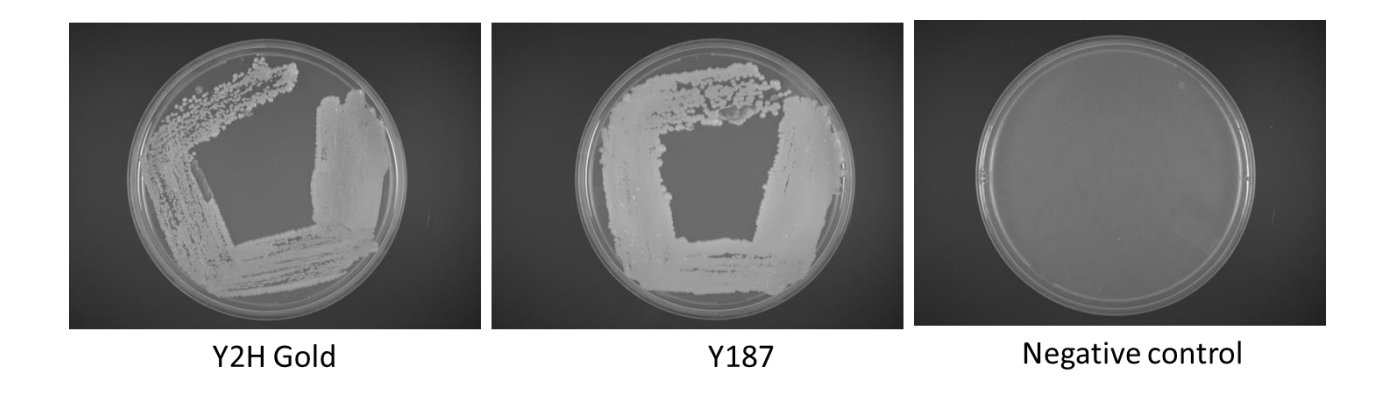


Figure 3. Representative SD agar plates showing the growth of Y2H Gold and Y187. Negative control was included to detect the possible non-specific growth.

Y2H Gold and Y187(prey strain) transformed with the control plasmids displayed growth on SD/-Trp and SD/-Lue agar plates (Figure 4). Colonies that appeared on the SD/-Trp and SD/-Lue plates were streaked onto the fresh plate to confirm their growth (Figure 4). Since the yeast transformed with control plasmids showed growth on selection media, the next step was to perform mating of Y2H Gold transformed pGBKT7-53 with prey strain transformed pGADT7 to demonstrate a positive interaction. Similarly, mating was also conducted between Y2H Gold transformed with pGBKT7-Lam and prey strain transformed with pGADT7-T interacts negatively. Subsequent cross mating among these two conjugants were plated on 2X YPD agar plates. Growth was observed for the conjugants both in the positive and negative interaction experiments (Figure 5). Yeast colonies from the 2X YPD plates were then streaked on to quadruple dropout (SD/-Trp/-Lue/-His/-Ade) agar plates. Growth was observed in conjugants resulting from the mating of Y2H Gold transformed pGBKT7-53 with prey strain transformed pGADT7-T, indicating a positive interaction (Figure 6). Growth was not observed in conjugants that were derived from Y2H Gold transformed with pGBKT7-Lam and prey strain transformed with pGADT7-T mating, indicating a negative interaction. Thus, the authenticity of the plasmids, mating and interaction was established (Figure 6).

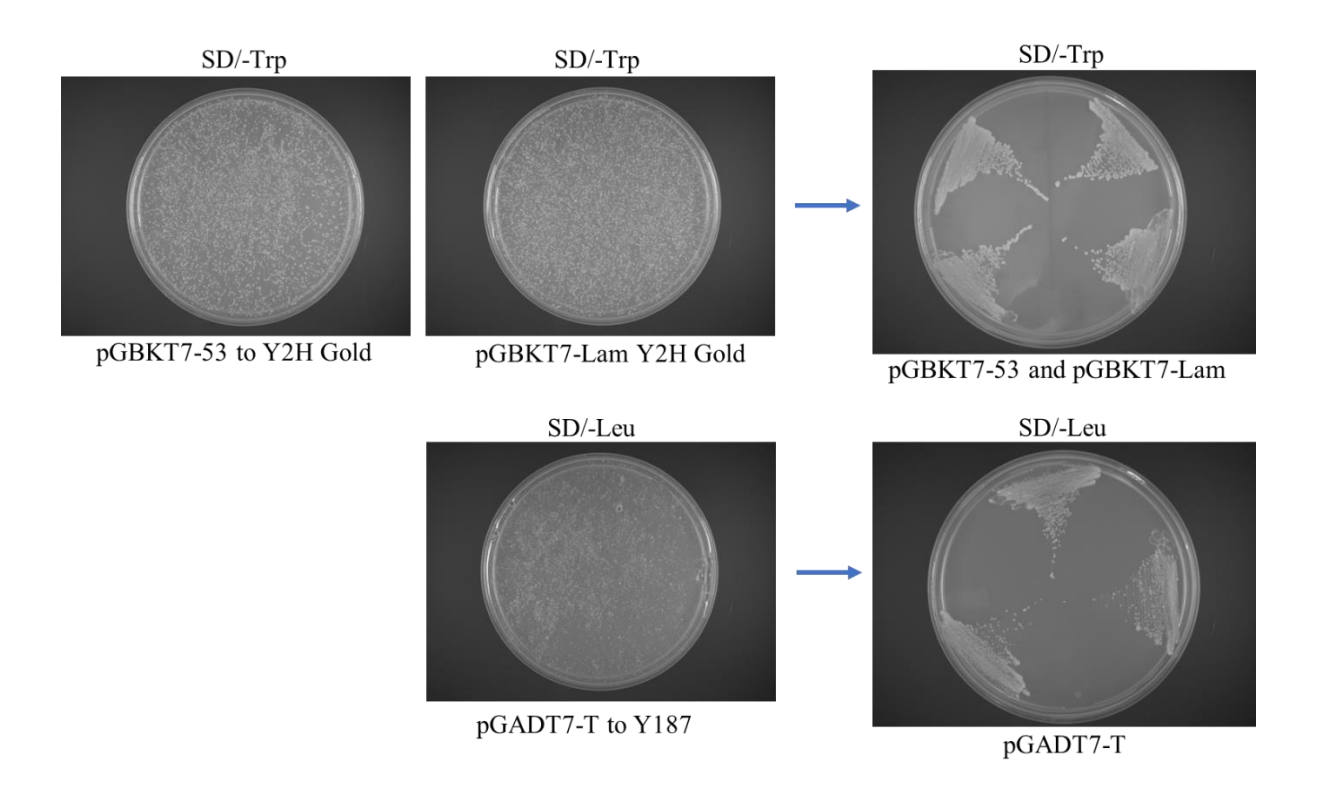


Figure 4. Representative SD/-Trp and SD/-Lue showing the growth of Y2H Gold and Y187 transformed with pGBKT7-53, pGBKT7-Lam and pGADT7 control experiments plasmids. Negative control was included to detect the possible non-specific growth. Colonies that appeared on SD/-Trp and SD/-Lue plates were streaked on to fresh SD/-Trp and SD/-Lue plates. Representative SD/-Trp and SD/-Lue agar plates showing the growth of Y2H Gold and Y187 transformed with control plasmids. Negative control was included to detect the possible non-specific growth.

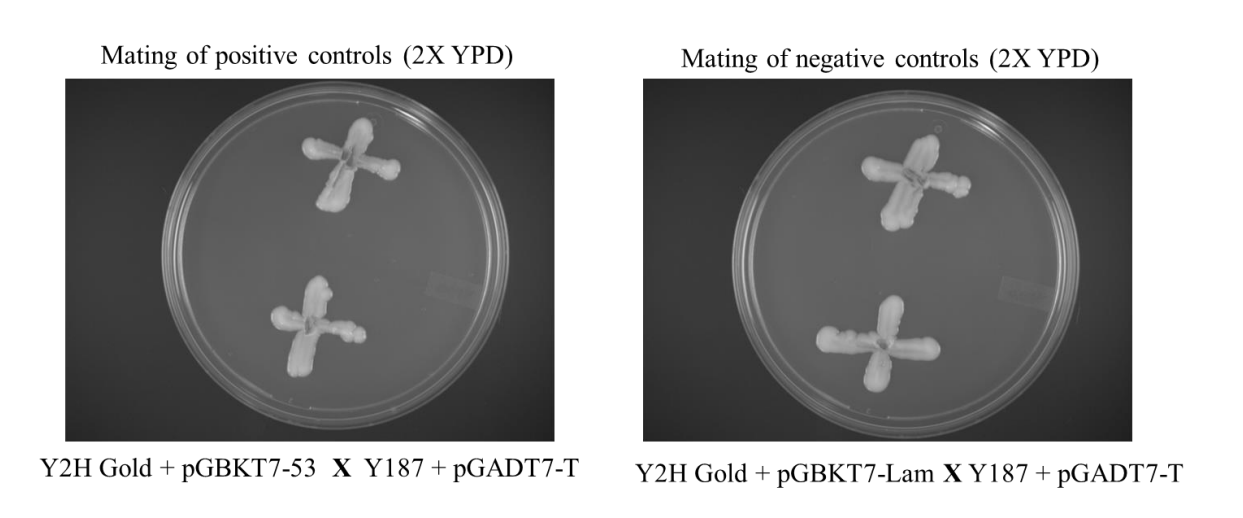
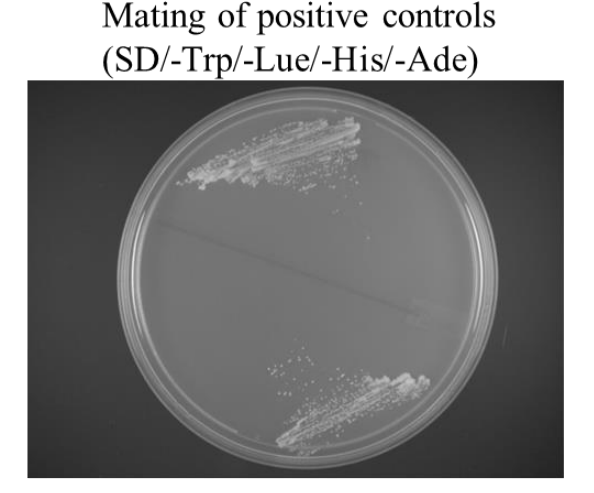


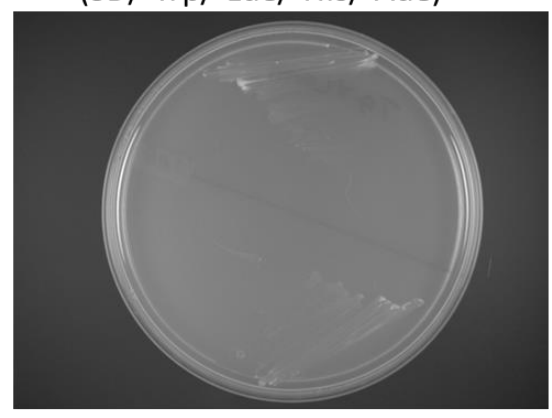
Figure 5.Mating of positive controls. Y2H Gold and Y187 were transformed with pGBKT7-53 and pGADT7-T, respectively. The two strains were cross-mated, and the conjugants streaked on 2X YPD agar plates. Mating of

negative controls. Y2H Gold and Y187 were transformed with pGBKT7-Lam and pGADT7-T, respectively. The two strains were cross-mated, and the conjugants streaked on 2X YPD agar plates. Representative 2X YPD plates showing the growth of conjugants.



Y2H Gold pGBKT7-53 X Y187 pGADT7-T

Mating of negative controls (SD/-Trp/-Lue/-His/-Ade)



Y2H Gold pGBKT7-Lam X Y187 pGADT7-T.

Figure 6. Mating of positive controls. Y2H Gold and Y187 were transformed with pGBKT7-53 and pGADT7-T, respectively. The two strains were mated, and the conjugants that showed growth on 2X YPD plates were then streaked on quadruple dropout (SD/-Trp/-Lue/-His/-Ade) agar plates. Mating of negative controls. Y2H Gold and Y187 were transformed with pGBKT7-Lam and pGADT7-T respectively. The two strains were mated, and the conjugants that showed growth on 2X YPD plates were then streaked on quadruple dropout (SD/-Trp/-Lue/-His/-Ade) agar plates. Representative SD agar plates show the growth of conjugants.

3.2.3. Cloning and testing the bait for auto-activation and toxicity

To determine the interaction partners of UPK1a and UPK2, primers were designed to amplify their coding sequence (Table 1). Using human testis cDNA, UPK1a was amplified. It was then cloned into pGBKT7 vector between the BamH1 and EcoR1 restriction digestion sites. The plasmid (pGBKT7-UPK1A) was then sequenced for the presence of the cloned fragment and proper orientation (Figure 7). Y2H Gold yeast were transformed with pGBKT7-UPK1A and pGBKT7-UPK2. Auto activation test was performed by plating the transformed with pGBKT7-UPK1A and pGBKT7-UPK2 plasmis on the SD/-Trp and SD/-Lue Plate. No growth was observed on SD/-Lue, indicating no auto-activation for these genes (Figure 8). Further, toxicity test was

performed by streaking Y2H Gold yeast transformed with pGBKT7-UPK1A, pGBKT7-UPK2 and pGBKT7 on to SD/-Trp agar plates. The same size colony growth was observed in both pGBKT7-UPK1A and pGBKT7 empty vector, indicating that the cloned genes both UPK1A and UPK2 were not toxic to the Y2H Gold cells (Figure 8).

Table 1. Primers used for cloning Upk1a and Upk2

Name	Sequence 5'-3'	RE site	Length (bp)	GC (%)	Tm ⁰ C	Size (bp)
H UPK1A pGBKT7 FP	gccgaattcATGGCGTCTGCGGCAGCAGC	EcoRI	29	66	68.6	840
H UPK1A pGBKT7 RP	ggcggatccTCAGGATGGCAAACCCAAACC	BamHI	30	60	67.1	
H UPK2 pGBKT7 FP	gccgaattcGACTTCAACATCTCAAGCCT	EcoRI	29	48	61.5	498
H UPK2 pGBKT7 RP	ggcggatccTTACTTGCGGGAGCCCAGTG	BamHI	29	66	68.6	

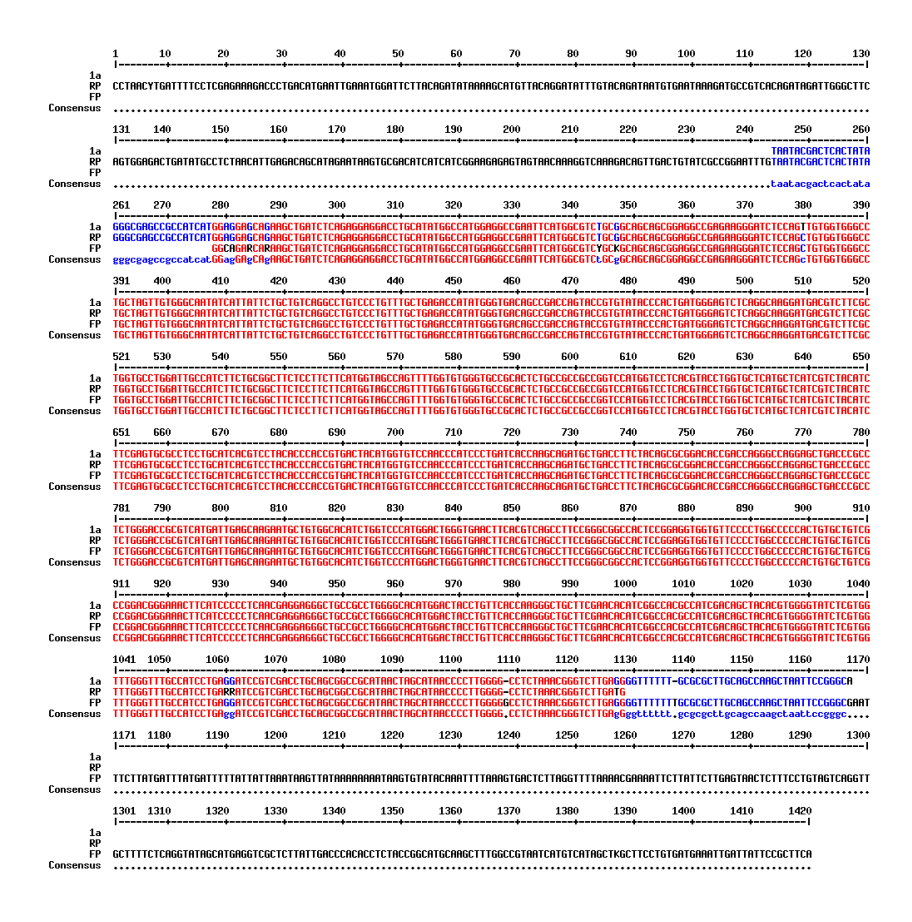


Figure 7. Sequence of the cloned human UPK1a in pGBKT7 vector



Figure 8. Autoactivation and toxicity tests. For determination of autoactivation, Y2H Gold yeast transformed with pGBKT7-UPK1A and pGBKT7-UPK2 were plated onto SD/-Trp and SD/-Lue agar plate. To determine toxicity, Y2H Gold yeast transformed with pGBKT7-UPK1A, pGBKT7-UPK2 and pGBKT7 empty vector were streaked on the SD/-Trp plate and growth was observed.

3.2.4. Identification of UPK1A / UPK2 interacting partners in the testis cDNA library

Y2H Gold yeast transformed with pGBKT7-UPK1A or pGBKT7-UPK2 were mated with Y187 yeast transformed with human testis cDNA library (Takara, Cat. No. 630470) were plated on SD/-Trp/-Lue agar plates. Resulting colonies were handpicked and streaked onto fresh SD/-Trp/-Lue agar plate. Representation of the pattern of streaking is shown in Figure 9. Colonies that showed growth on SD/-Trp/-Lue plates were then streaked onto double (SD/-Trp/-Leu), triple (SD/-Trp/-Leu/-His) and quadruple (SD/-Trp/-Leu/-His/-Ade) dropout agar plates. The number of colonies picked for UPK1A and UPK2 are shown in tables 2 and 5. Colonies that showed growth on quadruple dropout plates were selected and colony PCR performed. The amplicon was then sequenced and the identity of the interacting partner was determined by using BLAST tool available at NCBI.

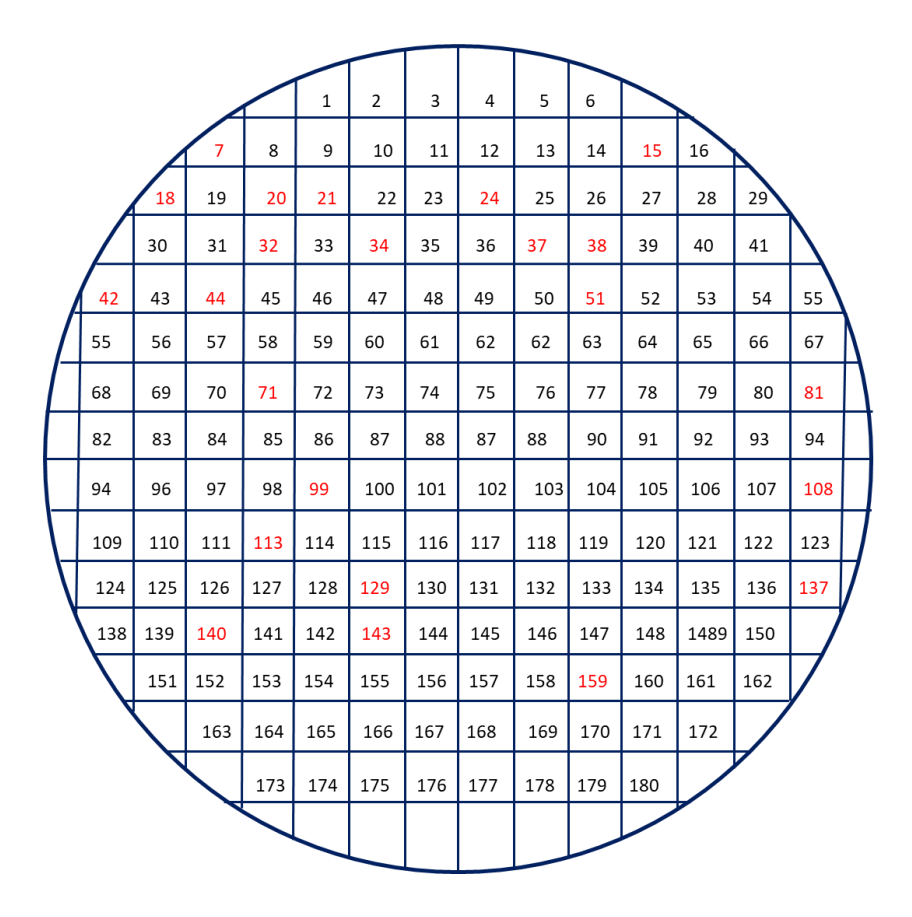


Figure 9. Representative diagram of the pattern of streaking of colonies on SD/-Trp/-Lue agar plate.

3.2.5. Confirmation of interaction

To confirm the interaction between human UPK1A and the possible partners, mammalian cell culture system was used. Upk1a was cloned immediately next to pDsRed2, a red fluorescent protein of pDsRed2-N1 vector, such that the expression of UPK1a-DsRed2 fusion protein is detected by the red color under a fluorescence microscope. Similarly, the interacting partner of UPK1a or UPK2 is cloned immediately next to EGFP, a green fluorescent protein, of pEGFP-N1 vector, such that the expression of interacting partner-EGFP fusion protein is detected by the green color under a fluorescence microscope. The cloned plasmids (3 ug) mentioned above mixed with P3000TM Reagent 6ul, LipofectamineTM 3000 Reagent 6ul (Invitrogen Cat, No. L3000008) 250 ul of Opti-MEM (GibcoTM, Cat. No. 11058021) were added to a culture of 1 x 10⁶ HEK adherent cells in a 60mm plate under Opti-MEM. The complete medium was than replaced after 5 hours. Twenty-four hours after the transfection, the cells were observed under a fluorescence microscope

(Lawrence & Mayo) with the excitation and emission set to 561 nm and 580 to 620nm band pass respectively to visualize the expression of UPK1A-DsRed2 (red color) and the interacting partner-EGFP with the excitation and emission 488nm and 500 to 550 band pass (green color). Further, to determine the probability of co-localization / interaction of UPK1A and its interacting partner, HEK cells expressing these proteins were subjected to high resolution microscopy (Leica TCS SP8 Laser Scanning confocal Microscope). Further analyzes these images with Leica, Software: LAS X Version 3.5.7.23225 and Fiji software 1.0.

3.3. Results

To determine the various molecular factors that may interact or assist UPK1a for its role in male reproductive tract, we directed our studies to determine the possible interaction factors using yeast two hybrid screening. We used the Matchmaker *GAL4* two-hybrid assay. In this assay, a bait protein is articulated as a fusion to the Gal4 DNA-binding domain (DNA-BD), and the libraries of prey proteins are expressed as fusions to the Gal4 activation domain. In the Matchmaker Gold Yeast Two-Hybrid System, when bait and library fusion proteins interact, the DNA-BD and AD are brought into proximity to activate the transcription of four independent reporter genes (*AUR1-C, ADE2, HIS3*, and *MEL1*).

3.3.1. Identifying the interaction partners of UPK1A and UPK2

Conjugants of Y2H Gold strain transformed with pGBKT7-UPK1A or pGBKT7-UPK2 and mated with Y187 strain transformed with testis cDNA library when plated on double drop out plates (SD/-Trp/-Leu) formed colonies. The colonies that appeared on double drop out SD-agar plates were then sequentially transferred to triple (SD/-Trp/-Lue/-His) and quadruple dropout (SD/-Trp/-Lue/-His/-Ade) agar plates. The number of colonies transferred from each of the plates are presented in table 2. The colonies that showed growth on the quadruple dropout plate were selected and yeast colony PCR was performed. The resulting amplicons were sequenced to know the identity of the interacting partner. From the sequencing results, we identified 36 possible interacting partners of UPK1A as shown in table 3. Among the 36 possible interaction partners identified, for a few of them, the coding region appears to be interacting with UPK1A (Table 4). We noticed that the sequence obtained for Regucalcin (RGN) and Proteasome subunit beta 1

(PSMB1) was completely matching with their full coding region and this region appears to interact with UPK1A. Hence, these two proteins were selected for further analyses.

Table 2. Details of colonies picked to identify the interacting partners of UPK1A

SD Plate	Colonies picked up (n)	Colonies observed (n)
SD/-Trp/-Lue (mated culture spreading)		So many
SD/-Trp/-Lue	1600	1600
SD/-Trp/-Lue/-His	1600	550
SD/-Trp/-Lue/-His/-Ade	550	200

Table 3. Possible interacting partners of UPK1A identified by colony PCR with Testicular cDNA library of Homo sapines

Colony	UPK1A interacting Sequence matched mRNAs
No	
34	Pecanex 1 (PCNX1)
51	Guanosine monophosphate reductase (GMPR)
99,3.113	Helicase for meiosis 1 (HFM1)
129	Tubulin alpha 3c (TUBA3C)
159,3.3	Threonyl-tRNA synthetase 2, mitochondrial (TARS2)
78	Long intergenic non-protein coding RNA 608 (LINC00608)
81	chromosome 8 clone RP11-300I14 map q24.13
121	Immunoglobulin lambda gene locus DNA, clone:288A10
127	Mitochondrial ribosomal protein L13 (MRPL13)
1	Collagen type XI alpha 1 chain (COL11A1)
3, 46	Chromosome 17, clone RP11-676J12
4	Y-chromosome specific repetitive DNA family (DYZ1)
5	Similar to ribosomal protein S8, clone IMAGE:3447074
11	Regucalcin (RGN), transcript variant 4
15	SET binding factor 2 (SBF2), RefSeqGene (LRG_267)
19	Acetyl-CoA carboxylase alpha (ACACA)
23	Methyltransferase like 26 (METTL26)
24	BAC clone RP11-323K15 from 7
25	S-transferase mu 3 (GSTM3)

26, 3	Structural maintenance of chromosomes 4 (SMC4)
33	Coiled-coil domain containing 87 (CCDC87)
35	cDNA clone IMAGE:4826441
36	Ornithine aminotransferase (OAT)
37	Zinc finger protein 17 (ZNF17)
39	TAR (HIV-1) RNA binding protein 1 (TARBP1)
40	Acetoacetyl-CoA synthetase (AACS)
42	Component of oligomeric golgi complex 7 (COG7)
47	Maestro heat like repeat family member 7 (MROH7)
51	Chromosome 5 clone CH17-477F8
52	Regulator of G protein signaling 22 (RGS22)
56	Striatin 4 (STRN4)
66	Proteasome subunit beta 1 (PSMB1)
66 2 nd	Clone HTL-S-45 testicular secretory protein Li 45 mRNA
88	SURP and G-patch domain containing 2 (SUGP2)
106	Cytoplasmic polyadenylation element binding protein 2 (CPEB2)
108	Tubulin alpha 3c (TUBA3C)

Table 4. Possible interacting partners in which the coding sequence may interact with UPK1A

Gene Name	3'UTR	CDS	3' that matches with known sequence UTR	CDS that matches with known sequence	No of Nucleotides	No of Amino acids	No of amino acids matched
Regucalcin (RGN)	1-990	991- 1674	No	1045- 1674	630	227	19- 227(210)
Glutathione S-transferase mu 3 (GSTM3)	1-310	311- 988	169-310	311-988	820	225	No
Ornithine aminotransferase (OAT)	1-253	254- 1573	No	1202- 1573	372	439	124
TAR (HIV-1) RNA binding protein 1 (TARBP1)	1-76	77- 4866	No	4276- 4866	591	1621	1425- 1621(197)
Regulator of G protein signaling 22 (RGS22)	1-128	129- 3923	101-128	129-182, 468-723	338	1264	1-18, 114- 199(104)
Striatin 4 (STRN4)	1-33	34- 2316	No	1647- 2316	670	760	539-760 (220)
Proteasome subunit beta 1 (PSMB1)	1-65	66-791	28-65	66-791	764	241	241
SURP and G-patch domain containing 2 (SUGP2)	1-92	93- 3341	No	1748- 2587	840	1082	553-831

Cytoplasmic	1-193	194-	No	3068-	126	999	959-999
polyadenylation element		3193		3193			(41)
binding protein 2 (CPEB2)							

In the case of UPK2A, the number of colonies that appeared on double drop out (SD/-Trp,-Lue) were sequentially transferred to triple (SD/-Trp/-Lue/-His) and quadruple dropout (SD/-Trp/-Tyr/-His/-Ade) agar plates is shown in table 5. Basing on the sequence of the amplicons obtained by colony PCR, 21 possible interacting partners were identified (Table 6). Of these 21, for a few of them, the coding region appears to be interacting with UPK2 (Table 7). The complete coding region of testis expressed 44 (TEX44) and small nuclear ribonucleoprotein polypeptide N (SNRPN) were found to be interacting with UPK2A (Table 7).

Table 5. Details of colonies picked to identify the interacting partners of UPK2

SD Plate	Colonies picked up (n)	Colonies observed (n)
SD/-Trp -Lue (mated culture spreading)		So many
SD/-Trp-Lue	600	600
SD/-Trp,-Lue-His	600	150
SD/-Trp-Lue-His-Ade	150	90

Table 6. Possible interacting partners of UPK2 identified by colony PCR with Testicular cDNA librariy of Homo sapines

Col No	Name of the Gene interacting partner for the UPK2
2	Premelanosome protein (PMEL)
6	Nischarin (NISCH)
8, 16, 55, 62,	Chromosome 17 open reading frame 80 (C17orf80)
15, 24,	Pseudopodium enriched atypical kinase 1 (PEAK1)
18	General transcription factor IIi pseudogene 20 (GTF2IP20),
19	Premelanosome protein (PMEL)
25	Signal recognition particle 68 (SRP68)
27	Pre-mRNA processing factor 6 (PRPF6)
29	Transformer 2 beta homolog (TRA2B)
32	Transmembrane p24 trafficking protein 10 (TMED10)
51	BAC clone RP11-33B1 from 4

67	Centromere protein U (CENPU)
73	Transmembrane p24 trafficking protein 10 (TMED10)
76	Sidekick cell adhesion molecule 1 (SDK1)
82	Integrin subunit beta 1 (ITGB1)
84	Testis expressed 44 (TEX44)
85	Solute carrier family 30 member 1 (SLC30A1)
87	Small nuclear ribonucleoprotein polypeptide N (SNRPN),
91	Signal recognition particle 68 (SRP68)
97	Mucin like 3 (MUCL3)
98	Arginine-glutamic acid dipeptide repeats (RERE)

 Table 7. Possible interacting partners in which the coding sequence of may interact with UPK2

Gene Name	3'UTR	CDS	5'UTR	3' that	CDS	No of	No of	No of
				matches	that	Nucleotides	Amino	amino
				with	matches	Matched	acids	acids
				known	with			matched
				sequence	known			
				UTR	sequence			
Premelanosome protein (PMEL)	1-86	87-2072	2072-	No	1350-	723	661	422-661
			2195		2072			(240)
Nischarin (NISCH)	1-38	39-4553	4554-	No	1739-	563	1504	567-754
			5139		2302			(188)
Homo sapiens chromosome 17 open	1-273	274-1995	1996-	No	540-1511	972	609	111-434
reading frame 80 (C17orf80)			3624					(324)
Homo sapiens pseudopodium enriched	1-576	577-5817	5818-		3817-	837	1746	1081-
atypical kinase 1 (PEAK1)			19319		4653			1359
								(279)
Homo sapiens general transcription	2947	No						
factor IIi pseudogene 20 (GTF2IP20),								
non-coding RNA								
Homo sapiens signal recognition	1-26	27-1910	1911-	No	861-1796	936	627	279-590
particle 68 (SRP68), transcript variant			2831					(312)
1								
Homo sapiens pre-mRNA processing	1-114	115-2940	2941-	No	1751-	1029	941	546-888
factor 6 (PRPF6)			3047		2778			(343)
Homo sapiens transformer 2 beta	1-114	115-1021	1022-	No	398-985	588	288	82-277
homolog (TRA2B)			4178					(196)
Homo sapiens transmembrane p24	1-33	34-694	695-	No	316-	378	219	95-219
trafficking protein 10 (TMED10)			4109		693+			(125)

Homo sapiens BAC clone RP11-33B1	130879	No						
from 4								
Homo sapiens centromere protein U	1-34	35-1291	1292-	12-34	34-880	846	418	1-282
(CENPU)			1494					(282)
Homo sapiens sidekick cell adhesion	1-335	3366977	6977-	No	4690-	1066		
molecule 1 (SDK1)			10593		5756			
Homo sapiens integrin subunit beta 1	1-86	87-2483	2484-	No	1909-	576	798	599-789
(ITGB1)			3735		2483			(191)
Homo sapiens testis expressed 44	1-88	89-1276	1277-	1-88	89-1033	945	395	1-315
(TEX44)			1420					(315)
Homo sapiens solute carrier family 30	1-549	550-2073	2074-	No	1161-	912	507	205-507
member 1 (SLC30A1)			5893		2073			(303)
Homo sapiens small nuclear	1-560	561-1283	1284-	94-560	561-1052	492	240	1-164
ribonucleoprotein polypeptide N			1562					(164)
(SNRPN)								
Mucin-like protein 3 precursor	1-27	28-4209	4210-	No	3286-	924	1393	1087-
			5813		4209			1393
								(307)
Homo sapiens arginine-glutamic acid	1-625	626-5326	5327-	No	641-1750	1110	1566	6-375
dipeptide repeats (RERE)			8009					(370)

3.3.2. Confirmation of the interaction of UPK1A with RGN and PSMB1

To further confirm the interaction of UPK1A with RGN we cloned these genes in two different fusion fluorescent-tagged vectors. The UPK1A was cloned such that it is expressed as a fusion protein with red fluorescent protein (RFP) whereas RGN or PSMB1 as a fusion protein with green fluorescent protein (GFP). HEK cells were co-transfected with plasmids that express UPK1A-RFP and RGN-EGFP displayed red and green fluorescence indicating the expression of these two fusion proteins (Figure 10). Overlay of images taken at higher magnification displayed the presence of red and green fluorescence in the same region of cells (Figure 11), indicating that UPK1A and RGN may be interacting. To gather further evidence on the co-localization / interaction, high-resolution imaging was performed. Co-localization of UPK1A and RGN was also evident in the images obtained by high resolution microscope (Figure 12). To obtain a quantitative assessment of the extent of localization / interaction, Pearson's correlation for multiple images was obtained (Table 8). From the Pearson's Correlation values it appears that the colocalization / interaction rate between UPK1A and RGN was around 57%.

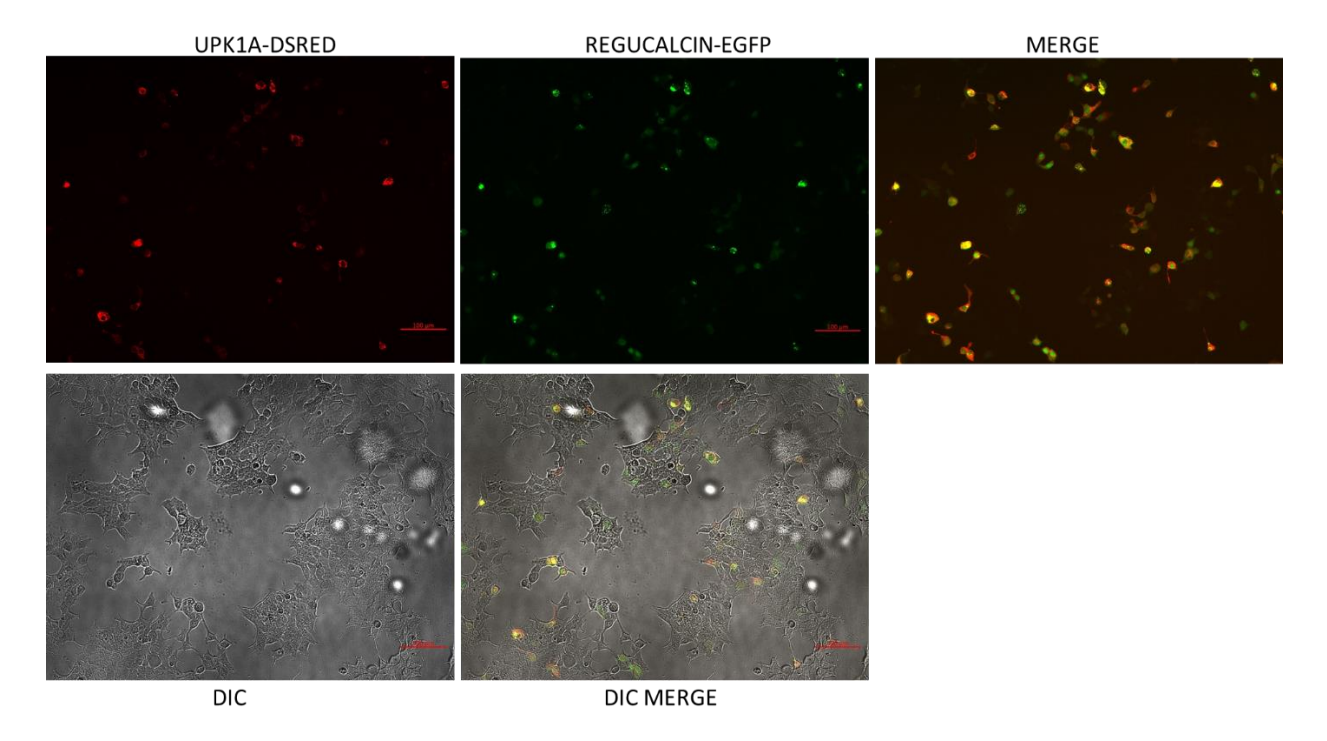


Figure 10. Localization of UPK1A and RGN in HEK cells. HEK cells were co-transfected with plasmids that express UPK1A-RFP and RGN-EGFP as fusion proteins. Red and green colour indicates the expression of UPK1A and RGN respectively. Scale bar: 100 μm.

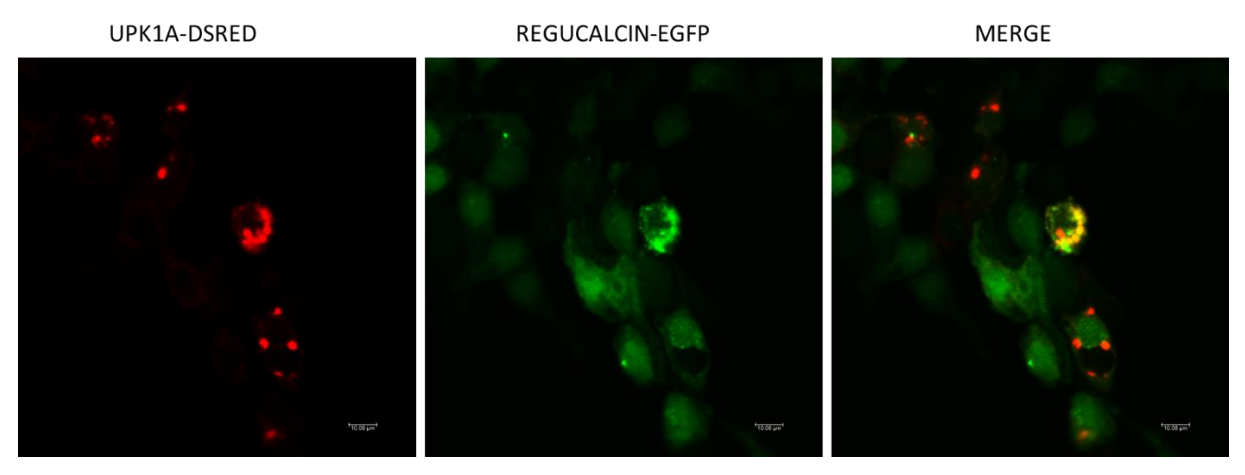


Figure 11. Localization of UPK1A and RGN in HEK cells at higher magnification. HEK cells were co-transfected with plasmids that express UPK1A-RFP and RGN-EGFP as fusion proteins. Red and green colour indicates the expression of UPK1A and RGN respectively. Scale bar: $100 \mu m$.

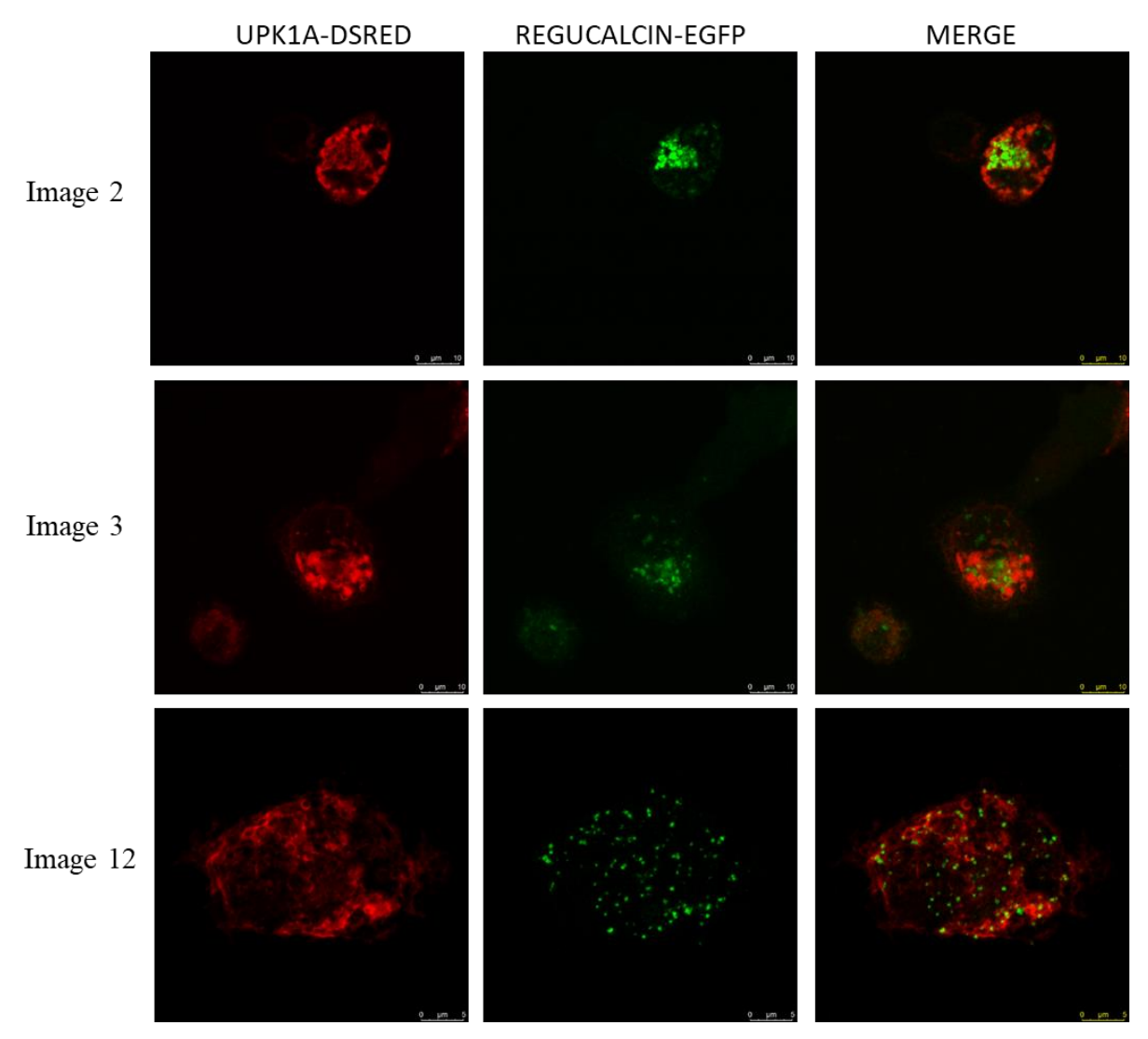


Figure 12. Localization of UPK1A and RGN by high resolution imaging. HEK cells were co-transfected with plasmids that express UPK1A-RFP and RGN-EGFP as fusion proteins. Red and green colour indicates the expression of UPK1A and RGN respectively. Scale bar: For Image 2 and 3, 10 µm, For Image 12, 5 µm.

Table 8. Pearson's correlation values for the localization / interaction between UPK1A and RGN.

Image Name	Pearson's Correlation	Overlap Coefficient	Colocalization Rate (%)
2	0.542	0.5819	46.07%
3	0.5513	0.6589	54.02%
5	0.2296	0.4273	15.96%
6	0.7246	0.7492	39.77%

7	0.4667	0.6498	77.04%
8	0.4294	0.6284	63.26%
9	0.5026	0.5787	56.83%
10	0.3182	0.6134	36.27%
11	0.6312	0.7543	87.08%
12	0.5786	0.7516	77.84%
13	0.4373	0.7034	71.98%
Average	0.491954545	0.645172727	56.92%

On the same lines, co-transfection of HEK cells with plasmids that express UPK1A-RFP and PSMB1-EGFP allowed the expression of these two fusion proteins, as indicated by the red and green florescence (Figure 13). High resolution microscopy based images also confirmed the co-localization of UPK1A-RFP and PSMB1-EGFP in HEK cells (Figure 14). The extent of colocalization / interaction between UPK1A and PMSB1 was approximately 40% as determined from the Pearson's Correlation values (Table 9).

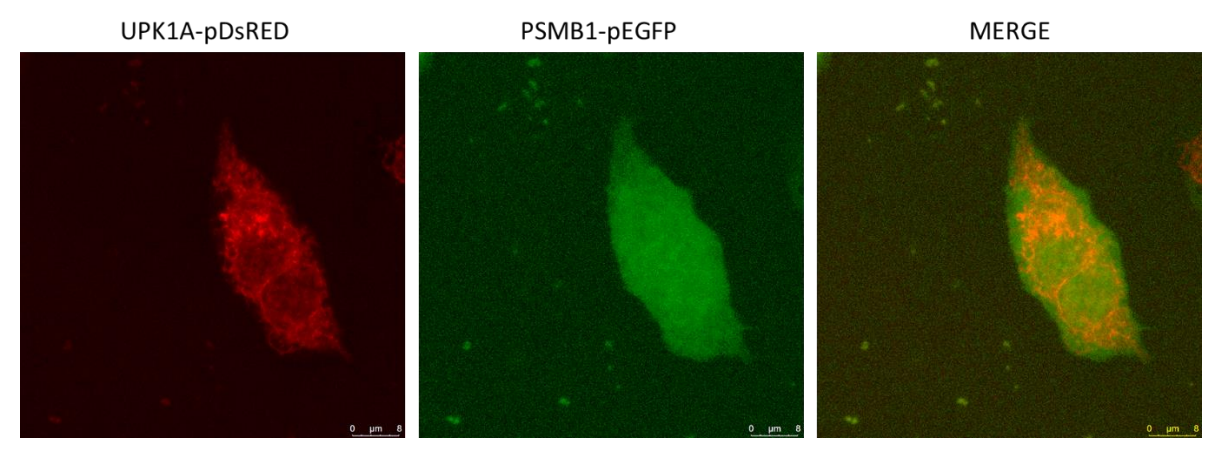


Figure 13. Localization of UP1A and PMSB1 in HEK cells at higher magnification. HEK cells were co-transfected with plasmids that express UPK1A-RFP and PMSB1-EGFP as fusion proteins. Red and green colour indicates the expression of UPK1A and RGN respectively. Scale bar: 8 µm.

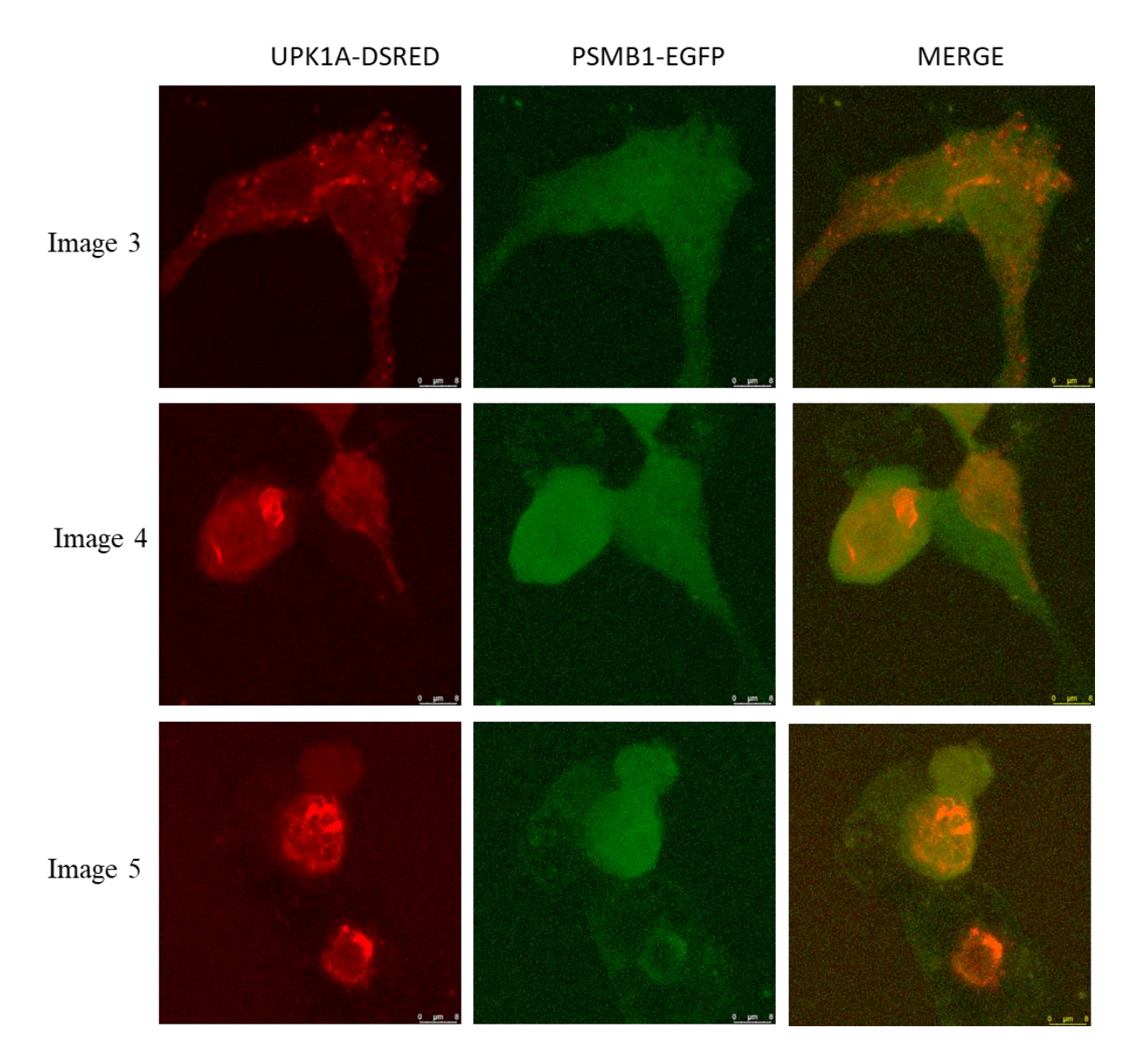


Figure 14. Localization of UPK1A and PMSB1 by high resolution imaging. HEK cells were co-transfected with plasmids that express UPK1A-RFP and PMSB1-EGFP as fusion proteins. Red and green colour indicates the expression of UPK1A and RGN respectively. Scale bar: 8 μm.

Table 9. Pearson's correlation values for the localization / interaction between UPK1A and PMSB1.

Image Name	Pearson's Correlation	Overlap Coefficient	Colocalization Rate
3	0.2986	0.5247	51.06%
4	0.3747	0.5909	55.53%
5	0.2681	0.5107	43.03%
6	0.3582	0.6584	39.27%
7	0.338	0.6088	72.46%
8	0.5009	0.6755	72.04%
9	0.4123	0.6668	67.57%
10	0.4331	0.7169	81.15%
11	0.4322	0.6533	60.55%
Average	0.379566667	0.622888889	60.30%

3.4. Discussion

Cell surface receptors (transmembrane proteins) play role in communication between the cells and biological functions, mainly involved in signal transduction. Their role in the male reproductive physiology, especially during gametogenesis, maturation and fertilization are reported. The ion channel linked receptors, namely, Calcium (Ca+2) channels participate in fertilization (Darszon, Nishigaki, Beltran, & Treviño, 2011). The enzyme-linked receptor, c-kit (CD117) type-III receptor tyrosine kinase is involved in proliferation of progenitor cells to gonocytes(Prabhu et al., 2006). Similary, the G protein-coupled receptor, FSHR, present on Sertoli cells contributes to spermatogenesis (Oduwole, Peltoketo, & Huhtaniemi, 2018). CD9, a tetraspanin, plays an important role in sperm-egg interaction (Jégou *et al.*, 2011). Uroplakins, being transmembrane proteins (monospanins and tetraspanins) are thought to primarily contribute to the urothelial integrity. However, their role as signaling molecules either individually or by interacting with other proteins are not explored. Hence, in this part of the study, we explored the possible interacting partners of UPK1A and UPK2 to determine whether proteins that are crucial to male gametogenesis, maturation and fertilization act in conjunction with Uroplakins.

Results of the yeast two hybrid analyses backed with fluorescence microscopy indicated a strong interaction between UPK1A and regucalcin (RGN), a highly conserved, calcium-binding protein that is preferentially expressed in the liver, kidney and other tissues. It plays an important role in calcium homeostasis and its mmultifunctional role in the regulation of cell functions in liver, kidney cortex, heart and brain is well studied. It primarily is involved in promotion of urinary calcium transport in the epithelial cells of kidney cortex (Yamaguchi, 2015). Interaction of UPK1A with RGN may have effects on calcium homeostasis and this probably indicates a novel role for UPK1A in the urothelium. Further, RGN contributes to the promotion of dormancy of prostate cancer (Sharma et al., 2021). UPK1A interaction with RGN and its implication on prostate cancer pathogenesis is a new area to be investigated. On the other hand, Ca²⁺ homeostasis in spermatogenesis and sperm function is crucial and its disruption causes male infertility (Laurentino et al., 2012). RGN is widely distributed in the male reproductive tract and exerts a suppressive effect on in vitro sperm capacitation (Pillai et al., 2017). UPK1A knockout caused subfertility in this study indicating a possible interaction between UPK1A and RGN is required for normal spermatogenesis needs to be addressed.

We also report the interaction of UPK1A with proteasome subunit beta type-1 (PSMB1) using yeast two hybrid screening and high resolution fluorescence microscopy. The non-catalytic component of the 20S core proteasome complex is involved in the proteolytic degradation of most intracellular proteins. PSMB1 recognizes degradable proteins, for protein quality control purpose or key regulatory protein components for dynamic biological processes. Compromised proteasome complex assembly and function leads to reduced proteolytic activities and the accumulation of damaged or misfolded protein species; leading to neurodegenerative, cardiovascular diseases, inflammatory responses and autoimmune diseases, and systemic DNA damage responses leading to malignancies. The role of PSMB family members in malel reproductive physiology are reported. Meiosis I progression in spermatogenesis requires a type of testis-specific 20S core proteasome (PSMA8) (Q. Zhang, Ji, Busayavalasa, Shao, & Yu, 2019). The proteasome subunit α4s is essential for formation of spermatoproteasomes and histone degradation during meiotic DNA repair in spermatocytes(Z. H. Zhang et al., 2021). Further, proteolysis required in spermatogenesis mediated by 20S-PA200 complex (UniProt, 2022). RhoS (a new member of Rho GTPases family specific to sperm) associates with PSMB5, a catalytic subunit of the proteasome, in a series of stage-specific spermatogenic cells (N. Zhang et al., 2010). Though the role of PSMB1 family

members in male reproductive physiology is reported by few studies, the role of PSMB1 in spermatogenesis, maturation and fertilizaton remains unexplored. The implication of UPK1A interaction with PSMB1 on the functioning of spermatoproteasome will be an interesting aspect to study further. In conclusion, we report the possible interaction of UPK1A with RGN and PSMB1 by yeast two hybrid screening and by high resolution microscopy. The implications of these interactions in the male reproductive physiology, especially in gametogenesis, sperm maturation and fertilization remains to be investigated further in detail.

3.5. References

- 1. Adrina, C., Fernanda, M. C., Gonzalez, E., Lucrecia, P., & Jorge, A. B. (1980). Interaction of Proteins of Epididymal Origin with Spermatozoa. *Biology of Reproduction*, 23(4), 737-742. doi:10.1095/biolreprod23.4.737
- Ansari-Pour, N., Razaghi-Moghadam, Z., Barneh, F., & Jafari, M. (2016). Testis-Specific Y-Centric Protein-Protein Interaction Network Provides Clues to the Etiology of Severe Spermatogenic Failure. *J Proteome Res*, 15(3), 1011-1022. doi:10.1021/acs.jproteome.5b01080
- 3. Barh, D., Chaitankar, V., Yiannakopoulou, E., Salawu, E., Chowbina, S., Ghosh, P., & Azevedo, V. (2014). In Silico Models: From Simple Networks to Complex Diseases. In A. Verma & A. Singh (Eds.), *Animal Biotechnology: Models in Discovery and Translation* (pp. 385-404): Academic Press.
- 4. Björkgren, I., & Sipilä, P. (2019). The impact of epididymal proteins on sperm function. *Reproduction*, 158(5), R155-r167. doi:10.1530/rep-18-0589
- 5. Darszon, A., Nishigaki, T., Beltran, C., & Treviño, C. L. (2011). Calcium channels in the development, maturation, and function of spermatozoa. *Physiological Reviews*, *91*(4), 1305-1355. doi:10.1152/physrev.00028.2010
- DK, T., P, S., Uppin, J., S, U., & CPD, G. (2018). Investigating the Influence of Hotspot Mutations in Protein–Protein Interaction of IDH1 Homodimer Protein: A Computational Approach. In R. Donev (Ed.), Advances in Protein Chemistry and Structural Biology (Vol. 111, pp. 243-261).

- 7. Hadziselimovic, F., Verkauskas, G., & Stadler, M. (2022). A novel role for CFTR interaction with LH and FGF in azoospermia and epididymal maldevelopment caused by cryptorchidism. *Basic Clin Androl*, 32(1), 10. doi:10.1186/s12610-022-00160-0
- 8. Hardcastle, I. (2016). Protein–Protein Interaction Inhibitors in Cancer. *Reference Module in Chemistry, Molecular Sciences and Chemical Engineering*. doi:10.1016/B978-0-12-409547-2.12392-3
- 9. Jégou, A., Ziyyat, A., Barraud-Lange, V., Perez, E., Wolf, J. P., Pincet, F., & Gourier, C. (2011). CD9 tetraspanin generates fusion competent sites on the egg membrane for mammalian fertilization. *Proceedings of the National Academy of Sciences of the United States of America*, 108(27), 10946-10951. doi:10.1073/pnas.1017400108
- 10. Kant, K., Tomar, A. K., Sharma, P., Kundu, B., Singh, S., & Yadav, S. (2019). Human Epididymis Protein 4 Quantification and Interaction Network Analysis in Seminal Plasma. *Protein Pept Lett*, 26(6), 458-465. doi:10.2174/0929866526666190327124919
- 11. Kotlyar, M., Pastrello, C., Rossos, A. E. M., & Jurisica, I. (2018). Protein-Protein Interaction Databases. In *Reference Module in Materials Science and Materials Engineering*.
- 12. Laurentino, S. S., Correia, S., Cavaco, J. E., Oliveira, P. F., de Sousa, M., Barros, A., & Socorro, S. (2012). Regucalcin, a calcium-binding protein with a role in male reproduction? *Molecular Human Reproduction*, 18(4), 161-170. doi:10.1093/molehr/gar075
- 13. Mariani, N. A. P., Camara, A. C., Silva, A. A. S., Raimundo, T. R. F., Andrade, J. J., Andrade, A. D., . . . Silva, E. J. R. (2020). Epididymal protease inhibitor (EPPIN) is a protein hub for seminal vesicle-secreted protein SVS2 binding in mouse spermatozoa. *Molecular and Cellular Endocrinology*, 506, 110754. doi:10.1016/j.mce.2020.110754
- 14. Oduwole, O. O., Peltoketo, H., & Huhtaniemi, I. T. (2018). Role of Follicle-Stimulating Hormone in Spermatogenesis. *Front Endocrinol (Lausanne)*, *9*, 763. doi:10.3389/fendo.2018.00763
- 15. Petit, F. G., Kervarrec, C., Jamin, S. P., Smagulova, F., Hao, C., Becker, E., . . . Primig, M. (2015). Combining RNA and protein profiling data with network interactions identifies genes associated with spermatogenesis in mouse and human. *Biology of Reproduction*, 92(3), 71. doi:10.1095/biolreprod.114.126250

- 16. Pillai, H., Shende, A. M., Parmar, M. S., A, A., L, S., Kumaresan, A., . . . Bhure, S. K. (2017). Regucalcin is widely distributed in the male reproductive tract and exerts a suppressive effect on in vitro sperm capacitation in the water buffalo (Bubalus bubalis). *Molecular Reproduction and Development*, 84(3), 212-221. doi:10.1002/mrd.22767
- 17. Prabhu, S. M., Meistrich, M. L., McLaughlin, E. A., Roman, S. D., Warne, S., Mendis, S., . . . Loveland, K. L. (2006). Expression of c-Kit receptor mRNA and protein in the developing, adult and irradiated rodent testis. *Reproduction*, 131(3), 489-499. doi:10.1530/rep.1.00968
- Schiza, C., Korbakis, D., Panteleli, E., Jarvi, K., Drabovich, A. P., & Diamandis, E. P. (2018). Discovery of a Human Testis-specific Protein Complex TEX101-DPEP3 and Selection of Its Disrupting Antibodies. *Molecular and Cellular Proteomics*, 17(12), 2480-2495. doi:10.1074/mcp.RA118.000749
- 19. Sharma, S., Pei, X., Xing, F., Wu, S. Y., Wu, K., Tyagi, A., . . . Watabe, K. (2021). Regucalcin promotes dormancy of prostate cancer. *Oncogene*, 40(5), 1012-1026. doi:10.1038/s41388-020-01565-9
- 20. Silva, J. V., Yoon, S., Domingues, S., Guimarães, S., Goltsev, A. V., da Cruz, E. S. E. F., . . . Fardilha, M. (2015). Amyloid precursor protein interaction network in human testis: sentinel proteins for male reproduction. *BMC Bioinformatics*, 16(1), 12. doi:10.1186/s12859-014-0432-9
- 21. UniProt. (2022). UniProtKB P20618 (PSB1_HUMAN): Proteasome subunit beta type-1. Retrieved from https://www.uniprot.org/uniprot/P20618
- 22. Yamaguchi, M. (2015). The potential role of regucalcin in kidney cell regulation: Involvement in renal failure (Review). *International Journal of Molecular Medicine*, 36(5), 1191-1199. doi:10.3892/ijmm.2015.2343
- 23. Zhang, N., Liang, J., Tian, Y., Yuan, L., Wu, L., Miao, S., . . . Wang, L. (2010). A novel testis-specific GTPase serves as a link to proteasome biogenesis: functional characterization of RhoS/RSA-14-44 in spermatogenesis. *Molecular Biology of the Cell*, 21(24), 4312-4324. doi:10.1091/mbc.E10-04-0310
- 24. Zhang, Q., Ji, S. Y., Busayavalasa, K., Shao, J., & Yu, C. (2019). Meiosis I progression in spermatogenesis requires a type of testis-specific 20S core proteasome. *Nat Commun*, 10(1), 3387. doi:10.1038/s41467-019-11346-y

25. Zhang, Z. H., Jiang, T. X., Chen, L. B., Zhou, W., Liu, Y., Gao, F., & Qiu, X. B. (2021). Proteasome subunit α4s is essential for formation of spermatoproteasomes and histone degradation during meiotic DNA repair in spermatocytes. *Journal of Biological Chemistry*, 296, 100130. doi:10.1074/jbc.RA120.016485



SUMMARY

Though UPKs have been well characterized in the urinary tract, their role in other organ systems is not well studied. The organs of the male reproductive system have many anatomical similarities with the urinary system and both these are subjected to infections by UPEC, the bacterial species that express the type 1 fimbriae. In light of these similarities and the scarcity of studies on the role of UPKs in other organ systems, is it important to analyze the expression pattern of *Upk* genes and their protein products in the male reproductive system and their possible functional role in male reproduction and innate immunity. Further, in-depth studies that explored the involvement of UPKs at the molecular level in the male reproductive tract are not yet reported. To explore such functional roles, the common practice is to use gene knockout mice. Thus, we generated *Upk1a* knockout mice and analyzed their fecundity, sperm function and responsiveness of the male reproductive tract tissues to UPEC infection. The physiological processes in an organ system are governed by complex interactions of genes and the absence of a specific gene may affect the normal function. Hence, it is important to determine the testicular transcriptome profile of *Upk1a* knockout mice to assess the global impact of under conditions of *Upk1a* gene ablation. Protein-protein interactions are crucial in many cellular and sub-cellular processes, such as signaling, ion transport, metabolite trafficking, protein folding, etc. The sperm proteins are extensively modified due to interaction with the epididymal luminal proteins and these interactions are crucial for sperm function and fertilization. Since UPKs are known to be expressed in the male reproductive tract tissues and on sperm, it is worth analyzing the possible interaction partners of UPKs and their relevance to sperm function. To accomplish this, yeast two-hybrid (Y2H) screening is the standard protocol. Thus, the interaction partners of UPKs were determined by Y2H.

Objective 1: In silico and in vivo characterization of rat Uroplakins

To the best of our knowledge, for the first time, we report the expression of UPKs in the male reproductive system. *Upk1a*, *Upk1b*, *Upk2*, and *Upk3b* mRNA and their corresponding proteins were abundantly expressed in the caput, cauda, testis, seminal vesicles, and the prostate. Their expression was not developmentally regulated. UPK protein expression was also localized on the spermatozoa, suggesting a role for these proteins in sperm function. In the rat testicular and epididymal cell lines, *Upk* mRNA levels increased in response to lipopolysaccharide challenge.

However, in the caput, cauda, testes, seminal vesicle, and prostate obtained from LPS-treated rats, *Upk* mRNA expression was significantly reduced. Results of this study indicate a role for UPKs in male reproductive physiology and innate immune responses.

Objective 2: Functional characterization of Uroplakin1a (Upk1a) using knock-out model

We report that *Upk1a* knockout mice are sub-fertile with compromised sperm count, but with normal sperm function (capacitation and acrosome reaction). Anatomical damage to the male reproductive tissues (caput, cauda, testis, prostate, and seminal vesicle) as well as non-reproductive tissues (bladder, pancreas, kidney, liver, and brain) were evident, suggesting that this gene plays role in the functioning of multiple organs. The lower efficiency of bacterial clearance in the tissues of *Upk1a* knock-out mice indicates the failure of initiating signaling mechanisms of the urothelium to sense and clear the invading pathogens. Differential expression of genes involved in a variety of physiological processes due to *Upk1a* ablation further reinforces the crucial role of this gene in normal and disease processes.

Objective 3: Evaluating the functional role of Uroplakin1a at the molecular level using Yeast Two-Hybrid Screening

Yeast two-hybrid screening was conducted to determine the interaction partners of Uroplakins (UPK1A and UPK2). 37 and 21 positive colonies were obtained on a quadruple plates for screening for UPK1A and UPK2. RGN and PSMB1 were identified as potential interaction partners and the co-localization was evident with immunofluorescence microscopy, high-resolution microscopy, and Pearson's coefficient. The role of regucalcin in sperm calcium dynamics and sperm capacitation is reported (39,40). Since UPK1A knockout caused subfertility in this study; a possible interaction between UPK1A and RGN is required for normal spermatogenesis needs to be addressed. The role of PSMBs in the meiotic progression during spermatogenesis and the formation of spermatoproteasomes is reported (41,42). The implication of UPK1A interaction with PSMB1 on the functioning of spermatoproteasome will be an interesting aspect to study further.



SIMILARITY INDEX

Characterization and elucidating the functional role of uroplakins in the male reproductive tract

by Suresh Babu Munipalli

Submission date: 20-Jul-2022 10:31AM (UTC+0530)

Submission ID: 1872906896

File name: SURESH BABU MUNIPALLI.docx (231.32K)

Word count: 20407

Character count: 113829

Characterization and elucidating the functional role of uroplakins in the male reproductive tract

ORIGINA	ALITY REPORT			
4 SIMILA	5% ARITY INDEX	11% INTERNET SOURCES	44% PUBLICATIONS	5% STUDENT PAPERS
PRIMAR	Y SOURCES			
1	Suresh E "Uroplak reproduc Compara Publication	JR is from the Students own be		
2	Submitte Hyderab Student Paper		of Hyderabad,	Dr. SUREST Professor Department of Animal Biolo School of Life Sciences University of Hyderabad University of Hyderabad Hyderabad-500046
3	en.wikip			<1%
4	"Transge and sper mixture	rm proteome in of pyrethroids a	resh Yenugu. cts on the fecun rats exposed to at doses similar to themosphere, 20	to
5	polen.itu Internet Source			<1%
6	www.bio			<1%



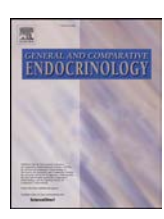
PUBLICATIONS

FISEVIER

Contents lists available at ScienceDirect

General and Comparative Endocrinology

journal homepage: www.elsevier.com/locate/ygcen



Uroplakin expression in the male reproductive tract of rat

Suresh Babu Munipalli, Suresh Yenugu*

Department of Animal Biology, University of Hyderabad, Hyderabad 500046, India



ARTICLE INFO

Keywords: Uroplakins Epididymis Testis Sperm Lipopolysaccharide

ABSTRACT

Uroplakins (UPKs) play an important role in the normal and pathophysiology of the urothelium. They protect the urothelium and play a crucial role during urothelial infections by Uropathogenic *E. coli*. However, their functions beyond this organ system remain unexplored. A wide variety of proteins secreted in the male reproductive tract tissues contribute to spermatogenesis, sperm maturation, fertilization and innate immunity. However, the presence of UPKs and their possible contribution to the male reproductive tract physiology is not yet reported. Hence, in this study, we characterized UPKs in the male reproductive tract of rats. To the best of our knowledge, for the first time, we report the expression of UPKs in the male reproductive system. *Upk1a, Upk1b, Upk2* and *Upk3b* mRNA and their corresponding proteins were abundantly expressed in the caput, cauda, testis, seminal vesicles and the prostate. Their expression was not developmentally regulated. UPK protein expression was also localized on the spermatozoa, suggesting a role for these proteins in sperm function. To study the role of UPKs in innate immunity, *Upk* mRNA expression in response to endotoxin challenge was evaluated *in vitro* and *in vivo*. In the rat testicular and epididymal cell lines, *Upk* mRNA levels increased in response to lipopolysaccharide challenge. However, in the caput, cauda, testes, seminal vesicle and prostate obtained from LPS treated rats, *Upk* mRNA expression was significantly reduced. Results of this study indicate a role for UPKs in male reproductive physiology and innate immune responses.

1. Introduction

Uroplakins (UPKs) are a group of proteins that form the major constituents of urothelial plaques. In the mammals, five UPKs, namely, UPK1a, UPK1b, UPK2, UPK3a and UPK3b (a minor isoform of UPK3a) are characterized. Besides these, UPK2b and UPK3c and UPK3d were identified in other species (Desalle et al., 2014, Garcia-Espana et al., 2006, Wu et al., 1994). Mammalian UPKs are divided into two groups. UPK1a and UPK1b belong to the tetraspanin family, whereas UPK2 and UPK3 are grouped under the monospanin family (Yu et al., 1994, Lin et al., 1994, Wu and Sun 1993). The former family of proteins span the plasma membrane four times whereas the later span the plasma membrane only once. The plaques formed by UPKs generates an asymmetric unit membrane (AUM), which in turn functions to provide permeability barrier and structural stability to the urothelium. The formation of plaques involves specific interaction between the UPKs. UPK1a interacts with UPK2 whereas UPK1b interacts with UPK3a (Wu et al., 1994, Hu et al., 2005, Tu et al., 2006, Tu et al., 2002).

The functional significance of UPKs vary across the species. In mammals, though their major function is important for development, differentiation and homeostasis of the urothelium (Carpenter et al.,

2016), in the Xenopus oocytes UPK3a and UPK1b form a complex to mediate sperm-egg interaction and fertilization (Sakakibara et al., 2005, Hasan et al., 2011, Mahbub Hasan et al., 2005). In the zebrafish, UPK3a related protein contributes to epithelial cell polarization and morphogenesis of pronephric tubules (Mahbub Hasan et al., 2005). A recent study indicates that the UPK2/3 proteins are related to phosphotyrosine phosphatases and thus may have a role in cellular signaling (Chicote et al., 2017). UPK knock out mice display renal failure and high rates of mortality (Kong et al., 2004, Hu et al., 2000). Mutations in the UPK genes resulted in renal hypo dysplasia, adysplasia and renal failure in humans (Jenkins et al., 2005, Schonfelder et al., 2006). Further, UPKs serve as anchors for Uropathogenic E. coli (UPEC) during infections (Wu et al., 2009). They allow binding of the type-1 fimbriae expressing UPEC strains and facilitate their binding to the urothelial surface and triggering a cascade of events that favor bacterial infection and migration not only in the bladder, but also in the upper urinary tract organs such as urethra and renal pelvic urothelia (Wu et al., 1996, Mulvey et al., 1998, Martinez et al., 2000). Altered levels of UPKs in urothelial carcinomas are considered as useful markers for the diagnosis, detection and prediction of urothelial carcinomas (Wu et al., 2009, Huang et al., 2007, Zupancic et al., 2011).

^{*} Corresponding author at: Department of Animal Biology, University of Hyderabad, P.O. Central University, Hyderabad 500046, India. E-mail addresses: ysnaidu@yahoo.com, sureshsl@uohyd.ernet.in (S. Yenugu).

ORIGINAL ARTICLE





Tlr1-13, Nod1/2 and antimicrobial gene expression in the epididymis and testis of rats with alloxan-induced diabetes

Suresh Babu Munipalli | Marri Reddy Mounika | Jamil Aisha | Suresh Yenugu 🗓

Department of Animal Biology, School of Life Sciences, University of Hyderabad, Hyderabad, India

Correspondence

Suresh Yenugu, Department of Animal Biology, School of Life Sciences, University of Hyderabad, Hyderabad - 500046, India. Emails: ysnaidu@yahoo.com; sureshsl@ uohyd.ernet.in

Funding information

Indian Council of Medical Research, Grant/ Award Number: 61/6/2011/BMS

Abstract

Pattern recognition receptors (PRRs) such as toll-like receptors (TLRs) and nuclear oligomerization domain (NOD) receptors along with antimicrobial proteins and peptides (AMPs) are crucial for innate immunity. The pathology of insulin-dependent diabetes mellitus is associated with the disrupted expression of TLRs, NODs and AMPs in the kidney, lungs and other organs. However, such a relation in the male reproductive tract is not yet investigated. In this study, we analysed the expression pattern of Tlr1-13, Nod1/2 receptors and AMPs (β-defensins and defensin-like proteins of the Sperm-Associated Antigen 11 (Spag11) family) in the male reproductive tissues (caput, cauda and testis) obtained from diabetic or insulin-treated diabetic or untreated control rats. Alterations in the expression pattern of Tlr1-13, Nod 1/2, Defb1, 2, 21, 24, 27, 30 and Spag11a/ c/t were observed under diabetic conditions. Administration of insulin to diabetic rats could modulate the expression pattern of only some these genes. Results of our study indicate perturbed gene expression profile of Tlrs, Nod1/2, Defbs and Spag11 isoforms in the epididymis and testis of diabetic rats, and this could be one of the important reasons for the increased risk of infections in the male genital tract.

KEYWORDS

antimicrobial, defensin, diabetes, toll-like

wileyonlinelibrary.com/journal/and

INTRODUCTION

Innate immune system confers immediate defence strategies against pathogen-associated molecular pattern molecules (PAMPs) and damage-associated molecular pattern molecules (DAMPs), and this is accomplished through the recruitment of pattern recognition receptors (PRRs) and production of antimicrobial molecules. PRRs involved are toll-like receptors 1-13 (TLRs 1-13), nuclear oligomerization domain 1 and 2 (NOD1 and NOD2) receptors, RIG-I-like receptors, AIM2-like receptors and the receptor for advanced glycation end products (RAGE; Tang, Kang, Coyne, Zeh, & Lotze, 2012). Signalling pathways effected by these receptors promote the production of antimicrobial proteins and peptides, and these processes are well characterised in reproductive and in other organ systems (Mukherjee, Karmakar, & Babu, 2016). We and other groups demonstrated the abundant expression

of Tlr1-13 in the male reproductive tract of different species (Biswas et al., 2009; Biswas & Yenugu, 2011; Liman, Alan, & Apaydin, 2019; Palladino, Johnson, Gupta, Chapman, & Ojha, 2007; Palladino, Savarese, Chapman, Dughi, & Plaska, 2008; Pioli et al., 2004). The general gene expression pattern and LPS/uropathogenic Escherichia coli-mediated induction of rat Defbs and DEFB-like proteins and peptides belonging to the Sperm-Associated Antigen 11 (SPAG11) family were reported in the male reproductive system (Biswas & Yenugu, 2011, 2013, 2014; Yenugu, Chintalgattu, et al., 2006; Yenugu, Hamil, French, & Hall, 2006). The involvement of TLR4 in modulating Defb and Spag11 gene expression via the NF-kB pathway and epigenetic mechanisms was reported (Biswas & Yenugu, 2013, 2014).

Disruption in the innate immune signalling cascades and the subsequent defects in the expression of antimicrobial peptides are a hallmark of autoimmune diseases, atherosclerosis and diabetes mellitus



The End